6-13-2014 12:00 AM

Investigating Microenvironmental Regulation of Human Chordoma Cell Behaviour

Priya Patel
The University of Western Ontario

Supervisor
Dr. Cheryle Séguin
The University of Western Ontario

Graduate Program in Anatomy and Cell Biology
A thesis submitted in partial fulfillment of the requirements for the degree in Master of Science

INVESTIGATING MICROENVIRONMENTAL REGULATION OF HUMAN CHORDOMA CELL BEHAVIOUR

(Thesis format: Integrated Article)

by

Priya Patel

Graduate Program in Anatomy and Cell Biology

A thesis submitted in partial fulfillment
of the requirements for the degree of
Master of Science

The School of Graduate and Postdoctoral Studies
The University of Western Ontario
London, Ontario, Canada

ABSTRACT

The tumor microenvironment is complex and often includes matricellular proteins and regions of hypoxia, which can promote stem and progenitor properties that regulate cancer cell biology. We hypothesized that hypoxia and CCN2 would promote notochord progenitor-like characteristics in human chordoma (U-CH1) cells, and assessed cell phenotype using Real-time qPCR and in vitro functional assays. We found the expression of CCN family members *CCN1, CCN2, CCN3* and *CCN5* in U-CH1 cells. We demonstrate that hypoxia and CCN2 promoted progenitor-like characteristics specific to the notochordal tissue of origin. Specifically, hypoxia had the greatest ability to promote progenitor characteristics (increase in notochord markers *T, CD24, FOXA1, ACAN* and *CA12*, sphere formation, cell growth and fewer vacuolated cells) and the effects of CCN2 were more pronounced under normoxia than hypoxia. This study highlights the importance of the tumor microenvironment and how these components can be used to regulate human chordoma behaviour.

Keywords: chordoma, notochord, hypoxia, connective tissue growth factor, microenvironment

ACKNOWLEDGEMENTS

I would first like to thank Dr. Cheryle Séguin for providing me with the opportunity to undertake my Master's degree and being there for me over the last few years not only in graduate school but as an undergraduate as well. Thank you for providing me with lots of great opportunities and guidance for the past few years. In addition, thank you to all the Séguin lab members (both past and present) for your motivation, humor and support. A special thank you to Courtney Brooks for your training, support and insightful feedback about my project.

Next, I would like to thank my supervisory committee, Drs. Alison Allan and Frank Beier, for providing me with feedback on ways to improve my project and guidance whenever it was needed.

A special thank you to my family and friends for your support and encouragement while I have been in graduate school. I love you for being there for me and I thank you for everything.

TABLE OF CONTENTS

LIST OF TABLES

LIST OF FIGURES

LIST OF APPENDICES

LIST OF ABBREVIATIONS

ACAN	aggrecan
ALDH	aldehyde dehydrogenase
ARNT	aryl hydrocarbon receptor nuclear translocator
bFGF	basic fibroblast growth factor
CA12	carbonic anhydrase XII
CCN1	CCN family member 1 (cysteine-rich, angiogenic inducer, 61)
CCN2	CCN family member 2 (connective tissue growth factor)
CCN3	CCN family member 3 (nephroblastoma overexpressed)
CCN5	CCN family member 5 (WNT1 inducible signaling pathway protein 2)
CD90	Thy-1 membrane glycoprotein
CD105	endoglin
CD133	prominin
cDNA	complementary deoxyribonucleic acid
CO_2	carbon dioxide
COL2A1	collagen type II alpha I
DAPI	4’-6’-diamino-2-phenylindole
DEAB	diethylaminobenzaldehyde
DNA	deoxyribonucleic acid
E	embryonic day
EGF	epidermal growth factor
EMA	epithelial marker antigen

EMT	epithelial-mesenchymal transition
FBS	fetal bovine serum
FOXA1	forkhead box A1
FOXA2	forkhead box A2
GLUT1	glucose transporter 1
HIF1-α	hypoxia-inducible factor 1-alpha
IGF	insulin-like growth factor
IgG	immunoglobulin G
IVD	intervertebral disc
kDA	kilodalton
LacZ	β-Galactosidase
mRNA	messenger ribonucleic acid
NOD/SCID	nonobese diabetic/severe combined immunodeficient
NP	nucleus pulposus
O_2	oxygen
P	passage
PBS	phosphate buffered saline
PBST	0.2% Triton X-100 in phosphate buffered saline
PCR	polymerase chain reaction
PTEN	phosphatase and tensin homolog
rCCN2	recombinant CCN2
$rCCN2_{domain4}$	recombinant CCN2 domain 4
RNA	ribonucleic acid
Shh	sonic hedgehog

SOX9	sry-type high mobility group box 9
SOX5	sry-type high mobility group box 5
SOX6	sry-type high mobility group box 6
SP	signal peptide
T	brachyury
TSP-1	thrombospondin-1 domain
VEGF	vascular endothelial growth factor
VWC	a von Willebrand type C domain

CHAPTER 1

Introduction

1.1 Overview of chordoma

1.1.1 Basic understanding of chordoma

Chordomas are rare, malignant and locally invasive tumors that occur most commonly at the base of the skull (32%) and sacrococcygeal region (29%), and less frequently in cervical, thoracic and lumbar vertebrae [1,2]. The cancer typically affects one in one million people each year in the United States with the median age of diagnosis being 49 for skull-based chordomas and 69 for sacral-based chordomas [1]. The median age of survival for patients affected with chordomas is 6 years and the tumors have a high rate of recurrence [3]. Studies report that males are more commonly affected than females, with the ratio of males to females with chordoma being approximately 1.6 to 1. The cancer has also been reported to less frequently affect African-American individuals compared to Caucasians [1]. Chordomas are low-grade tumors that have a high rate of recurrence and are capable of metastasizing to areas including the lungs, liver, bone and skin [4].

The clinical presentation of chordoma varies depending on the anatomical region affected. Patients affected by skull-based chordomas often present with headaches, neck pain or double vision whereas patients with sacral-based chordomas have changes in bowel/bladder function, pain, numbness or weakness in the legs and arms [5]. A major setback for patients remains the limited treatment options, as the tumors are often resistant to traditional chemotherapy and radiation therapy [6-7]. As a result, surgical resection is the major form of treatment, however complete resection is often difficult to achieve due to the invasive behaviour and proximity of tumors to the spinal cord [6,8].

Currently, there are a limited number of studies that examine the biology of these tumors and their malignant transformation from the pre-cancerous cell of origin (notochord cells). This paradigm highlights the importance of gaining a basic understanding of this cancer, as this could contribute to the development of more effective treatment options for patients.

1.1.2 Development of the notochord and vertebral column

The vertebral column is comprised of vertebral bone separated by intervertebral discs. During formation of the vertebral column, the notochord is the embryonic structure that acts as the primitive axis of the embryo and induces patterning of surrounding tissues [9]. Using murine models, it has been shown that the notochord elongates at embryonic day (E) 7.5 from a structure known as the node, which originates from the mesoderm [10]. In humans, complete formation of the notochord occurs at E20 (**Figure 1.1A**); at this time the notochord is surrounded by a structure called the notochord sheath, which helps maintain the rod-like structure of the notochord [11-12]. At the end of embryonic week 5, segmented blocks of paraxial mesoderm called somites divide and encircle the notochord. These somites segment and produce alternating condensed and non-condensed regions that will give rise to the annulus fibrosus and vertebral bodies, respectively [13-14]. The notochord enlarges between the vertebral bodies to form the future nucleus pulposus, which is located in the middle of the intervertebral disc [13,15] (**Figure 1.1B**). In humans, the notochord cells are thought to disappear a few years after birth. There remains controversy surrounding whether notochord cells develop into chondrocyte-like nucleus pulposus cells or if they die and are replaced by cells that migrate into the nucleus

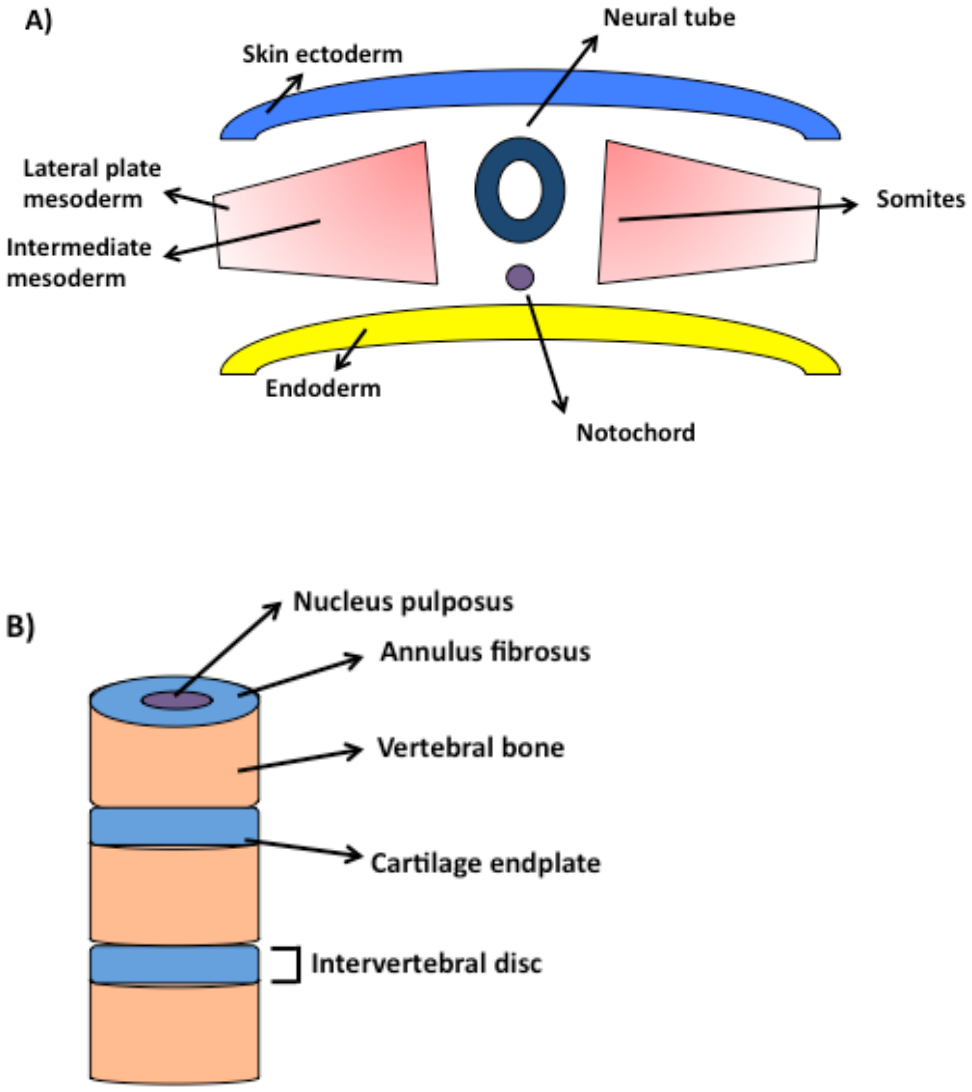

Figure 1.1. Illustration of the notochord that forms the nucleus pulposus in humans. **(A)** Shows the formation of the notochord at E20 surrounded by somites. **(B)** Shows the notochord derived nucleus pulposus in the middle of the intervertebral disc surrounded by the outer annulus fibrosus.

pulposus from the inner annulus fibrosus or cartilage endplate [13-16]. Recent studies using lineage tracing in the murine model have established that all cells of the mature nucleus pulposus are derived from the embryonic notochord [16,19].

One of the factors involved in notogenesis is T, the founding member of the T-box family of transcription factors. T is expressed in the notochord and to a lesser extent in the nucleus pulposus, and is critical to notochord formation [19,20]. The complete loss of *T* in mice has been shown to cause embryonic lethality at E10.0 due to impaired axial development and allantoic defects [21,22]. In comparison, knockdown of *T* in mice resulted in notochord formation but the cells were not able to differentiate and mice exhibited axial skeletal defects [23]. *T* has also been shown to be highly expressed in nucleus pulposus tissue in rats at 12 months of age compared to rats at 21 months of age, where there was a significant decrease in expression [24]. In humans, DNA sequence analysis has correlated a missense mutation in the *T* locus to vertebral malformations [25].

Aggrecan (ACAN) is a proteoglycan that is expressed in a variety of tissues including the notochord and notochord sheath [26]. In addition, ACAN is expressed in the extracellular matrix of normal (non-degenerate) human nucleus pulposus disc tissue and confers water bearing capacity to the disc due to osmotic pressure provided by its chondroitin sulphate chains [27, 28]. SOX9 is a transcription factor that is a member of the SOX (Sry-type high mobility group box) family of genes and that has been shown to increase expression from the aggrecan gene promoter in human chondrocyte cells [29]. Interestingly, this effect was found to be cell-type dependent, as SOX9 enhancement of

ACAN promoter activity was not found in osteoblast-like osteosarcoma cells. In addition, SOX9 is important for notochord development as *SOX9*-null mice do not form a continuous notochord, with regions in the cervical and thoracic sections disrupted at E10.5 [30]. After E10.5, these mice displayed a progressive rostral to caudal loss of the notochord. *SOX9* is also expressed in normal (non-degenerate) human nucleus pulposus tissues [28].

In addition to SOX9, the transcription factors SOX5 and SOX6 and forkhead box A1 and A2 (FOXA1 and FOXA1) are important for notochord development. Both SOX5 and SOX6 are expressed in murine notochord cells and their expression decreases as notochord cells differentiate into mature nucleus pulposus cells [31]. *SOX5*$^{-/-}$*;SOX6*$^{-/-}$ mice lack formation of the notochord sheath. In addition, the notochord cells of these mice underwent apoptosis and were not able to form nucleus pulposi, although the inner annulus was present [31]. FOXA1 is expressed in the notochord and floor plate, whereas FOXA2 is expressed in the node, notochord and floorplate [32]. Mice lacking both *FOXA1* and *FOXA2* show deformed nucleus pulposi that were small and compressed at E17.5. These mice also demonstrated abnormal notochord sheath formation and the lack of a visible notochord at the forelimb level [33].

Although in the field of spine research there is a general lack of notochord and nucleus pulposus-specific markers, heat stable antigen CD24 is a cell surface receptor that has been shown to be expressed in the notochord of rats and nucleus pulposus of humans [34,35]. In addition, carbonic anhydrase XII (CA12) has been shown to be expressed

exclusively in the notochord in mice and the nucleus pulposus of young human subjects while its expression decreases in older subjects [32-34].

1.1.3 Notochordal cell and the origin of chordoma

Our lab and others have demonstrated that notochord cells act as tissue-specific progenitor cells within the murine intervertebral disc, through a traditional fate mapping study [19, 16]. Using a novel Noto$^{Cre/+}$ mouse crossed with a LacZ reporter mouse, where Cre recombinase was expressed specifically in the node and posterior notochord through targeting of the *Noto* locus, this study permanently labeled cells of notochordal origin [19]. This genetic strategy demonstrated that all cells of mature nucleus pulposus were derived from the embryonic notochord and also identified small clusters of notochord cells within the vertebrae of skeletally mature mice (**Figure 1.2**). In the study, the presence of notochord remnants (i.e. benign notochord cell tumors) was reported in at least one vertebrae in >90% of skeletally mature mice. A similar study that used fate-mapping analysis to examine cells of notochord origin with *Shh*^{Cre} mice also noted the presence of notochord remnant cells in all mice examined along the entire length of the vertebral column [16].

Similar to findings in the mouse model, a study using 100 human cadavers noted the presence of benign notochord cell tumors in 20% of the cadavers [39]. The anatomical distribution of the tumors was similar to that of chordomas (11.5% clivus, 5% cervical vertebrae, 2% lumbar vertebrae 12% sacro-coccygeal vertebrae). Another study used 82

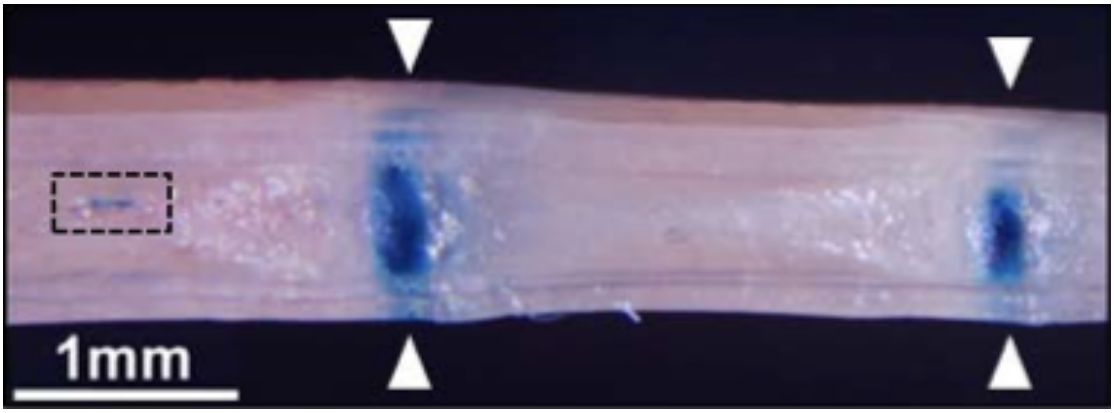

Figure 1.2. Localization of notochord-derived cells in skeletally mature mice (postnatal day 100). Linage tracing of notochord-derived cells using notochord-specific Cre mouse ($Noto^{CRE}$) crossed with the Rosa26 ^{LacZ} reporter demonstrates the localization of notochordal cells to the nucleus pulposus of the intervertebral discs (white arrow heads) as well as clusters of notochordal remnants within the vertebral bone (black dotted box). *(Reproduced with permission from McCann et al. Dis Model Mech., 2012)*

human cadavers and found that 7.3% of cadavers contained benign notochord cell tumors [40]. The age of cadavers with these tumors ranged from 40-70 years old; however, another study found that these benign tumors could be found in patients as young as 14 years old [41]. Since the occurrence of chordoma is rare (1 in 1 million cases per year), it has been suggested that these benign notochord cell tumors lay dormant throughout a person's lifetime unless stimulated by other factors. Chordomas are believed to arise from these benign notochord cell tumors, based on histological association in three separate patient cases. In the first case, a resected chordoma from the coccyx was found adjacent to an benign notochord cell tumor in a 57-year old patient [42]. In the next two cases, the presence of an incipient chordoma was found alongside benign notochord cell tumors [43]. Histologically, the chordomas appeared as cords of tumor cells that contained a myxoid (mucoid) matrix with eccentrically located nuclei and physaliferous cells [43]. The major difference between chordomas and benign notochord cell tumors is the lack of a mucoid matrix and nuclear atypia [44]. Furthermore, the benign notochord tumors and chordomas stained positively for epithelial marker antigen (EMA), vimentin, cytokeratin and S-100, which are also markers of the embryonic notochord [45–47].

1.1.4 Human chordoma cell lines

An overarching issue associated with the use of chordoma cell lines for research are concerns that many of the chordoma cell lines generated from primary tumors do not accurately represent human chordomas [48]. For example, the CCL3 [49], CCL4 [50], GB60 [51] and CM319 [52] cell lines lack genetic alterations typical of human cancers and lack copy number aberrations that have been associated with chordomas, such as losses on

chromosome 3p, or cell morphology that is not consistent with the typical physaliferous morphology of chordoma cells [48]. The human chordoma cell lines U-CH1 [53], U-CH2 [48], MUG-Chor1 [54] and JHC7 [6] are generally considered the most representative models of chordoma.

The current study was conducted using U-CH1, a cell-line derived from a 46-year old male with a recurrent sacral chordoma [53]. When cultured *in vitro*, the cell line is a heterogenous population containing both vacuolated "physaliferous" cells and small non-vacuolated cells (**Figure 1.3**). U-CH1 cells express S-100, vimentin, EMA, CD24 and cytokeratin, which are typical markers of chordomas [39,43-53]. In addition, gene expression analysis has shown that U-CH1 expresses *T* 10-fold higher than the U-CH2 cell line [53]. U-CH1 has been shown to have a loss of the PTEN tumor suppressor gene, consistent with chordoma tumors [48]. U-CH1 was directly compared to the parent tumor from which cells were isolated, which confirmed similar physaliferous cells and positive staining for cytokeratin [53]. U-CH1 has also been used to create a mouse xenograft model of chordoma following injection of cells into the NOD/SCID/interleukin 2 receptor-null mouse [55]. The study demonstrated that the U-CH1 xenograft was morphologically similar to chordoma and that cells expressed T.

1.2 The tumor microenvironment and role of matricellular proteins

1.2.1 Basic overview of the CCN family members

The CCN family is comprised of six matricellular proteins (CCN1, CCN2, CCN3, CCN4, CCN5 and CCN6) that bind to cell-surface receptors, components of the

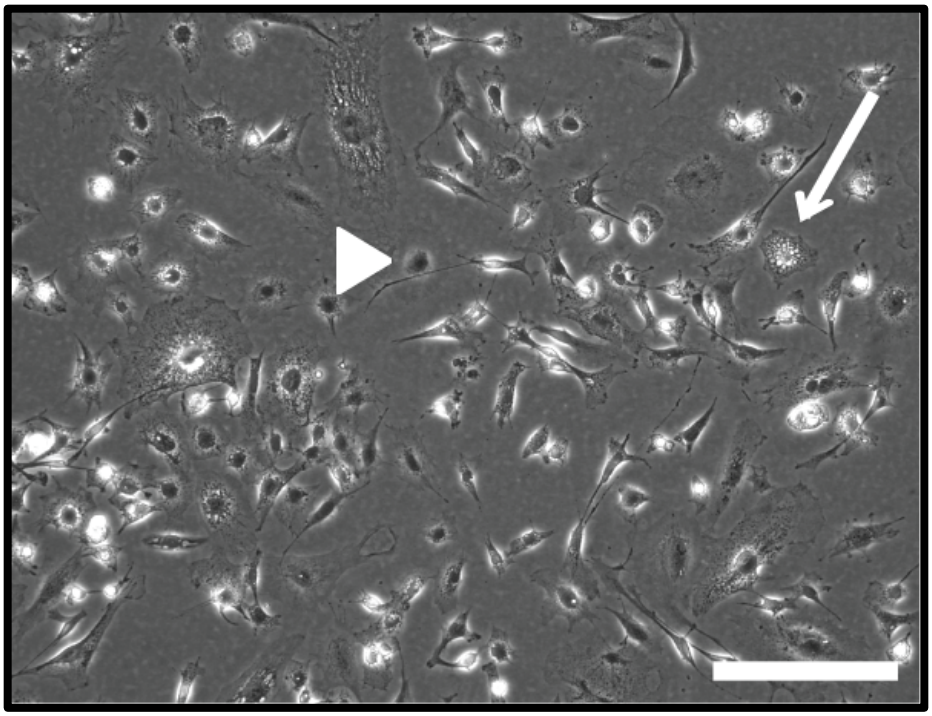

Figure 1.3. Morphological appearance of U-CH1 human chordoma cell line. Representative phase contrast image of UCH-1 cells maintained in monolayer culture (P39), as previously described. White arrow indicates a vacuolated ("physaliferous") cell and arrowhead indicates a non-vacuolated cell. (Scale bar = 250 μm)

extracellular matrix, proteases and signaling molecules such as cytokines and hormones [56-57]. As a result, these proteins have a variety of functions that regulate cell adhesion, mitosis, apoptosis, migration and extracellular matrix production in a variety of different cell types [58]. Members of the CCN family play roles in development, wound healing and diseases including cancer.

CCN proteins are composed of four modules: the insulin-like growth factor binding protein domain (module 1), a Von Willebrand factor domain (module II), a thrombospondin-homology domain (module III) and a cysteine knot, heparin-binding domain (module IV). The one exception is CCN5 which lacks module IV [59] (**Figure 1.4**). Domains II and III are linked by hinge regions that can be cleaved by proteases [58]. The CCN proteins share 40-60% of their amino acid sequences and have a gene structure consisting of five exons and four introns [58].

1.2.2 Role of CCN proteins in cancer

The tumor microenvironment is composed of a variety of different cell types including cancer cells, stromal fibroblasts, endothelial cells, as well as secreted proteins, oxygen levels, matricellular proteins and components of the extracellular matrix [60] (**Figure 1.5**). CCN proteins contribute to the regulation of various aspects of tumor progression such as epithelial-mesenchymal transition (EMT), angiogenesis, cell proliferation, cell migration and extracellular matrix degradation.

CCN1 has been implicated in prostate cancer, glioma, pancreatic cancer and

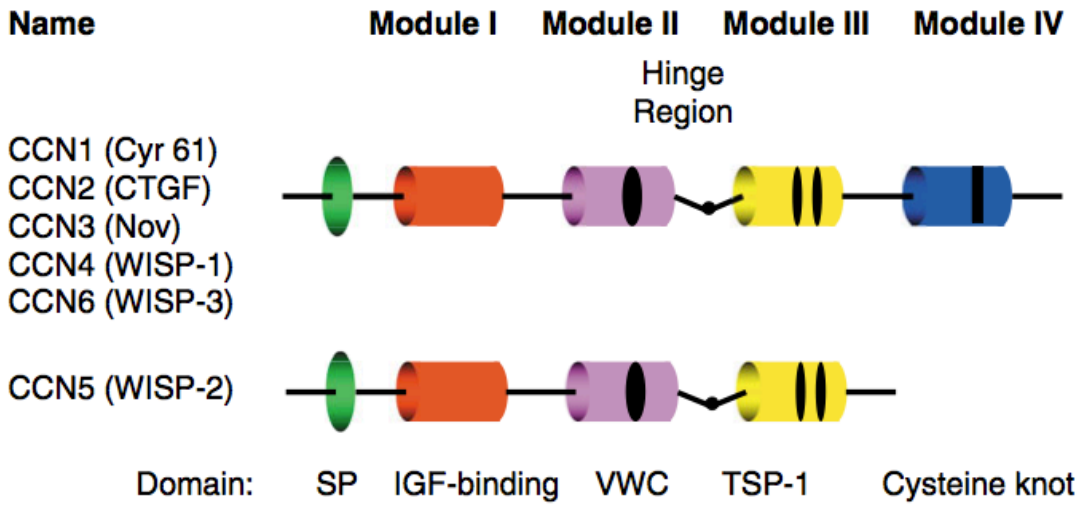

Figure 1.4. Schematic illustration depicting the structure of CCN family proteins. CCN family members share a secretory signal peptide (SP) and four domains: (1) IGF-binding domain, (2) a von Willebrand type C domain (VWC), (3) a thrombospondin-1 domain (TSP-1) and (4) a cysteine knot domain. The exception is CCN5, which lacks a cysteine knot domain. There is a hinge region between domains II and III that is susceptible to cleavage. *(Reproduced with permission from Leask et al. J Cell Sci., 2006)*

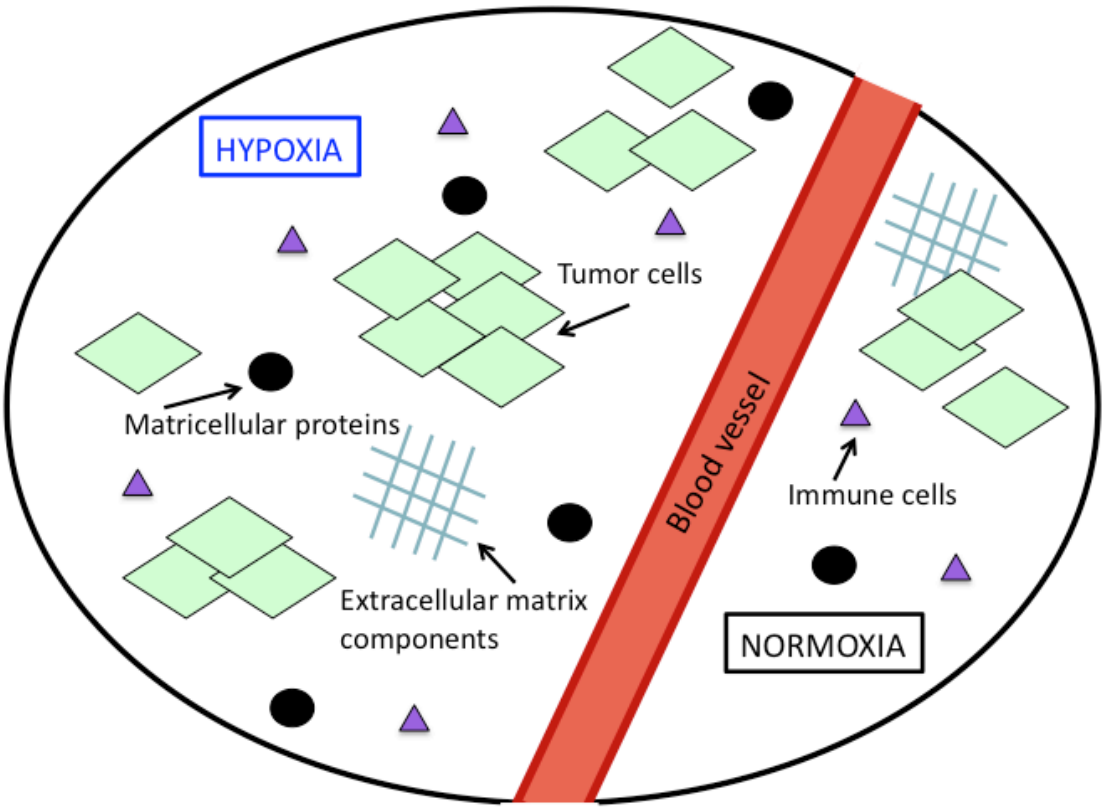

Figure 1.5. Example of a tumor microenvironment. Schematic representation depicting components of the tumor microenvironment including tumor cells, blood vessels, immune cells, extracellular matrix components, matricellular proteins and regions of hypoxia and normoxia.

breast cancer. In prostate carcinoma cells, CCN1 has been shown to enhance cell adhesion through $\alpha_6\beta_1$ and $\alpha_6\beta_4$ integrin binding and heparan sulfate proteoglycan binding and also to increase cell proliferation [61-62]. CCN1 was detected in pancreatic cancer cells, and blocking of CCN1 inhibited cell migration [63]. Studies in breast cancer cell lines show that CCN1 expression is correlated to increased invasiveness, anchorage-independent growth, tumor progression and VEGF secretion through $\alpha_5\beta_3$ integrin binding [66-67].

CCN2 has been shown to play a role in a variety of cancers including lung, gallbladder, leukemia, breast and pancreatic cancer. In lung adenocarcinoma cells, CCN2 has been shown to induce anoikis, which in turn suppresses metastasis [66]. Studies using gallbladder cancer cell lines demonstrated that CCN2 knockdown reduces cell viability, colony formation and anchorage-independent growth [67]. A study using five leukemia cell lines showed that *CCN2* is expressed in all of the cell lines and that silencing of this gene resulted in suppressed cell growth [68]. In breast cancer, overexpression of CCN2 in MCF-7 cells resulted in reduced cell proliferation, increased migration and increased angiogenesis [69]. An *in vivo* mouse model of bone metastasis using breast cancer cells (MDA231) showed that blocking of CCN2 resulted in reduced osteolytic bone metastasis and decreased tumor proliferation and migration [70]. Lastly, overexpression of CCN2 in pancreatic cancer cells significantly increased colony formation [71]. Studies using recombinant CCN2 (rCCN2) have found that this protein can both promote and reduce the ability of cells to differentiate. For example, a study using hepatic progenitor cells found that rCCN2 peptide promoted hepatic differentiation [72]. Another study found that

treatment of mesenchymal stem cells with full length rCCN2 peptide reduced their ability to differentiate [73].

CCN3 has been implicated in prostate and breast cancer, and also chondrosarcoma. Studies have shown that breast cancer patients with bone metastasis show elevated CCN3 in their tumors [70]. Furthermore, *CCN3* knockdown inhibits cell migration, tumor growth in bone and bone metastasis in an *in vivo* mouse model of prostate cancer [71]. CCN3 is also expressed in bone metastases from patients with breast cancer [76]. A study demonstrated that overexpression of *CCN3* in breast cancer cells (66cl4) increased bone metastases when cells were injected into the left cardiac ventricle of mice [76]. Mice with ectopic expression of *CCN3* were found to have increased bone metastases (31%) compared to control mice (14%). CCN3 has also been shown to have a role in glioma, where overexpression of *CCN3* in glioma cells demonstrated an anti-proliferative effect [77]. Furthermore, studies using the JJ012 human chondrosarcoma cell line found that *CCN3* expression promoted cell migration [78].

CCN5 has been shown to play a role in breast and pancreatic cancers. A study using an invasive breast cancer cell line (MDA-MB-231) showed that overexpression of *CCN5* reduced cell proliferation and invasiveness, and that the loss of *CCN5* expression promoted breast cancer progression [81-82]. A study using human pancreatic adenocarcinoma cell lines showed that overexpression of *CCN5* promoted epithelial-mesenchymal transition [79].

To date, there are no studies examining the role of CCN proteins in chordoma. Thus far, there is evidence suggesting that CCN2 may play a role in chordoma pathogenesis through its interaction with T, which is amplified in sporadic chordomas and duplicated in familial chordomas [57,82]. A recent study examined the T transcriptional network in UCH-1 chordoma cells and identified CCN2 as a direct downstream target [82].

1.2.3 Role of CCN2 in notochordal cells

Studies have shown that CCN2 is enriched in the notochord and nucleus pulposus of mice (**Figure 1.6**) [85-86] and is secreted by notochord cells in the nucleus pulposus of non-chondrodystrophic dogs [85]. In zebrafish, knockdown of *Ccn2* resulted in disrupted notochord development, including tail buds that failed to elongate [86]. Recently, our lab generated a mouse strain with targeted deletion of CCN2 in notochord and notochord-derived cells [83]. This study found that loss of *CCN2* in notochord-derived cells disrupted extracellular matrix composition within the IVD at postnatal day 1, with decreased levels of ACAN and collagen type II alpha I (COL2A1) in the putative nucleus pulposus. These mice also displayed accelerated age-related disc degeneration in 12 and 17 month old mice compared to wild-type controls. Studies in humans have shown that CCN2 is more highly expressed in degenerated IVDs than normal IVDs, leading to a debate regarding the role played by CCN2 in accelerating disc degeneration or contributing to a reparative tissue response [89-90].

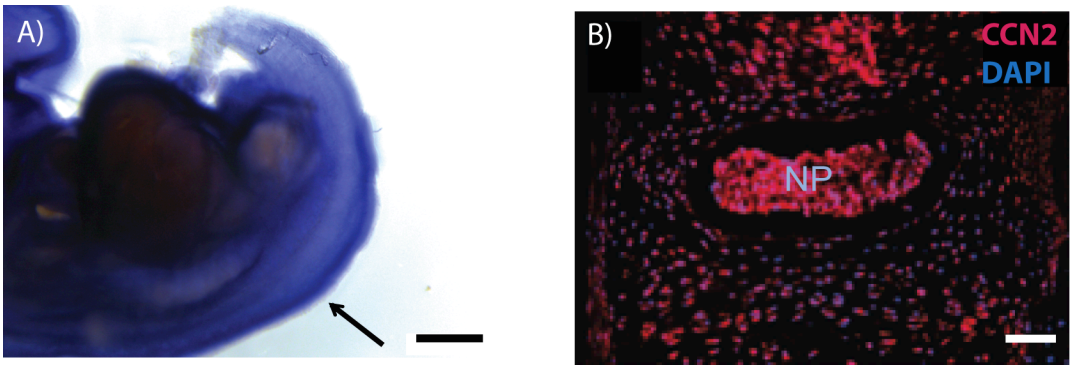

Figure 1.6. CCN2 localization in notochord and notochord-derived tissues of the murine intervertebral disc. Representative images demonstrating localization of CCN2 in mice. (A) Depicts CCN2 mRNA localization by *in situ* hybridization in the posterior aspect of the embryo as E12.5 (indicated by the black arrow; Scale bar = 500 μm). *(Matthew McCann, unpublished data)* (B) Immunolocalization of CCN2 protein in the newly formed intervertebral disc at postnatal day 1. (Scale bar = 50 μm) *(Reproduced with permission from Bedore et al., Arthritis & Rheum., 2013)*.

1.3 The tumor microenvironment and role of hypoxia

1.3.1 The effects of hypoxia in cancer

As previously described, tumor microenvironments are highly complex and are often marked by oxygen tension levels distinct from those of surrounding healthy tissues. The normal oxygen level in tissues is approximately 20% O_2 (normoxia), which is oxygen in air at normal atmospheric pressure [89]. Solid tumors often create hypoxic environments (usually between 1-3% O_2 but can vary depending on the type of tumor) due to a limited oxygen supply [89]. Hypoxic conditions result from inadequate oxygen supply to the tumor, which is usually caused by limited ability for blood to carry oxygen, reduced tissue perfusion and inconsistencies in blood flow diffusion [90]. Normally, these conditions would be harmful to cells but cancer cells adapt to these conditions by undergoing genetic changes promoting survival [91].

In hypoxic conditions, cells often show increased levels of hypoxia-inducible factor 1-alpha (HIF1-α). HIF1-α belongs to a family of HIF proteins that respond to low oxygen conditions and are involved in regulating many pathways, such as its interaction with the Notch signaling network [92]. Under normoxic conditions, the α subunit of the HIF1-α protein is rapidly degraded through hydroxylation of two key proline residues in the oxygen-dependent degradation domain [93]. However, under hypoxic conditions HIF1-α becomes stabilized and heterodimerizes with the aryl hydrocarbon receptor nuclear translocator (ARNT) in the nucleus. Upon heterodimerization, HIF1-α binds to hypoxia-response elements within the genome, inducing the expression of many hypoxia-response genes. The activated genes can be involved in a variety of processes including cell

proliferation, angiogenesis, metabolism, migration and apoptosis [91]. For example, vascular endothelial growth factor (VEGF) and glucose transporter 1 (GLUT1) are immediate downstream targets of HIF1-α involved in angiogenesis and glycolysis [94].

1.3.2 Effects of hypoxia on stem and progenitor stem cell populations

The effect of hypoxia on stem cell and progenitor cell populations is an area of active investigation, as hypoxia has been shown to have different effects on the differentiation of stem and progenitor cells. In general, progenitor cells are early descendants of stem cells that can differentiate to form one or more kinds of cells but are more limited in the kinds of cells they can become and cannot self-renew indefinitely.

Murine bone marrow cells have been shown to have an increased number of progenitor cells and a higher stem cell potential in hypoxia (1% O_2) compared to cells maintained in normoxia for 8 days [95]. The cells maintained under hypoxia also demonstrated increased colony formation compared to cells in normoxia. Hematopoietic progenitor cells also show similar responses to hypoxic environments, with a reported four-fold expansion in the number of $CD34^+$ cells (a marker for primitive blood and bone marrow-derived progenitor cells) in hypoxia (1% O_2) compared to normoxia [96]. In contrast, hypoxia (5% O_2) has been shown to promote cell differentiation in neuronal stem cells [97]. Interestingly, differentiation of human mesenchymal stem cells into osteoblastic or adipogenic lineages was not affected by culture in hypoxia; however, cells demonstrated a nine-fold increase in proliferation under hypoxia (2% O_2) compared to normoxia [98].

The effect of hypoxia on cancer stem cell and progenitor populations is still an active area of research. Studies conducted using glioma and glioblastoma cells demonstrated that hypoxia (1-2% O_2) promoted a more stem-like phenotype, with the upregulation of the pluripotency markers OCT4, NANOG and the cancer stem cell marker CD133 [99–101]. These cells were able to form spheres faster and demonstrated reduced cell differentiation compared to cells in normoxia. In addition, ovarian cancer cells (ES-2 and OVCAR-3) have been shown to upregulate cancer stem cell markers CD44 and CD133 under hypoxia and also demonstrate increased sphere formation *in vitro* [102]. In addition, hypoxia has been shown to have different effects on cell migration, where it has increased migration of glioblastoma cells (U87) and decreased the migration of human prostate cancer cells compared to normoxia [103, 104].

To date, no studies have examined the effects of hypoxia on the maintenance on a cancer stem cell or progenitor cell population in chordomas. A previous report assessed the expression of stem cell markers on UCH-1 cells and reported that a subset of cells were positive for CD90 (11.82%), CD105 (5.66%), CD166 (4.76%), CD73 (0.46%), CD45 (8.2%), CD34 (2.66%) or CD133 (2.6%) [105]. In another study, primary human chordoma tumor samples were stained with stem cell surface marker CD44, which was detected in 50% (8 out of 16) chordoma patient tumor samples[106]. One limitation to the claim that CD44 and CD133 mark chordoma cancer stem cells is the lack of functional studies isolating or characterizing CD44+ or CD133+ populations using standard xenograft models. The MUG-Chor1 human chordoma cell line was assessed for aldehyde dehydrogenase (ALDH) activity and reported a small (0.3%) population of $ALDH^{high}$

cells [107]. ALDH is a cystolic enzyme responsible for retinoic acid metabolism and cellular self-protection from oxidative damage, and has been found in cancer stem populations in various cancers such as breast and pancreatic cancer [108, 113–116].

1.3.3 Effects of hypoxia on chordoma cells

Determining the effects of hypoxia on chordoma cell biology is important, as a study using positron electron tomography on a sacrococcygeal chordoma demonstrated that a large volume of the chordoma tumor is hypoxic [117]. There are currently a limited number of studies investigating the effects of hypoxia on chordoma cell biology. One study reported that chordoma cells (CH8, GB60, U-CH1) cultured in hypoxic conditions (5% O_2) showed no differences in cell proliferation when compared to cells grown in normoxia over 7 days [118]. However, another study used a primary human chordoma cell line and found that culture in hypoxia (5% O_2) increased cell proliferation compared to cells maintained in normoxia over 5 days [50].

1.3.4 Effects of hypoxia on the nucleus pulposus

The intervertebral disc is an avascular structure that demonstrates a range of oxygen concentrations across the intervertebral disc. The central nucleus pulposus (NP) is a hypoxic environment and as a result, the NP cells have developed mechanisms to maintain their function and survival in this environment. For example, *HIF1-α* expression is higher in the NP compared to the annulus fibrosus or cartilage endplate tissues of the disc [119]. Studies using primary NP cells from rat, human and sheep reported that HIF1-α protein levels were not significantly increased when cells were placed under hypoxic (2%

O_2) conditions compared to normoxic conditions [119]. The authors therefore suggested that NP cells maintain high HIF1-α levels, regardless of the oxygen environment.

Furthermore, studies reported that exposure to hypoxia increased levels of *ACAN* gene expression in NP cells isolated from rat (2% O_2) [120], bovine (5% O_2) [121] and human (3.5% O_2) [122] samples and increased levels of *COL2A1* and *SOX9* in the human samples compared to cells maintained in normoxia. Human NP cells also show increased proliferation in hypoxic conditions [122]. Hypoxia has also been shown to have a role in preventing cell apoptosis, as rat NP cells grown in hypoxic conditions survive serum starvation better (12-15% of cells underwent apoptosis) than cells in normoxia (35-40% of cells underwent apoptosis) [123]. Lastly, hypoxia has been shown to influence *CCN2* expression in rat NP cells [124]. Cells cultured in hypoxia showed a significant decrease in *CCN2* gene expression and protein expression. The overexpression of *HIF1-α* in these cells resulted in suppression of *CCN2* promoter activity, suggesting that hypoxia decreases CCN2 expression and promoter activity in a HIF1-α-dependent manner. This is in contrast to chondrocytic cells, which showed the addition of rCCN2 increased *HIF1-α* mRNA and protein levels [125].

The effects of hypoxia and CCN2 on human chordoma cells remain largely unknown. As previously mentioned, studies have demonstrated that a large volume of chordoma is hypoxic and that CCN2 is a direct downstream target of the known chordoma marker brachyury (T), whose mutations are associated with sporadic and familial chordomas [34-35]. In the current study, we sought to better understand the role

played by the tumor microenvironment in regulating chordoma cell biology by specifically investigating the effects of hypoxia and CCN2 on the regulation of human chordoma (U-CH1) cells, as they have both been implicated in regulating cancer cell biology and stem and progenitor properties in other cell types.

1.4 Rationale, hypothesis and objectives

Rationale: We sought to investigate microenvironmental regulation of human chordoma cells (U-CH1). We chose to specifically study the effects of CCN2 and hypoxia, as studies have shown that these are important factors in the tumor microenvironment that may regulate chordoma pathogenesis.

Hypothesis: Hypoxic conditions and/or increased levels of CCN2 will alter the phenotype and functional properties of human chordoma cells, promoting progenitor-like characteristics specific to the notochordal tissue of origin.

Objectives: In order to test our hypothesis, we developed two specific objectives:

1) To examine the effect of hypoxia on human U-CH1 chordoma cells.

2) To examine the effect of CCN2 and the additive effects of CCN2 and hypoxia on human U-CH1 chordoma cells.

1.5 References

1. McMaster ML, Goldstein M, Bromley CM, Ishibe N & Parry DM. Chordoma: incidence and survival patterns in the United States, 1973-1995. *Cancer Causes Control.* **12**, 1–11 (2001).

2. Bjornsson J, Wold LE, Ebersold MJ & Laws ER. Chordoma of the mobile spine. A clinicopathologic analysis of 40 patients. *Cancer.* **71**, 735–40 (1993).

3. Chugh R, Tawbi H, Lucas DR, Biermann JS, Schuetze SM & Baker LH. Chordoma: the nonsarcoma primary bone tumor. *Oncologist.* **12**, 1344–50 (2007).

4. Chambers PW & Schwinn CP. Chordoma. A clinicopathologic study of metastasis. *Am. J. Clin. Pathol.* **72**, 765–776 (1979).

5. Rich TA, Schiller A, Suit HD & Mankin HJ. Clinical and pathologic review of 48 cases of chordoma. *Cancer*. **56**, 182–7 (1985).

6. Hsu W, Mohyeldin A, Shah SR, ap Rhys CM, Johnson LF, Sedora-Roman NI, Kosztowski TA, Awad OA, McCarthy EF, Loeb DM, Wolinsky JP, Gokaslan ZL & Quiñones-Hinojosa A. Generation of chordoma cell line JHC7 and the identification of Brachyury as a novel molecular target. *J. Neurosurg.* **115**, 760–9 (2011).

7. Adams DS, Keller R & Koehl MA. The mechanics of notochord elongation, straightening and stiffening in the embryo of Xenopus laevis. *Development*. **110**, 115–30 (1990).

8. Fourney DR, Rhines LD, Hentschel SJ, Skibber JM, Wolinsky JP, Weber KL, Suki D, Gallia GL, Garonzik I & Gokaslan ZL. En bloc resection of primary sacral tumors: classification of surgical approaches and outcome. *J. Neurosurg. Spine*. **3**, 111–122 (2005).

9. Beddington RS & Robertson EJ. Axis development and early asymmetry in mammals. *Cell*. **96**, 195–209 (1999).

10. Yamanaka Y, Tamplin OJ, Beckers A, Gossler A & Rossant J. Live imaging and genetic analysis of mouse notochord formation reveals regional morphogenetic mechanisms. *Dev. Cell* **13,** 884–96 (2007).

11. Peter Raven GJ. *Biology*. 1224–1225 (McGraw-Hill, 2002).

12. Choi KS & Harfe BD. Hedgehog signaling is required for formation of the notochord sheath and patterning of nuclei pulposi within the intervertebral discs. *Proc. Natl. Acad. Sci. U. S. A.* **108,** 9484–9 (2011).

13. Theiler K. Vertebral malformations. *Adv Anat Embryol Cell Biol.* **112,** 1–99 (1988).

14. Goto S & Uhthoff HK. Notochord action on spinal development. A histologic and morphometric investigation. *Acta Orthop Scand.* **57,** 85–90 (1986).

15. Walmsley R. The development and growth of the intervertebral disc. *Edinb Med J.* **60,** 341–64 (1953).

16. Choi KS, Cohn MJ & Harfe BD. Identification of nucleus pulposus precursor cells and notochordal remnants in the mouse: implications for disk degeneration and chordoma formation. *Dev. Dyn.* **237,** 3953–3958 (2009).

17. Henriksson H, Thornemo M, Karlsson C, Hägg O, Junevik K, Lindahl A & Brisby H. Identification of Cell Proliferation Zones, Progenitor Cells and a Potential Stem Cell Niche in the Intervertebral Disc Region: A Study in Four Species. *Spine (Phila. Pa. 1976).* **34,** 2278- 87 (2009).

18. Illien-Jünger S1, Pattappa G, Peroglio M, Benneker LM, Stoddart MJ, Sakai D, Mochida J, Grad S & Alini M. Homing of Mesenchymal Stem Cells in Induced Degenerative Intervertebral Discs in a Whole Organ Culture System. *Spine (Phila. Pa. 1976).* **37,** 1865-73 (2012).

19. McCann MR, Tamplin OJ, Rossant J & Séguin CA. Tracing notochord-derived cells using a Noto-cre mouse: implications for intervertebral disc development. *Dis. Model. Mech.* **5,** 73–82 (2012).

20. Wilkinson DG, Bhatt S & Herrmann BG. Expression pattern of the mouse T gene and its role in mesoderm formation. *Nature.* **343**, 657-9 (1990).

21. Herrmann BG. Expression pattern of the Brachyury gene in whole-mount embryos mutant. *Development.* **917,** 913–917 (1991).

.22. Gluecksohn-Schoenheimer, S. The development of normal and homozygous brachy (T/T) mouse embryos in the extraembryonic coelom of the chick. *Proc Natl Acad Sci U S A.* **30**, 134-40. (1944).

23. Pennimpede T, Proske J, König A, Vidigal JA, Morkel M, Bramsen JB, Herrmann BG & Wittler L. In vivo knockdown of Brachyury results in skeletal defects and urorectal malformations resembling caudal regression syndrome. *Dev Biol.* **372,** 55–67 (2012).

24. Tang X, Jing L & Chen J. Changes in the Molecular Phenotype of Nucleus Pulposus Cells with Intervertebral Disc Aging. *PLoS One*. **7,** e52020 (2012).

25. Ghebranious N, Blank RD, Raggio CL, Staubli J, McPherson E, Ivacic L, Rasmussen K, Jacobsen FS, Faciszewski T, Burmester JK, Pauli RM, Boachie-Adjei O, Glurich I & Giampietro PF. A Missense T (Brachyury) Mutation Contributes to Vertebral Malformations. *J Bone Miner Res.* **23,** 1576–1583 (2008).

26. Bundya J, Rogersa R, Hoffman S & Conwaya SJ. Segmental expression of aggrecan in the non-segmented perinothochordal sheath underlines normal segmentation of the vertebral column. *Mech Dev.* **79,** 213–217 (1998).

27. Urban JP & Roberts S. Degeneration of the intervertebral disc. *Arthritis Res Ther.* **5,** 120-30 (2003).

28. Sive JI, Baird P, Jeziorsk M, Watkins A, Hoyland JA & Freemont AJ. Expression of chondrocyte markers by cells of normal and degenerate intervertebral discs. *Mol Pathol*. **55**, 91–98 (2002).

29. Sekiya I. SOX9 Enhances Aggrecan Gene Promoter/Enhancer Activity and Is Up-regulated by Retinoic Acid in a Cartilage-derived Cell Line, TC6. *J. Biol. Chem.* **275,** 10738–10744 (2000).

30. Barrionuevo F, Taketo MM, Scherer G & Kispert A. Sox9 is required for notochord maintenance in mice. *Dev. Biol.* **295,** 128–40 (2006).

31. Smits P. Sox5 and Sox6 are required for notochord extracellular matrix sheath formation, notochord cell survival and development of the nucleus pulposus of intervertebral discs. *Development.* **130,** 1135–1148 (2003).

32. Besnard V1, Wert SE, Hull WM & Whitsett JA. Immunohistochemical localization of Foxa1 and Foxa2 in mouse embryos and adult tissues. *Gene Expr. Patterns.* **5,** 193–208 (2004).

33. Maier JA, Lo Y & Harfe BD. Foxa1 and Foxa2 are required for formation of the intervertebral discs. *PLoS One.* **8,** e55528 (2013).

34. Tang X, Jing L & Chen J. Changes in the Molecular Phenotype of Nucleus Pulposus Cells with Intervertebral Disc Aging. *PLoS One*. **7,** e52020 (2012).

35. Fujita N, Miyamoto T, Imai J, Hosogane N, Suzuki T, Yagi M, Morita K, Ninomiya K, Miyamoto K, Takaishi H, Matsumoto M, Morioka H, Yabe H, Chiba K, Watanabe S, Toyama Y & Suda T. CD24 is expressed specifically in the nucleus pulposus of intervertebral discs. *Biochem. Biophys. Res. Commun.* **338,** 1890–6 (2005).

36. Visel A, Thaller C & Eichele G. GenePaint.org: an atlas of gene expression patterns in the mouse embryo. *Nucleic Acids Res.* **32,** D552–6 (2004).

37. Diez-Roux G, Banfi S, Sultan M, Geffers L, Anand S, Rozado D, Magen A, Canidio E, Pagani M, Peluso I, Lin-Marq N, Koch M, Bilio M, Cantiello I, Verde R, De Masi C, Bianchi SA, Cicchini J, Perroud E, Mehmeti S, Dagand E, Schrinner S, Nürnberger A, Schmidt K, Metz K, Zwingmann C, Brieske N, Springer C, Hernandez AM, Herzog S, Grabbe F, Sieverding C, Fischer B, Schrader K, Brockmeyer M, Dettmer S, Helbig C, Alunni V, Battaini MA, Mura C, Henrichsen CN, Garcia-Lopez R, Echevarria D, Puelles E, Garcia-Calero E, Kruse S, Uhr M, Kauck C, Feng G, Milyaev N, Ong CK, Kumar L, Lam M, Semple CA, Gyenesei A, Mundlos S, Radelof U, Lehrach H, Sarmientos P, Reymond A, Davidson DR, Dollé P, Antonarakis SE, Yaspo ML, Martinez S, Baldock RA, Eichele G & Ballabio A. A high-resolution anatomical atlas of the transcriptome in the mouse embryo. *PLoS Biol.* **9,** e1000582 (2011).

38. Power KA, Grad S, Rutges JP, Creemers LB, van Rijen MH, O'Gaora P, Wall JG, Alini M, Pandit A & Gallagher WM. Identification of cell surface-specific markers to target human nucleus pulposus cells: expression of carbonic anhydrase XII varies with age and degeneration. *Arthritis Rheum.* **63,** 3876–86 (2011).

39. Yamaguchi T, Suzuki S, Ishiiwa H & Ueda Y. Intraosseous benign notochordal cell tumours: overlooked precursors of classic chordomas. *Histopathology.* **44**, 597–602 (2004).

40. Deshpande V, Nielsen GP, Rosenthal DI & Rosenberg AE. Intraosseous benign notochord cell tumors (BNCT): further evidence supporting a relationship to chordoma. *Am. J. Surg. Pathol.* **31,** 1573–7 (2007).

41. Kyriakos M, Totty WG & Lenke LG. Case Report Giant Vertebral Notochordal Rest A Lesion Distinct From Chordoma: Discussion of an Evolving Concept. *Am J Surg Pathol.* **27,** 396–406 (2003).

42. Yamaguchi T, Yamato M & Saotome K. First histologically confirmed case of a classic chordoma arising in a precursor benign notochordal lesion: differential

diagnosis of benign and malignant notochordal lesions. *Skeletal Radiol.* **31,** 413–8 (2002).

43. Yamaguchi T, Watanabe-Ishiiwa H, Suzuki S, Igarashi Y & Ueda Y. Incipient chordoma: a report of two cases of early-stage chordoma arising from benign notochordal cell tumors. *Mod. Pathol.* **18,** 1005–10 (2005).

44. Amer HZ & Hameed M. Intraosseous benign notochordal cell tumor. *Arch. Pathol. Lab. Med.* **134,** 283–8 (2010).

45. Lehtonen E, Stefanovic V & Saraga-Babic M. Changes in the expression of intermediate filaments and desmoplakins during development of human notochord. *Differentiation.* **59,** 43–9 (1995).

46. Salisbury JR. Demonstration of cytokeratins and an epithelial membrane antigen in chondroid chordoma. *J. Pathol.* **153,** 37–40 (1987).

47. Nakamura Y, Becker LE & Marks A. S100 protein in human chordoma and human and rabbit notochord. *Arch. Pathol. Lab. Med.* **107,** 118–120 (1983).

48. Brüderlein S, Sommer JB, Meltzer PS, Li S, Osada T, Ng D, Möller P, Alcorta DA & Kelley MJ. Molecular Characterization of Putative Chordoma Cell Lines. *Sarcoma*. **2010,** 630129 (2010).

49. Ostroumov E & Hunter CJ. Identifying Mechanisms for Therapeutic Intervention in Chordoma: c-Met Oncoprotein. *Spine (Phila. Pa. 1976)*. **33,** 2774-80 (2008).

50. Ostroumov E & Hunter CJ. The role of extracellular factors in human metastatic chordoma cell growth in vitro. *Spine (Phila. Pa. 1976)*. **32,** 2957–64 (2007).

51. Ricci-Vitiani L, Lombardi DG, Pilozzi E, Biffoni M, Todaro M, Peschle C & De Maria R. Identification and expansion of human colon-cancer-initiating cells. *Nature.* **445,** 111–5 (2007).

52. Zhang DZ, Ma BA, Fan QY, Chang H & Wen YH. Establishment and characteristics of a human chordoma cell line. *Zhonghua Zhong Liu Za Zhi.* **25,** 234–7 (2003).

53. Scheil S, Brüderlein S, Liehr T, Starke H, Herms J, Schulte M & Möller P. Genome-wide analysis of sixteen chordomas by comparative genomic hybridization and cytogenetics of the first human chordoma cell line, U-CH1. *Genes. Chromosomes Cancer.* **32,** 203–11 (2001).

54. Rinner B, Froehlich EV, Buerger K, Knausz H, Lohberger B, Scheipl S, Fischer C, Leithner A, Guelly C, Trajanoski S, Szuhai K & Liegl B. Establishment and detailed functional and molecular genetic characterisation of a novel sacral chordoma cell line, MUG-Chor1. *Int. J. Oncol.* **40,** 443–51 (2012).

55. Presneau N, Shalaby A, Ye H, Pillay N, Halai D, Idowu B, Tirabosco R, Whitwell D, Jacques TS, Kindblom LG, Brüderlein S, Möller P, Leithner A, Liegl B, Amary FM, Athanasou NN, Hogendoorn PC, Mertens F, Szuhai K & Flanagan AM. Role of the transcription factor T (brachyury) in the pathogenesis of sporadic chordoma: a genetic and functional-based study. *J. Pathol.* **223,** 327–35 (2011).

56. Jiang WG, Watkins G, Fodstad O, Douglas-Jones A, Mokbel K & Mansel RE. Differential expression of the CCN family members Cyr61, CTGF and Nov in human breast cancer. *Endocr Relat Cancer*. **11**, 781–791 (2004).

57. Bornstein P. Matricellular proteins : an overview. *J Cell Commun Signal*. **3**, 163–165 (2009).

58. Leask A & Abraham DJ. All in the CCN family : essential matricellular signaling modulators emerge from the bunker. *J Cell Sci.* **119**, 4803-10. (2006).

59. Zuo GW, Kohls CD, He BC, Chen L, Zhang W, Shi Q, Zhang BQ, Kang Q, Luo J, Luo X, Wagner ER, Kim SH, Restegar F, Haydon RC, Deng ZL, Luu HH, He TC & Luo Q. The CCN proteins: important signaling mediators in stem cell differentiation and tumorigenesis. *Histol Histopathol.* **25,** 795–806 (2011).

60. Chong HC, Tan CK, Huang RL & Tan NS. Matricellular proteins: a sticky affair with cancers. *J. Oncol.* **2012,** 351089 (2012).

61. Leask A. A sticky situation: CCN1 promotes both proliferation and apoptosis of cancer cells. *J. Cell Commun. Signal.* **4,** 71–2 (2010).

62. Franzen CA, Chen CC, Todorović V, Juric V, Monzon RI & Lau LF. The matrix protein CCN1 is critical for prostate carcinoma cell proliferation and TRAIL-induced apoptosis. *Mol Cancer Res.* **7,** 1045–1055 (2010).

63. Haque I, Mehta S, Majumder M, Dhar K, De A, McGregor D, Van Veldhuizen PJ, Banerjee SK & Banerjee S. Cyr61/CCN1 signaling is critical for epithelial-mesenchymal transition and stemness and promotes pancreatic carcinogenesis. *Mol. Cancer.* **10,** 8 (2011).

64. Espinoza I, Menendez JA, Kvp CM & Lupu R. CCN1 promotes vascular endothelial growth factor secretion through αvβ 3 integrin receptors in breast cancer. *J. Cell Commun. Signal.* **1**, 23-7 (2013).

65. Tsai MS, Bogart DF, Castañeda JM, Li P & Lupu R. Cyr61 promotes breast tumorigenesis and cancer progression. *Oncogene.* **21,** 8178–85 (2002).

66. Chang CC, Yang MH, Lin BR, Chen ST, Pan SH, Hsiao M, Lai TC, Lin SK, Jeng YM, Chu CY, Chen RH, Yang PC, Chin YE & Kuo ML. CCN2 inhibits lung cancer metastasis through promoting DAPK-dependent anoikis and inducing EGFR degradation. *Cell Death Differ.* **20,** 443–55 (2013).

67. Garcia P, Leal P, Ili C, Brebi P, Alvarez H & Roa JC. Inhibition of connective tissue growth factor (CTGF/CCN2) in gallbladder cancer cells leads to decreased growth in vitro. *Int. J. Exp. Pathol.* **94,** 195–202 (2013).

68. Lu H, Kojima K, Battula VL, Korchin B, Shi Y, Chen Y, Spong S, Thomas DA, Kantarjian H, Lock RB, Andreeff M & Konopleva M. Targeting connective tissue growth factor (CTGF) in acute lymphoblastic leukemia preclinical models: anti-

CTGF monoclonal antibody attenuates leukemia growth. *Ann. Hematol.* **93**, 485-92. (2013).

69. Chien W, O'Kelly J, Lu D, Leiter A, Sohn J, Yin D, Karlan B, Vadgama J, Lyons KM & Koeffler HP. Expression of connective tissue growth factor (CTGF/CCN2) in breast cancer cells is associated with increased migration and angiogenesis. **38,** 1741–1747 (2013).

70. Shimo T, Kubota S, Yoshioka N, Ibaragi S, Isowa S, Eguchi T, Sasaki A & Takigawa M. Pathogenic Role of Connective Tissue Growth Factor (CTGF/CCN2) in Osteolytic Metastasis of Breast Cancer. *J Bone Miner Res*. **21**, 1045-59 (2006).

71. Bennewith KL, Huang X, Ham CM, Graves EE, Erler JT, Kambham N, Feazell J, Yang GP, Koong A & Giaccia AJ. The role of tumor cell-derived connective tissue growth factor (CTGF/CCN2) in pancreatic tumor growth. *Cancer Res.* **69,** 775–84 (2009).

72. Yang AT, Wang P, Tong XF, Cong M, Liu TH, Cong R, Wu P, Jia JD, Wang BE & You H. Connective tissue growth factor induces hepatic progenitor cells to differentiate into hepatocytes. *Int J Mol Med.* **32,** 35–42 (2013).

73. Lee CH, Shah B, Moioli EK & Mao JJ. CTGF directs fibroblast differentiation from human mesenchymal stem/stromal cells and defines connective tissue healing in a rodent injury model. *J Clin Invest.* **120,** 3340-9 (2010).

74. Chen PC, Cheng HC & Tang CH. CCN3 promotes prostate cancer bone metastasis by modulating the tumor-bone microenvironment through RANKL-dependent pathway. *Carcinogenesis.* **34,** 1669–79 (2013).

75. Chen PC, Lin TH, Cheng HC & Tang CH. CCN3 increases cell motility and ICAM-1 expression in prostate cancer cells. *Carcinogenesis* **33,** 937–45 (2012).

76. Ouellet V, Tiedemann K, Mourskaia A, Fong JE, Tran-Thanh D, Amir E, Clemons M, Perbal B, Komarova SV & Siegel PM. CCN3 impairs osteoblast and stimulates osteoclast differentiation to favor breast cancer metastasis to bone. *Am. J. Pathol.* **178,** 2377–88 (2011).

77. Gupta N, Wang H, McLeod TL, Naus CC, Kyurkchiev S, Advani S, Yu J, Perbal B & Weichselbaum RR. Inhibition of glioma cell growth and tumorigenic potential by CCN3 (NOV). *Mol. Pathol.* **54,** 293–9 (2001).

78. Tzeng HE, Chen JC, Tsai CH, Kuo CC, Hsu HC, Hwang WL, Fong YC & Tang CH. CCN3 increases cell motility and MMP-13 expression in human chondrosarcoma through integrin-dependent pathway. *J. Cell. Physiol.* **226,** 3181–9 (2011).

79. Dhar G, Mehta S, Banerjee S, Gardner A, McCarty BM, Mathur SC, Campbell DR, Kambhampati S & Banerjee SK. Loss of WISP-2/CCN5 signaling in human pancreatic cancer: a potential mechanism for epithelial-mesenchymal-transition. *Cancer Lett.* **254,** 63–70 (2007).

80. Banerjee SK & Banerjee S. CCN5/WISP-2: A micromanager of breast cancer progression. *J. Cell Commun. Signal.* **6,** 63–71 (2012).

81. Yang, XR, Ng D, Alcorta DA, Liebsch NJ, Sheridan E, Li S, Goldstein AM, Parry DM & Kelley MJ. T (Brachyury) gene duplication confers major susceptibility to familial chordoma. *Nat. Genet.* **41,** 1176–1178 (2010).

82. Nelson AC, Pillay N, Henderson S, Presneau N, Tirabosco R, Halai D, Berisha F, Flicek P, Stemple DL, Stern CD, Wardle FC & Flanagan AM. An integrated functional genomics approach identifies the regulatory network directed by brachyury (T) in chordoma. *J Pathol*. **228**, 274–285 (2012).

83. Bedore J, Sha W, McCann MR, Liu S, Leask A & Séguin CA. Impaired Intervertebral Disc Development and Premature Disc Degeneration in Mice With Notochord-Specific Deletion of CCN2. *Arthritis Rheum.* **65,** 2634–2644 (2013).

84. Tamplin OJ, Cox BJ & Rossant J. Integrated microarray and ChIP analysis identifies multiple Foxa2 dependent target genes in the notochord. *Dev. Biol.* **360,** 415–25 (2011).

85. Erwin WM, Ashman K, O'Donnel P & Inman RD. Nucleus pulposus notochord cells secrete connective tissue growth factor and up-regulate proteoglycan expression by intervertebral disc chondrocytes. *Arthritis Rheum.* **54,** 3859–67 (2006).

86. Chiou M, Chao T, Wu J, Kuo C & Chen J. The physiological role of CTGF/CCN2 in zebrafish notochond development and biological analysis of the proximal promoter region. *Biochem Biophys Res Commun.* **349,** 750–758 (2006).

87. Ali R, Le Maitre CL, Richardson SM, Hoyland JA & Freemont AJ. Connective tissue growth factor expression in human intervertebral disc: implications for angiogenesis in intervertebral disc degeneration. *Biotech. Histochem.* **83,** 239–45 (2008).

88. Peng B, Chen J, Kuang Z, Li D, Pang X & Zhang X. Expression and Role of Connective Tissue Growth Factor in Painful Disc Fibrosis and Degeneration. *Spine (Phila. Pa. 1976).* **34,** E178-82 (2009).

89. McKeown SR. Defining normoxia, physoxia and hypoxia in tumours-implications for treatment response. *Br. J. Radiol.* **87,** 20130676 (2014).

90. Höckel M & Vaupel P. Tumor hypoxia: definitions and current clinical, biologic, and molecular aspects. *J. Natl. Cancer Inst.* **93,** 266–76 (2001).

91. Harris AL. Hypoxia--a key regulatory factor in tumour growth. *Nat. Rev. Cancer* **2,** 38–47 (2002).

92. Gustafsson MV, Zheng X, Pereira T, Gradin K, Jin S, Lundkvist J, Ruas JL, Poellinger L, Lendahl U & Bondesson M. Hypoxia requires notch signaling to maintain the undifferentiated cell state. *Dev. Cell* **9,** 617–28 (2005).

93. Keith B & Simon MC. Hypoxia-inducible factors, stem cells, and cancer. *Cell.* **129,** 465–72 (2007).

94. Tammela T, Enholm B, Alitalo K & Paavonen K. The biology of vascular endothelial growth factors. *Cardiovasc. Res.* **65 ,** 550–563 (2005).

95. Ivanović Z, Bartolozzi B, Bernabei PA, Cipolleschi MG, Rovida E, Milenković P, Praloran V & Dello Sbarba P. Incubation of murine bone marrow cells in hypoxia ensures the maintenance of marrow-repopulating ability together with the expansion of committed progenitors. *Br. J. Haematol.* **108,** 424–9 (2000).

96. Ivanović Z, Dello Sbarba P, Trimoreau F, Faucher JL & Praloran V. Primitive human HPCs are better maintained and expanded in vitro at 1 percent oxygen than at 20 percent. **40,** 1482–1488 (2000).

97. Morrison SJ, Csete M, Groves AK, Melega W, Wold B & Anderson DJ. Culture in reduced levels of oxygen promotes clonogenic sympathoadrenal differentiation by isolated neural crest stem cells. *J. Neurosci.* **20,** 7370–6 (2000).

98. Grayson WL, Zhao F, Bunnell B & Ma T. Hypoxia enhances proliferation and tissue formation of human mesenchymal stem cells. *Biochem. Biophys. Res. Commun.* **358,** 948–53 (2007).

99. Heddleston JM, Li Z, McLendon RE, Hjelmeland AB & Rich JN. The hypoxic microenvironment maintains glioblastoma stem cells and promotes reprogramming towards a cancer stem cell phenotype. *Cell cycle.* **8,** 3274–3284 (2010).

100. Soeda A, Park M, Lee D, Mintz A, Androutsellis-Theotokis A, McKay RD, Engh J, Iwama T, Kunisada T, Kassam AB, Pollack IF & Park DM. Hypoxia promotes expansion of the CD133-positive glioma stem cells through activation of HIF-1alpha. *Oncogene.* **28,** 3949–59 (2009).

101. Li P, Zhou C, Xu L & Xiao H. Hypoxia enhances stemness of cancer stem cells in glioblastoma: an in vitro study. *Int. J. Med. Sci.* **10,** 399–407 (2013).

102. Liang D, Ma Y, Liu J, Trope CG, Holm R, Nesland JM & Suo Z. The hypoxic microenvironment upgrades stem-like properties of ovarian cancer cells. *BMC Cancer.* **12,** 201 (2012).

103. Zhu LL, Wu LY, Yew DT & Fan M. Effects of Hypoxia on the Proliferation and Differentiation of NSCs. *Mol Neurobiol.* **31,** 231–242 (2005).

104. Mamede AC, Abrantes AM, Pedrosa L, Casalta-Lopes JE, Pires AS, Teixo RJ, Gonçalves AC, Sarmento-Ribeiro AB, Maia CJ & Botelho MF. Beyond the limits of oxygen: effects of hypoxia in a hormone-independent prostate cancer cell line. *ISRN Oncol.* **2013,** 918207 (2013).

105. Aydemir E, Bayrak OF, Sahin F, Atalay B, Kose GT, Ozen M, Sevli S, Dalan AB, Yalvac ME, Dogruluk T & Türe U. Characterization of cancer stem-like cells in chordoma. *J Neurosurg.* **116,** 810–820 (2012).

106. Horiguchi H, Sano T, Qian ZR, Hirokawa M, Kagawa N, Yamaguchi T, Hirose T, Nagahiro S. Expression of cell adhesion molecules in chordomas : an immunohistochemical study of 16 cases. *Acta Neuropathol.* **107**, 91–96 (2004).

107. Lohberger B, Rinner B, Stuendl N, Absenger M, Liegl-Atzwanger B, Walzer SM, Windhager R, Leithner A. Aldehyde Dehydrogenase 1 , a Potential Marker for Cancer Stem Cells in Human Sarcoma. *PLoS One.* **7**, e43664 (2012).

108. Hess DA, Wirthlin L, Craft TP, Herrbrich PE, Hohm SA, Lahey R, Eades WC, Creer MH & Nolta JA. Selection based on CD133 and high aldehyde dehydrogenase activity isolates long-term reconstituting human hematopoietic stem cells. *Blood.* **107,** 2162–2169 (2006).

109. Hess DA, Meyerrose TE, Wirthlin L, Craft TP, Herrbrich PE, Creer MH & Nolta JA. Functional characterization of highly purified human hematopoietic repopulating cells isolated according to aldehyde dehydrogenase activity. *Blood*. **104,** 1648–1655 (2004).

110. Cai J, Cheng A, Luo Y, Lu C, Mattson MP, Rao MS & Furukawa K. Membrane properties of rat embryonic multipotent neural stem cells. *J. Neurochem.* **88,** 212–226 (2003).

111. Pearce DJ, Taussig D, Simpson C, Allen K, Rohatiner AZ, Lister TA & Bonnet D. Characterization of cells with a high aldehyde dehydrogenase activity from cord blood and acute myeloid leukemia samples. *Stem Cells.* **23,** 752–60 (2005).

112. Storms RW, Green PD, Safford KM, Niedzwiecki D, Cogle CR, Colvin OM, Chao NJ, Rice HE & Smith CA. Distinct hematopoietic progenitor compartments are delineated by the expression of aldehyde dehydrogenase and CD34. *Blood.* **106,** 95–102 (2005).

113. Corti S, Locatelli F, Papadimitriou D, Donadoni C, Del Bo R, Crimi M, Bordoni A, Fortunato F, Strazzer S, Menozzi G, Salani S, Bresolin N & Comi GP. Transplanted ALDHhiSSClo neural stem cells generate motor neurons and delay disease progression of nmd mice, an animal model of SMARD1. *Hum. Mol. Genet.* **15,** 167–87 (2006).

114. Ginestier C, Hur MH, Charafe-Jauffret E, Monville F, Dutcher J, Brown M, Jacquemier J, Viens P, Kleer CG, Liu S, Schott A, Hayes D, Birnbaum D, Wicha MS & Dontu G. ALDH1 is a marker of normal and malignant human mammary stem cells and a predictor of poor clinical outcome. *Cell stem cell.* **1,** 555–567 (2008).

115. Feldmann G, Dhara S, Bedja D, Beaty R, Mullendore M, Karikai C, Alvarez H, Iacobuzio C, Jimeno A, Gabrielson KL & Matsui W. Blockade of Hedgehog Signaling Inhibits Pancreatic Cancer Invasion and Metastases: A New Paradigm for Combination Therapy in Solid Cancers. *Cancer Res.* **67,** 2187–2196 (2011).

116. Balicki D. Moving forward in human mammary stem cell biology and breast cancer prognostication using ALDH1. *Cell Stem Cell.* **1,** 485–7 (2007).

117. Park SA & Kim HS. F-18 FDG PET/CT evaluation of sacrococcygeal chordoma. *Clin. Nucl. Med.* **33,** 906–8 (2008).

118. Yang C, Hornicek FJ, Wood KB, Schwab JH, Choy E, Iafrate J, Rosenberg A, Nielsen GP, Xavier RJ, Mankin H & Duan Z. Characterization and analysis of human chordoma cell lines. *Spine (Phila Pa 1976).* **35,** 1257–1264 (2013).

119. Risbud MV, Guttapalli A, Stokes DG, Hawkins D, Danielson KG, Schaer TP, Albert TJ & Shapiro IM. Nucleus pulposus cells express HIF-1 alpha under normoxic culture conditions: a metabolic adaptation to the intervertebral disc microenvironment. *J. Cell. Biochem.* **98,** 152–9 (2006).

120. Agrawal A, Guttapalli A, Narayan S, Albert TJ, Shapiro IM & Risbud MV. Normoxic stabilization of HIF-1 alpha drives glycolytic metabolism and regulates aggrecan gene expression in nucleus pulposus cells of the rat intervertebral disk. *Am J Physiol Cell Physiol.* **19107,** 621–631 (2007).

121. Mwale F, Ciobanu I, Giannitsios D, Roughley P, Steffen T & Antoniou J. Effect of Oxygen Levels on Proteoglycan Synthesis by Intervertebral Disc Cells. *Spine (Phila. Pa. 1976).* **36,** E131-8 (2011).

122. Yang SH, Hu MH, Sun YH & Lin FH. Differential phenotypic behaviors of human degenerative nucleus pulposus cells under normoxic and hypoxic conditions: influence of oxygen concentration during isolation, expansion, and cultivation. *Spine J.* **13,** 1590–6 (2013).

123. Risbud MV, Fertala J, Vresilovic EJ, Albert TJ & Shapiro IM. Nucleus Pulposus Cells Upregulate PI3K / Akt and MEK / ERK Signaling Pathways Under Hypoxic Conditions and Resist Apoptosis Induced by Serum Withdrawal. *Spine (Phila. Pa. 1976.)* **30,** 882–889 (2005).

124. Tran CM, Fujita N, Huang BL, Ong JR, Lyons KM, Shapiro IM & Risbud MV. Hypoxia-inducible Factor (HIF) -1alpha and CCN2 Form a Regulatory Circuit in Hypoxic Nucleus Pulposus Cells. *J Biol Chem.* **288**, 12654-66 (2013).

125. Nishida T, Kondo S, Maeda A, Kubota S, Lyons KM & Takigawa M. CCN family 2/connective tissue growth factor (CCN2/CTGF) regulates the expression of Vegf through Hif-1a expression in a chondrocytic cell line, HCS-2/8, under hypoxic condition. *Bone*. **44,** 24–31 (2009).

CHAPTER 2

Investigating Microenvironmental Regulation of Human Chordoma Cell Behaviour

Co-Authorship Statement

Patel P, Brooks C, Seneviratne A, Hess D and Séguin CA. Investigating microenvironmental regulation of human chordoma cell behaviour. (Manuscript submitted to PLOS One, July 2014).

PP: Figs. 2.1, 2.2, 2.3, 2.4, 2.5, 2.6, 2.7, 2.8, and 2.9.

CB: Figs. 2.2, 2.8 and 2.9.

AS: Figs. 2.8 and 2.9.

DH: Figs. 2.8 and 2.9.

PP and CAS contributed to experimental design, and writing of the manuscript.

2.1 Introduction

Chordomas are rare, malignant and locally invasive tumors that originate in bones of the skull and spine and are thought to arise from cellular remnants of the embryonic notochord. These tumors occur most commonly at the base of the skull (32%) and sacrococcygeal region (29%), and less frequently in cervical, thoracic and lumbar vertebrae [1-2]. The cancer typically affects one in one million people each year in the United States, with the median age of diagnosis being 49 for skull-based chordomas and 69 for sacral-based chordomas [1].

During embryonic development, notochord cells act as tissue-specific progenitor cells that give rise to the nucleus pulposus of the intervertebral disc [3-4]; however, during spine formation some of these notochord cells get trapped within bone and are referred to as benign notochord remnants. Since these benign notochord remnants give rise to chordomas [3-9], it can be suggested that factors associated with the regulation of embryonic notochord development may likewise be associated with the development of chordomas. For example, studies have demonstrated that brachyury (T), a factor necessary for the formation and maintenance of the notochord [8-9], is amplified in sporadic chordomas and duplicated in familial chordomas[10-11]. In addition to T, there are various other factors that are involved in normal notochord development such as SOX (sry-type high mobility group box) family members SOX5, SOX6 and SOX9. Studies have shown that all of these members are involved in notochord development and that SOX9 is also expressed in the nucleus pulposus [12-13]. In addition, aggrecan (ACAN) and forkhead box

protein A1 (FOXA1) are also involved in the formation of the notochord [14-15], and ACAN is also a critical component of the nucleus pulposus [16].

There are a limited number of studies that examine the effects of the tumor microenvironment on human chordoma cell biology. Two important components that are often found in the tumor microenvironment are hypoxia and matricellular proteins including CCN proteins. Hypoxic conditions (usually between 1-3% O_2 but vary depending on the type of tumor [17]) often result from inadequate oxygen supply to the tumor, which can be caused by low oxygen tension in arterial blood, limited ability for blood to carry oxygen, reduced tissue perfusion or inconsistencies in blood flow diffusion [18]. Normally, these conditions would be detrimental to cells but cancer cells adapt to these conditions; for example, under hypoxia prostate cancer cells show increased cell proliferation[19], and prostate [19], breast [20] and colon [21] cancer cells display increased migration compared to cells cultured under normoxia. In addition, studies have shown that hypoxia can promote stem and progenitor cell properties in various cancers including glioma and glioblastoma [22] and ovarian cancer cells [23].

Connective tissue growth factor (CCN2) is part of the CCN family of matricellular proteins. CCN2 is expressed in many tissues including the notochord [24] and nucleus pulposus [25] and is important in notochord development [26]. CCN2 also has a role in cancer cell biology and has been shown to promote cell proliferation, colony formation, migration and angiogenesis in a cell type-specific manner [27-28]. CCN2 has also been shown to modulate stem and progenitor cell properties; mesenchymal stem cells

treated with recombinant CCN2 (rCCN2) demonstrated reduced differentiation, whereas the addition of rCCN2 to hepatic progenitor cells promoted hepatocytic differentiation [29-30].

The specific effects of hypoxia and CCN2 on chordoma cells are largely unknown. Studies have demonstrated that a large volume of chordoma tumors are hypoxic [31] and that CCN2 is a direct downstream target of T in chordoma [32]. In this study, we sought to better understand the role of the tumor microenvironment by specifically investigating the effects of hypoxia and CCN2 on the regulation of human chordoma cells using the U-CH1 cell line [33]. Through characterization of gene expression and functional analyses, we demonstrate that exposure of U-CH1 cells to hypoxic conditions or increased levels of CCN2 promoted progenitor-like characteristics specific to the notochordal tissue of origin. Interestingly, exposure of chordoma cells to hypoxia induced more pronounced changes in *in vitro* cell behavior than did exposure of cells to CCN2. We found an additive effect when CCN2 and hypoxia were combined in the cell microenvironment on the expression of a subset of notochord progenitor markers.

2.2 Materials and Methods

2.2.1 Cell lines and cell culture

All experiments were conducted using the previously characterized U-CH1 chordoma cell line [33] obtained from Dr. Michael Kelley (Duke University, North Carolina, United States). Cells were maintained using previously established protocols in IMDM/RPMI (4:1) (Invitrogen, Life Technologies) supplemented with 10% fetal bovine

serum (Invitrogen, Life Technologies) (chordoma media) on 0.1% gelatin coated cell culture plates. U-CH1 cells were maintained until monolayer cultures reached 80-90% confluency, and cells were enzymatically dissociated using 0.25% Trypsin (Gibco, Life Technologies) and plated at a ratio of 1:3-1:6 for cell expansion.

Recombinant human CCN2 (PHG0286, Life Technologies) was resuspended in 0.1% bovine serum albumin in phosphate buffered saline (PBS) (17513F, Lonza); this 11.2 kDa amino acid peptide fragment corresponds to amino acids 253-349 of the full length human CCN2 and contains the cysteine knot domain ($rCCN2_{domain4}$). U-CH1 cells were treated with $rCCN2_{domain4}$ at 50, 100 or 200 ng/mL in IMDM/RPMI (4:1) with 5% FBS.

All cell culture was carried out at 37°C in a humidified atmosphere of 5% CO_2 in either normoxic (20% O_2) or hypoxic (2% O_2) conditions. Cells were maintained for at least 1-2 passages in either normoxia or hypoxia before experiments were performed.

2.2.2 Immunocytochemistry

Monolayer cultures of U-CH1 cells (70-80% confluence) were fixed in 4% paraformaldehyde (37°C) for 10 minutes. Fixed cells were washed three times in 0.2% Triton X-100 in PBS (PBST) and then blocked using 5% species-specific serum in PBST for 30 minutes at room temperatures. Cells were then incubated overnight at 4° C in 5% species-specific serum in PBST containing primary antibodies against human CCN1 (1:200; sc13100, Santa Cruz Biotechnology), CCN2 (1:200; sc14939, Santa Cruz

Biotechnology), CCN3 (1:200); AF1976, R&D Systems), brachyury (1:400; sc17743, Santa Cruz Biotechnology) or HIF1-α (1:200; sc13515, Santa Cruz Biotechnology). Following incubation, cells were washed three times with PBST and incubated with fluorescence conjugated species-specific secondary antibodies (donkey anti-goat IgG (A11055), goat anti-rabbit IgG (A11008) or donkey anti-mouse IgG (A11001), all from Life Technologies) in PBST for 45 minutes at room temperature. Cells were then washed three times with PBST and incubated with 4'-6'-diamino-2-phenylindole (DAPI) at a concentration of 0.001 mg/mL for 20 minutes at room temperature. Cells were then washed twice with PSBT and covered with PBS. Images were obtained with a Leica Microsystems DM1000 fluorescence microscope and Leica Microsystems DFC360FX camera. U-CH1 cells cultured under normoxia or hypoxia were stained in parallel, and images were captured with the same microscope settings (i.e. exposure, gain and intensity) to allow direct comparison, at 10X and 20X lens objective using glass bottom culture dishes (P35G014C, MatTek Corporation). IgG controls were run in parallel with experimental samples to detect non-specific binding.

2.2.3 Real-time PCR

Cells were harvested directly in TRIzol® Reagent (Invitrogen, Life Technologies). Total RNA was extracted according to the manufacturer's protocol and quantified using a NanoDrop 2000 spectrophotometer (Thermo Scientific). For each sample, 0.5 μg RNA was used for cDNA synthesis using iScript Reverse Transcriptase (Bio-Rad Laboratories). Real-time PCR was performed using the Bio-Rad CFX384 system. PCR reactions were run in triplicate using 27 ng of cDNA per reaction and 25

μm forward and reverse primers (sequences provided in Table 1.1) with 2X SsoFast EvaGreen Supermix (Bio-Rad Laboratories). The PCR program was an initial 2 minutes at 95° C for denaturing; 10 seconds at 95° C for denaturing; 20 seconds annealing/elongation at 60° C for a total of 40 cycles. Gene expression was normalized relative to a standard curve (1/5 serial dilution with initial input of 0.1 μg/μL) made from a mixture containing human chordoma cells (U-CH1), human foreskin fibroblast cells and human embryonic stem cell (CA2) RNA in a 2:2:1 ratio. (n=3; N=3-4).

2.2.4 Cell growth assay

U-CH1 cells were plated at a density of 3,430 cells/cm^2 in chordoma media or with rCCN2$_{domain4}$ media in 12-well plates (Nunc, Thermo Scientific) and maintained under either normoxic or hypoxic conditions. Cells were then trypsinized and counted with a hemocytomter using Trypan Blue to exclude non-viable cells (15250, Gibco) in triplicate on a phase contrast light microscope every 24 hours over 8 days (n=3; N=3).

2.2.5 Cell migration assay

U-CH1 cells were plated in chordoma media at 25,714 cells/cm^2 in 12-well plates (Nunc, Thermo Scientific) and maintained under either normoxic or hypoxic conditions. After 24 hours, media was changed to IMDM/RPMI (4:1) with 0.2% FBS to permit cell survival but minimize confounding effects of cell proliferation. After 24 hours, an artificial "scratch wound" was created using a 200 μl pipette tip. Cells were imaged at 0, 12, 24, 36 and 48 hours at the exact location of the scratch. Every 24 hours, cells were

Table 1.1. Primer sequences used for real-time PCR gene expression analysis.

Gene Name	Primer Sequence (5' to 3')
CCN1	Fwd- ACCGCTCTGAAGGGGATCT Rev- ACTGATGTTTACAGTTGGGCTG
CCN2	Fwd- TCCCAAAATCTCCAAGCCTA Rev- GTAATGGCAGGCACAGGTCT
CCN3	Fwd- AGTGATGGTCATTGGGACCTG Rev- CCTCTGGTAGTCTTCAGCTCC
CCN5	Fwd- GCGACCAACTCCACGTCTG Rev- TCCCCTTCCCGATACAGGC
T	Fwd- TGAGACCCAGTTCATAGCGG Rev- TGCTGGTTCCAGGAAGAAGC
CD24	Fwd- CTCCTACCCACGCAGATTTATTC Rev- AGAGTGAGACCACGAAGAGAC
ACAN	Fwd- TGAGGAGGGCTGGAACAAGTACC Rev- GGAGGTGCTAATTGCAGGGAACA
FOXA1	Fwd- GCAATACTCGCCTTACGGCT Rev- TACACACCTTGGTAGTACGCC
CA12	Fwd- TGGCATTCTTGGCATCTGTA Rev- TTGGTGGCTGGCTTGTAAAT
SOX5	Fwd- CAGCCAGAGTTAGCACAATAGG Rev- CTGTTGTTCCCGTCGGAGTT
SOX6	Fwd- TACCTCTACCTCACCACATAAGC Rev- ACATCGGCAAGACTCCCTTTG
SOX9	Fwd- AGCGAACGCACATCAAGAC Rev- CTGTAGGCGATCTGTTGGGG
HIF1A	Fwd- ATCCATGTGACCATGAGGAAATG Rev- TCGGCTAGTTAGGGTACACTTC
VEGFA	Fwd- AGGGCAGAATCATCACGAAGT Rev- AGGGTCTCGATTGGATGGCA
GLUT1	Fwd- GGCCAAGAGTGTGCTAAAGAA Rev- ACAGCGTTGATGCCAGACAG

briefly washed with PBS and media was replaced. Images were exported to ImageJ software and the polygon selection tool was used to calculate the area of new cell migration at each time point. The percentage of wound closure was calculated using the formula "$[(Area_{t\text{-}0h} - Area_{t\text{-}\Delta h})/Area_{t\text{-}0h}] \times 100\%$", as previously reported [34] (n=4; N=4).

2.2.6 Sphere formation assay

U-CH1 cells were plated using standard protocols for sphere formation [35], at 1,500 cells per well in 24-well non-adherent plates (Nunc, Thermo Scientific) and grown for 10 days in serum-free DMEM/F12 (Invitrogen, Life Technologies) supplemented with B27 (1:50 dilution), bFGF (20 ng/mL), EGF (20 ng/mL) and 1% methylcellulose (R&D Systems). For $rCCN2_{domain4}$ experiments, the above media was supplemented with 100 ng/mL rCCN2. Cells were fed every other day with the media added cumulatively (i.e. not aspirated) at each feeding and spheres (defined as ≥ 50 μM) were counted after 10 days. The efficiency of sphere formation (number of spheres per 1000 cells) was calculated, as previously described [35] (N=3-4).

2.2.7 Flow cytometry

U-CH1 cells were harvested from monolayer by enzymatic dissociation in 0.25% Trypsin and resuspended in 10% FBS in PBS. Cells were counted and resuspended at a concentration of 1×10^6 cells/mL in Aldefluor buffer (Stemcell Technologies). 2 μl/mL Aldefluor reagent (Stemcell Technologies) was added to determine aldehyde dehydrogenase (ALDH) activity, with a separate ALDH inhibitor (diethylaminobenzaldehyde (DEAB)) to act as a negative control (Stemcell

Technologies). Samples were incubated for 30 minutes and then centrifuged at 470g for 7 minutes. Media was then aspirated and cells were resuspended in Aldefluor buffer (1×10^6 cells in 200 µl) with fluorochrome-conjugated antibodies specific to human CD90 (Thy-1 membrane glycoprotein) (555596, BD Biosciences), CD105 (endoglin) (562380, BD Biosciences) and CD133 (prominin) (130090826, Miltenyi Biotec) and appropriate IgG controls for 30 minutes. After incubation, 500 µl of Aldefluor buffer was added to each tube and then cells were centrifuged at 470 *g* for 7 minutes. Media was then aspirated to the seam line of tubes and ALDH and cell surface expression was acquired using a LSR II flow cytometer (BD Biosciences) at the London Regional Flow Cytometry Facility, and analyzed on FlowJo software program. U-CH1 cells were also characterized based on side scatter using cluster gating with FlowJo software, as previously described [36]. Both ALDH and antibodies were titrated beforehand to determine the appropriate concentration for experiments. The amount of ALDH and cell surface receptors in experimental samples were then determined using their respective isotype (IgG) controls. The effects of $rCCN2_{domain4}$ were assessed following 6 days of treatment. For these experiments, cells were maintained in chordoma media supplemented with 5% or 10% FBS and 100 ng/mL $rCCN2_{domain4}$.

2.2.8 Statistical analysis

All data was collected and statistical analysis was performed using GraphPad Prism 6.0 Software. An unpaired Student's t test (between 2 groups); 1-way ANOVA (between ≥3 groups; comparing one condition) or 2-way ANOVA (between ≥3 groups; comparing two conditions) with either a Tukey's multiple comparisons test or Dunnett's

test to examine differences compared to a control group were performed on respective experiments.

2.3 Results

2.3.1. Expression of T and matricellular proteins in U-CH1 cells

The expression of the known chordoma marker T and the matricellular proteins CCN1 and CCN2 were first assessed in U-CH1 cells grown using established protocols [37]. Immunocytochemistry demonstrated nuclear localization of T in a subset of U-CH1 cells (both vacuolated and non-vacuolated cell morphologies) (**Figure 2.1A**), which is in keeping with previous reports [38]. It is important to note that vacuolated cells were defined as cells that had more than 2 vacuoles. There were no significant changes in the number of nuclei of cells positive for T under normoxia (20.4 ± 2.1%) compared to hypoxia (22.6 ± 2%). We also found expression of CCN1 and CCN2 (in both vacuolated and non-vacuolated cell morphologies), localized to perinuclear and cytoplasmic region of cells (**Figure 2.1B**). The corresponding IgG controls for cell staining indicated no detection non-specific staining (**Figure 2.2**).

2.3.2. Effects of hypoxia on U-CH1 gene expression

To determine the effects of changes in oxygen levels in the cell microenvironment on the chordoma gene expression profile, U-CH1 cells were grown in either normoxic (20% O_2) or hypoxic (2% O_2) conditions and a panel of genes were investigated. We first assessed expression of CCN family members, specifically *CCN1* [39-40], *CCN2* [41-42], *CCN3* [43-44] and *CCN5* [45-46] which have been implicated in modulating cell proliferation, cell

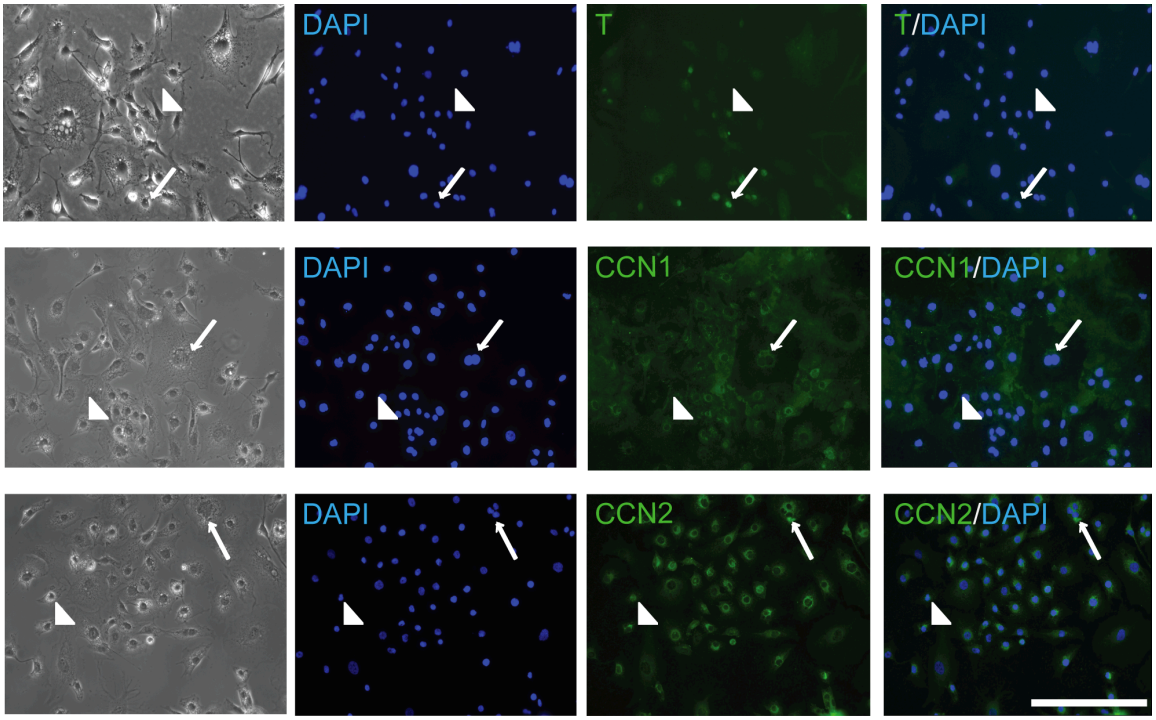

Figure 2.1. Localization of T, CCN1 and CCN2 in U-CH1 cells maintained using established culture protocols. Representative images demonstrate nuclear localization of T and perinuclear and diffuse cytoplasmic localization of CCN1 and CCN2 in U-CH1 cells. Interestingly, protein expression is detected throughout the heterogenous cell population in both vacuolated (arrow) and non-vacuolated (arrowhead) cells. (n=3; N=3; scale bar= 250 μm)

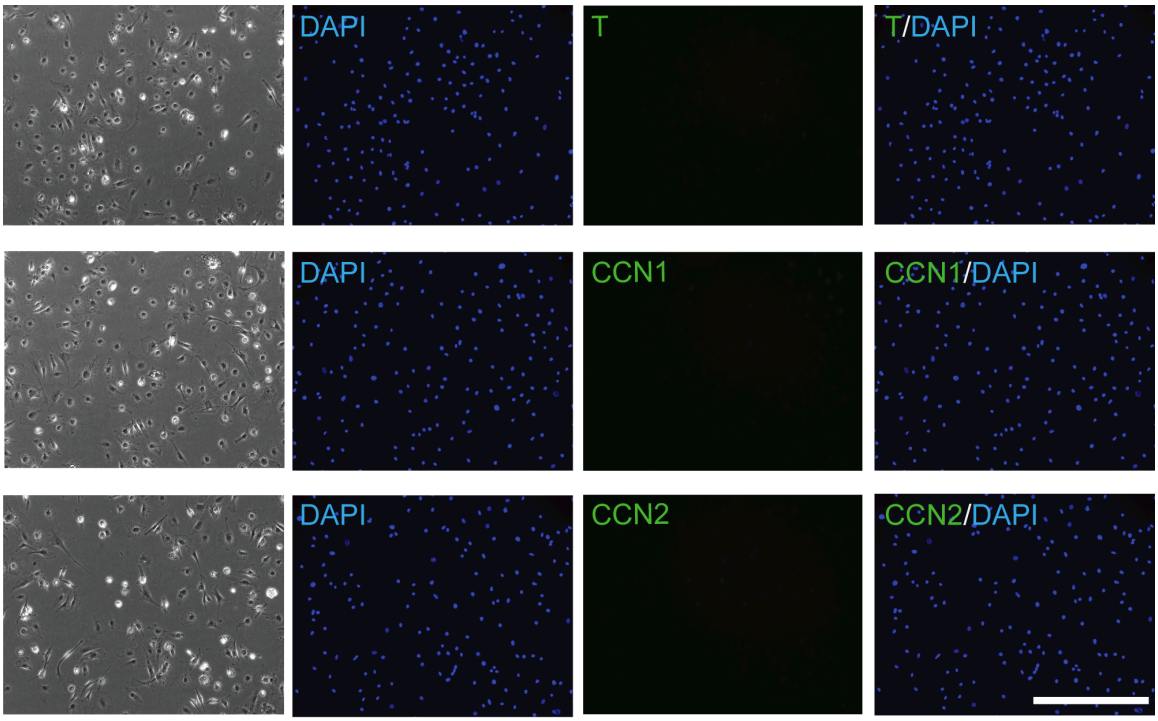

Figure 2.2. IgG controls for immunocytochemistry of T, CCN1, and CCN2 in UCH-1 cells. (n=3; N=3; scale bar = 500 μm)

adhesion, angiogenesis, cell migration, metastasis and epithelial-mesenchymal transition in a variety of cancers. Our results indicate that culture of U-CH1 cells in hypoxia promotes increased expression of *CCN3* and *CCN5* compared to normoxia, while no change in *CCN1* or *CCN2* expression was detected (**Figure 2.3A**). We next investigated the expression of SOX family members *SOX5, SOX6* and *SOX9*. Our results demonstrate that hypoxia induces a significant increase in *SOX6* and and *SOX9* but not *SOX6* expression in U-CH1 cells compared to cells in normoxia (**Figure 2.3B**). In order to determine if the gene expression of early notochord progenitor markers was changed in U-CH1 cells under hypoxic conditions, we examined the expression of *T, CD24, FOXA1, ACAN* and *CA12* (**Figure 2.3C**). Under hypoxia, we found that there was significant up-regulation in the expression of all these markers, with *T* and *CA12* having the most significant increase ($P< 0.001$) followed by *CD24* and *ACAN* ($P<0.01$) and then *FOXA1* ($P<0.05$). Together, these data suggest that hypoxia may be promoting a progenitor-like phenotype in U-CH1 cells. Lastly, to determine if HIF1-α was preferentially activated under hypoxic conditions, we interrogated the expression of *HIF1α* and its downstream targets *VEGF-A* and *GLUT1* (**Figure 2.3D**). Although no change was detected in the expression of *HIF1α*, chordoma cells in hypoxia demonstrated a significant increase in the expression of both *VEGF-A* and *GLUT1* compared to cells in normoxia.

2.3.3. Changes in CCN1 localization under hypoxia

Protein localization in U-CH1 cells maintained in either hypoxic or normoxic conditions was directly compared (**Figure 2.4** and **2.5**). Under hypoxia, CCN1 demonstrated cytoplasmic and cell surface localization compared to cells maintained in

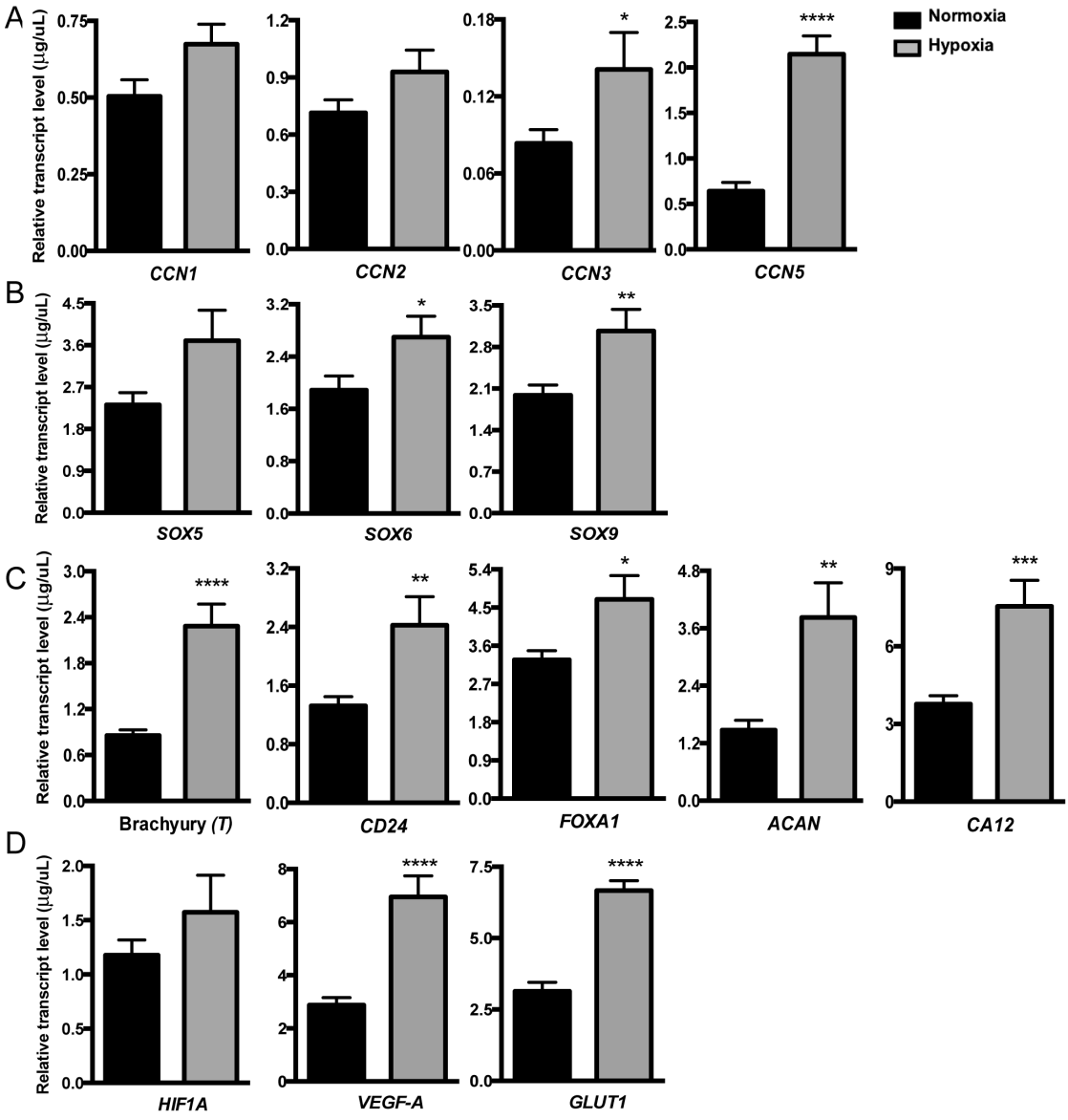

Figure 2.3. Effect of hypoxia on gene expression of U-CH1 cells. Gene expression was assessed in U-CH1 cells maintained in either normoxic (20% O_2) or hypoxic (2% O_2) conditions by real-time PCR. Expression of **(A)** members of the CCN family *(CCN1, CCN2, CCN3, CCN5)*, **(B)** members of the SOX transcription factor family *(SOX5, SOX6, SOX9)*, **(C)** notochord markers *(CD24, T, AGG, FOXA1, CA12)* and **(D)** hypoxia inducible factor (*HIF1A*) and its downstream targets (*VEGF-A, GLUT1*) were investigated. (Unpaired Student's t test; n=3; N=3-4; *= $P \leq 0.05$, **= $P \leq 0.01$, ***=$P \leq 0.001$, ****=$P \leq 0.0001$)

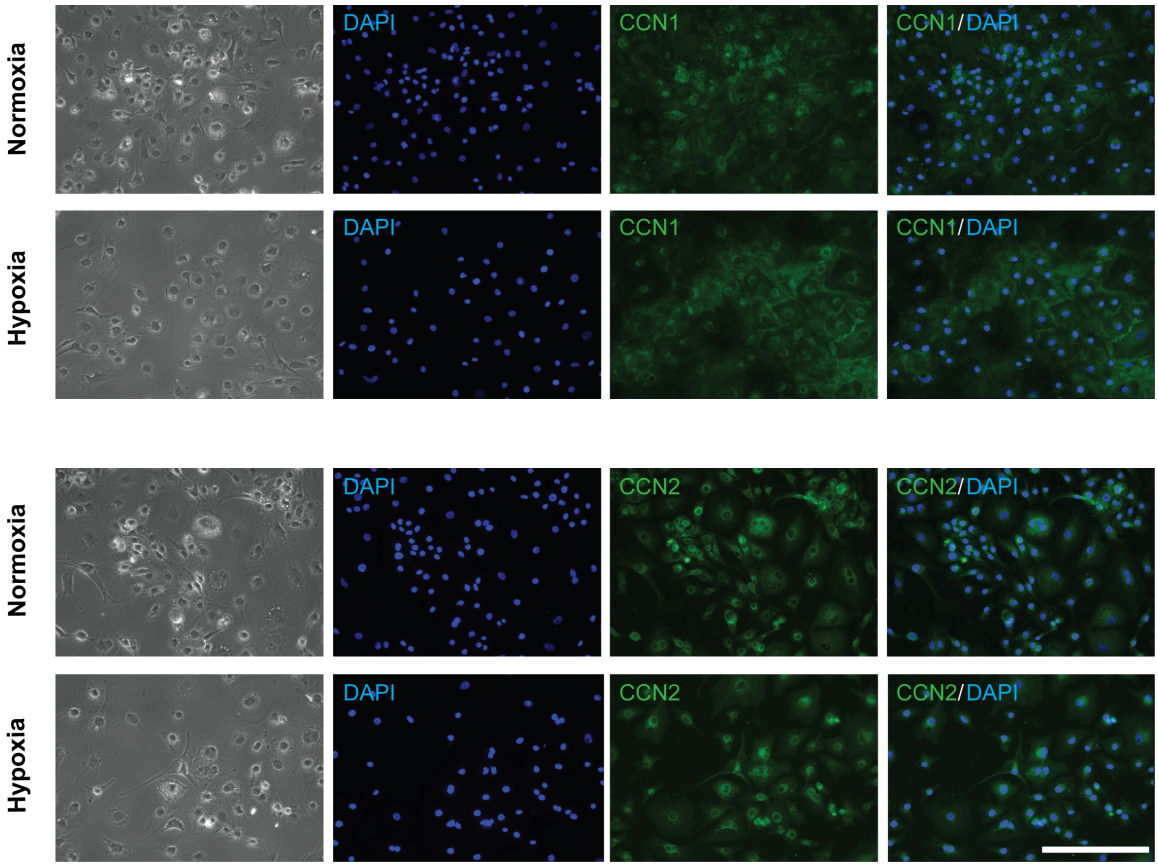

Figure 2.4. Expression and localization of CCN1 and CCN2 in U-CH1 cells maintained under normoxic (20% O_2) or hypoxic (2% O_2) conditions. CCN1 is localized to the perinuclear and cytoplasmic region under normoxia and cytoplasmic and cell surface region of cells under hypoxia. CCN2 is localized to the nuclear and cytoplasmic region under normoxia and hypoxia. (n=3; N=3; scale bar = 250 μm)

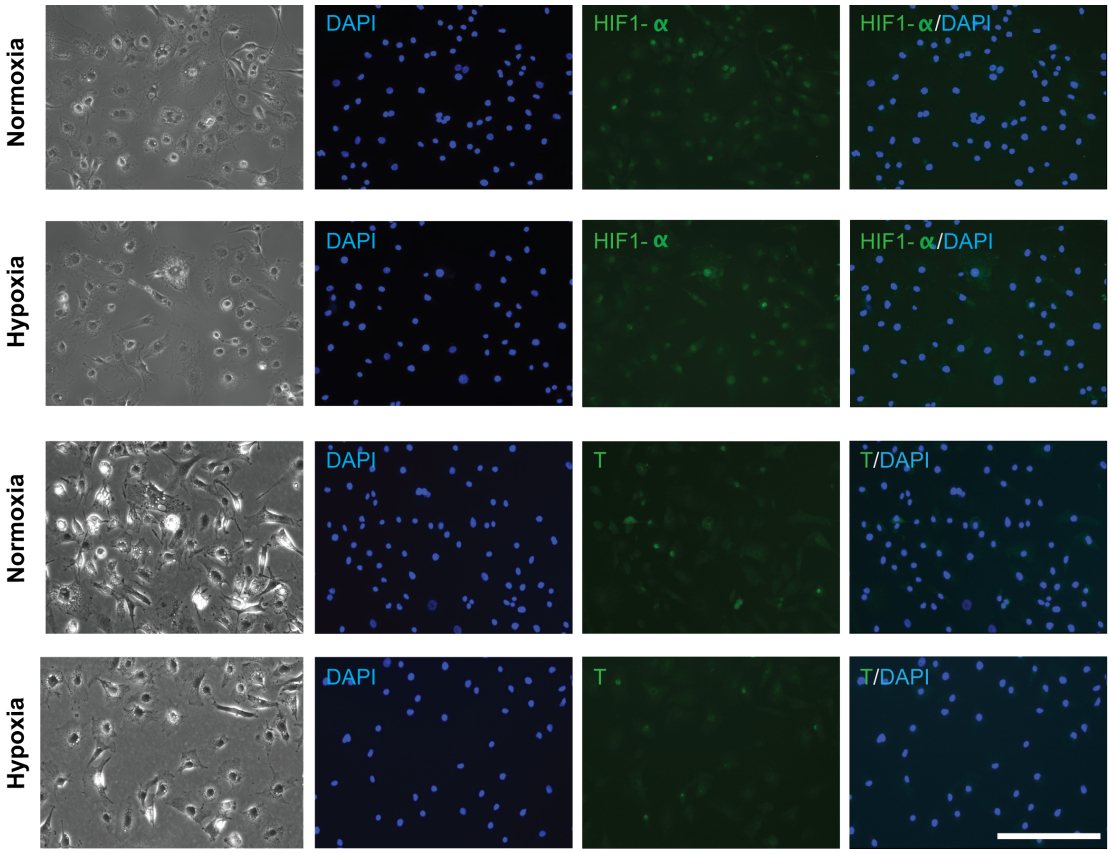

Figure 2.5. Expression and localization of HIF1-α and T in U-CH1 cells maintained under normoxic (20% O_2) or hypoxic (2% O_2) conditions. HIF1-α is primarily localized to nucleus under normoxia and hypoxia. T is localized to the nuclear region under both normoxia and hypoxia (n=3; N=3; scale bar = 250 μm)

normoxia, where CCN1 was localized primarily to the perinuclear region and cytoplasm. HIF1-α was detected primarily in the nucleus of U-CH1 cells under both normoxia and hypoxia. In addition, there were no changes detected in either CCN2 or T localization in U-CH1 cells under normoxia or hypoxia.

2.3.4. Hypoxia promotes U-CH1 cell growth and sphere formation but reduced cell migration

In order to investigate cell growth, U-CH1 cell numbers were counted every 24 hours over 8 days under either normoxic or hypoxic conditions (**Figure 2.6A**). U-CH1 cells demonstrated increased growth in hypoxia compared to normoxia at days 6, 7 and 8. In addition to changes at specific time points, there was also a significant increase in the rate of cell growth under hypoxia compared to normoxia when a linear regression was performed on cell counts plotted on a logarithmic scale. Interestingly, we found that there was no increase in cell growth at days 5 and 6 under normoxia. This was an unusual finding of our study and we suggest that future studies measure apoptosis throughout the assay to determine if it could have contributed to this finding.

To investigate stem-like properties, sphere formation assays were conducted using U-CH1 cells maintained under normoxic or hypoxic conditions (**Figure 2.6B**). Quantification of sphere formation following 10 days of culture demonstrated a significant 10-fold increase in sphere formation in U-CH1 cells maintained under hypoxia compared to normoxia.

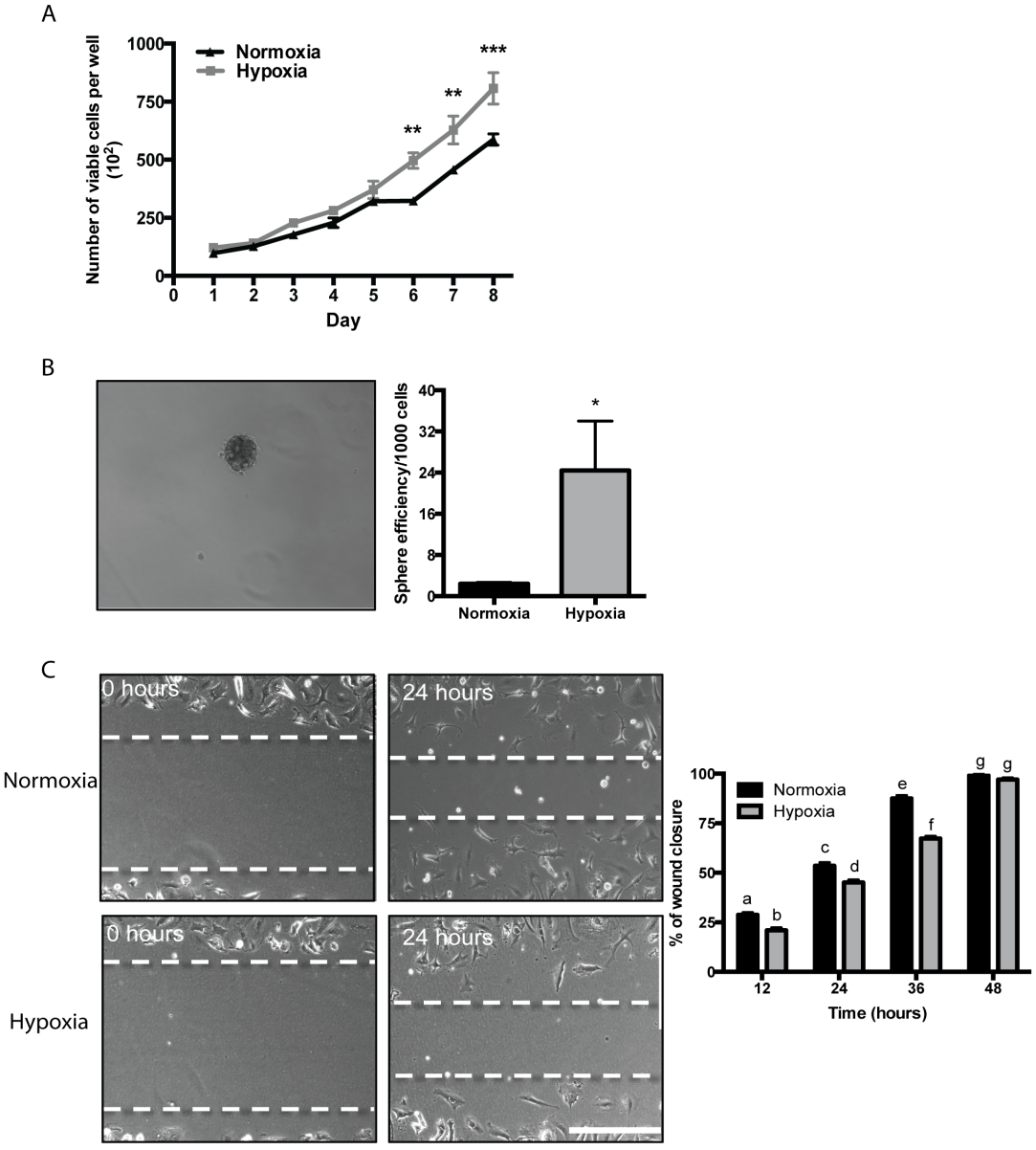

Figure 2.6. Cell growth, migration and sphere formation of U-CH1 cells in normoxic (20% O_2) or hypoxic (2% O_2) conditions. (A) U-CH1 cells were counted every 24 hours over 8 days and demonstrate increased growth in hypoxia versus normoxia at days 6-8 (n=3; N=3). **(B)** U-CH1 cells were grown in suspension and spheres were counted after 10 days. Cells maintained under hypoxic conditions demonstrate a significant increase in sphere formation compared to normoxic conditions (N=3). **(C)** U-CH1 cells were plated and an artificial "scratch wound" was created. Cells were imaged at 12, 24, 36 and 48 hours and the area of new cell migration borders was determined. Maintenance of cells in hypoxia significantly decreased cell migration at 12, 24 and 36 hours compared to cells in normoxia at the same time-point (n=4; N=4). (2-way ANOVA with Tukey's test (A and C); Unpaired Student's t test (B); *= $P \leq 0.05$; **= $P \leq 0.001$; ***= $P \leq 0.0001$; scale bar= 250 μm)

To evaluate changes in U-CH1 cell migration in normoxia compared to hypoxia, a "scratch wound" assay was conducted to quantify cell migration over 48 hours (**Figure 2.6C**). U-CH1 cells maintained under hypoxia demonstrate a significant decrease in migration at 12, 24 and 36 hours compared to cells maintained under normoxia at the same time-points. This difference was no longer apparent at 48 hours, as the majority of the wound appeared to be closed under both conditions. Taken together, these findings suggest that hypoxia could be promoting progenitor-like properties in U-CH1 cells.

2.3.5. 11.2 kDa rCCN2 fragment promotes *ACAN* and *COL2A1* gene expression in U-CH1 cells

Previous studies have demonstrated up-regulation of *ACAN* and *COL2A1* gene expression in nucleus pulposus cells following stimulation with CCN2 [47–49]. In order to ensure bioactivity of $rCCN2_{domain4}$ peptide in U-CH1 cells, we quantified expression of *ACAN* and *COL2A1* in U-CH1 cells following 24 hour treatment with 50, 100 or 200 ng/mL $rCCN2_{domain4}$. Treatment of cells with 100 ng/mL $rCCN2_{domain4}$ resulted in a significant increase in *ACAN* and *COL2A1* under normoxia and hypoxia and treatment with 200 ng/mL $rCCN2_{domain4}$ significantly increased *COL2A1* under normoxia (**Figure 2.7**). We therefore used a concentration of 100 ng/mL of $rCCN2_{domain4}$ for all remaining assays.

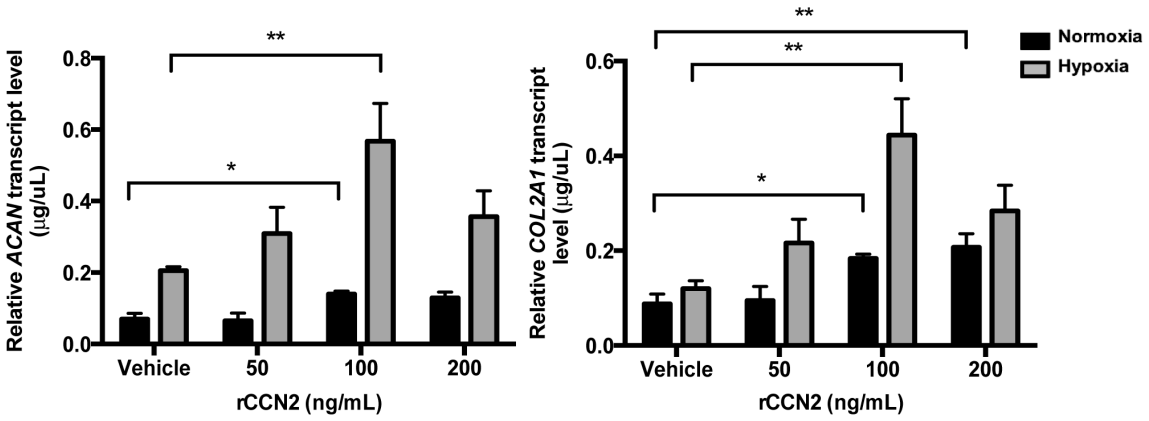

Figure 2.7. Effect of recombinant rCCN2 on *ACAN* and *COL2A1* gene expression in U-CH1 cells maintained under normoxic (20% O_2) or hypoxic (2% O_2) conditions. U-CH1 cells were treated with 50, 100 or 200 ng/mL of rCCN2 for 24 hours and harvested for gene expression analysis. Treatment of cells with 100 ng/mL of $rCCN2_{domain4}$ promoted a significant increase in *ACAN* and *COL2A1* gene expression in cells maintained in normoxia and hypoxia; treatment with 200 ng/mL of $rCCN2_{domain4}$ significantly increased *COL2A1* gene expression under normoxia. (1-way ANOVA with Dunnet's test; n=3; N=3; *= $P \leq 0.05$; **= $P \leq 0.001$)

2.3.6. Effects of $rCCN2_{domain4}$ on U-CH1 gene expression under normoxia and hypoxia

To determine the effects of $rCCN2_{domain4}$ on the chordoma gene expression profile, U-CH1 cells were grown with $rCCN2_{domain4}$ under either normoxic or hypoxic conditions for 24 hours, and a panel of genes was investigated. We first assessed expression of *CCN1, CCN2, CCN3* and *CCN5* and found a significant increase in all of these genes with the addition of $rCCN2_{domain4}$ under either normoxia or hypoxia (**Figure 2.8A**). Interestingly, we noted differences in in the expression levels of CCN family members between vehicle controls and the baseline gene expression presented in Figure 2.2. This may be due to differences in the media used for cell culture, since FBS was reduced from 10% to 5% in rCCN2 treatment conditions.

We also assessed the expression of SOX family members and found a significant increase in *SOX5* and *SOX6* gene expression with the addition of $rCCN2_{domain4}$ under normoxia (**Figure 2.8B**). Lastly, we investigated the expression of early notochord markers *(T, CD24, FOXA1, ACAN* and *CA12)* (**Figure 2.8C**). U-CH1 cells treated with $rCCN2_{domain4}$ in normoxia demonstrated a significant increase in the expression of early notochord development markers (*T, CD24, FOXA1* and *ACAN*) compared to untreated controls. In hypoxia, treatment of U-CH1 cells with $rCCN2_{domain4}$ induced a significant increase in the expression of *T, CD24* and *ACAN*. Interestingly, the combined effect of $rCCN2_{domain4}$ and hypoxia produced an additive response in a subset of gene expression, specifically for *T, CD24* and *ACAN*. Together, these data suggest that $rCCN2_{domain4}$ may

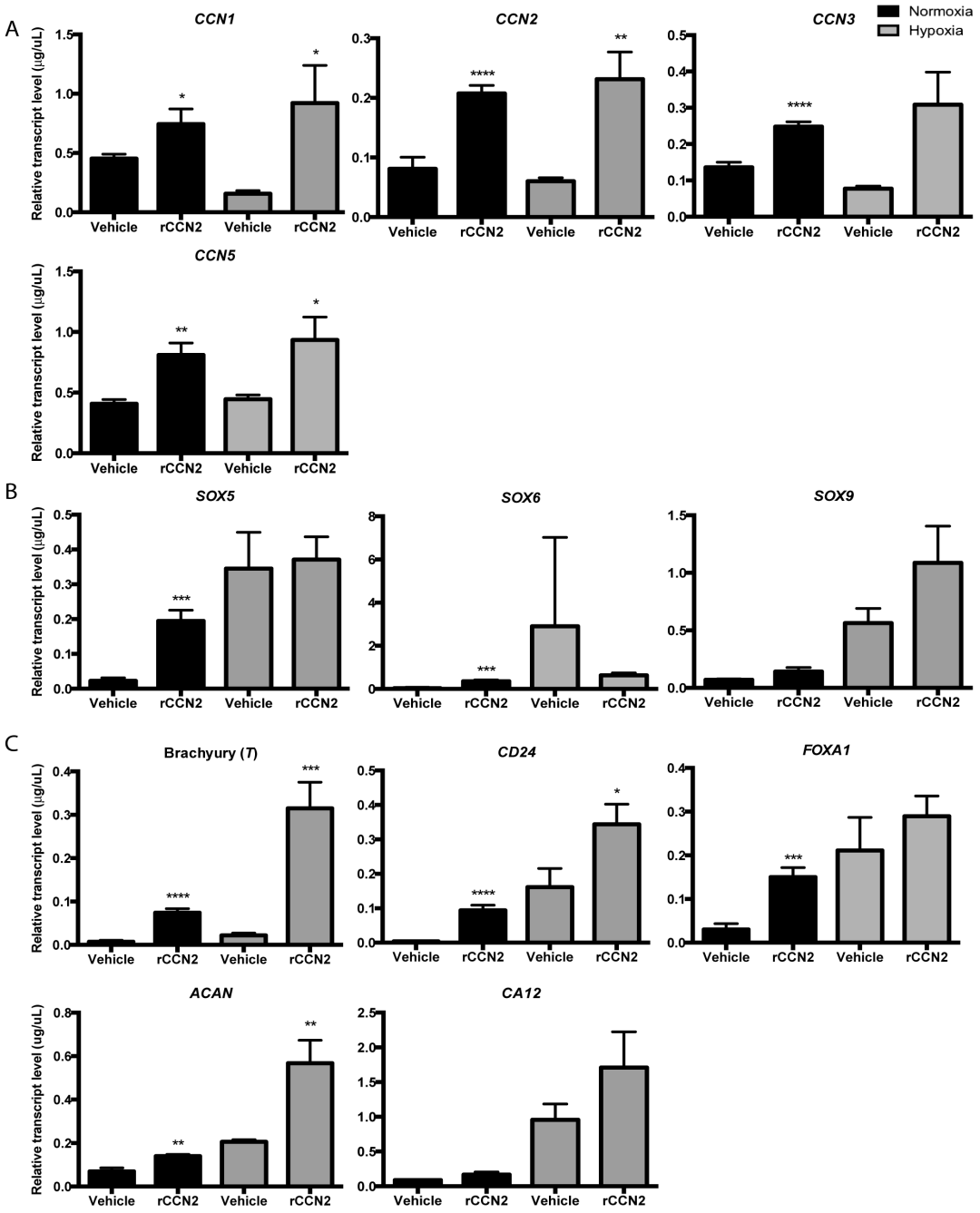

Figure 2.8. Effect of rCCN2$_{domain4}$ **on U-CH1 gene expression in normoxic (20% O_2) and hypoxic (2% O_2) culture environments.** Expression of **(A)** members of the CCN family *(CCN1, CCN2, CCN3, CCN5)*, **(B)** members of the SOX transcription factor family *(SOX5, SOX6, SOX9)* and **(C)** notochord markers *(T, CD24, FOXA1, ACAN, CA12)* were investigated in U-CH1 cells treated with 100 ng/mL of rCCN2 for 24 hours in either normoxic or hypoxic conditions. (Unpaired Student's t test; n=3, N=3; *= $P \leq 0.05$, **= $P \leq 0.01$, ***=$P \leq 0.001$, ****=$P \leq 0.0001$)

be promoting a progenitor-like phenotype in U-CH1 cells, with the effects being more robust under normoxia than hypoxia.

2.3.7. In normoxia rCCN2$_{domain4}$ significantly increases U-CH1 sphere formation but does not increase cell growth

Sphere formation was determined for U-CH1 cells grown in either normoxia or hypoxia with the addition of rCCN2$_{domain4}$ for 10 days. We found a significant 1.7-fold increase in sphere formation with the addition of rCCN2$_{domain4}$ compared to vehicle control in normoxia. In contrast, no changes in the efficiency of sphere formation were observed in the presence of rCCN2$_{domain4}$ in hypoxia (**Figure 2.9A**). We then assessed U-CH1 cell growth in the presence of rCCN2$_{domain4}$ in normoxia, as these culture conditions increased more progenitor markers and sphere formation in U- CH1 cells. Over 8 days, treatment of U-CH1 cells with rCCN2$_{domain4}$ did not alter cell growth (**Figure 2.9B**). We also performed a linear regression analysis of the data plotted on a logarithmic scale and found no changes in the rate of cell growth between U-CH1 cells treated with rCCN2$_{domain4}$ and vehicle control.

2.3.8. Maintenance of U-CH1 cells in hypoxia leads to a decrease in the number of vacuolated cells

To determine if culture of U-CH1 cells in hypoxia or the treatment of cells with rCCN2$_{domain4}$ affected the morphological characteristics of the heterogeneous chordoma cell population, we assessed intracellular complexity (side scatter) of cells by flow cytometry. Recent studies have suggested that non-vacuolated chordoma cells (with low

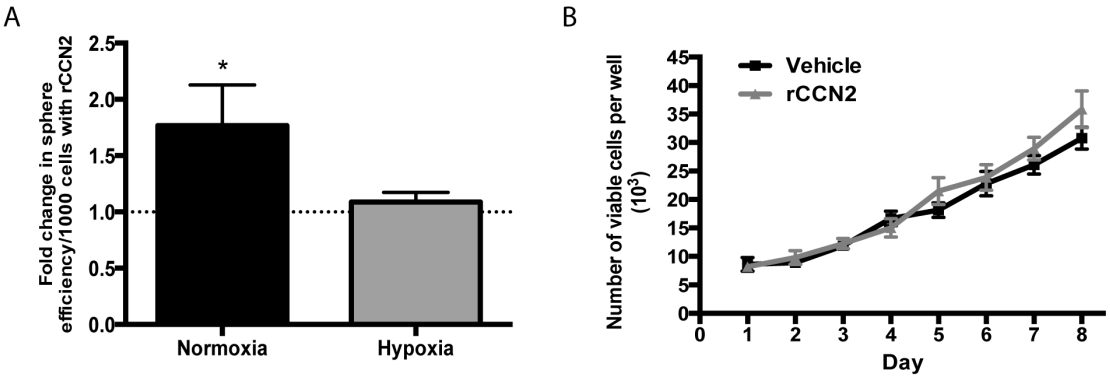

Figure 2.9. Sphere formation and cell growth in U-CH1 cells treated with rCCN2$_{domain4}$. (A) Sphere formation was assessed in U-CH1 cells treated with rCCN2$_{domain4}$ (100 ng/mL) in either normoxic or hypoxic conditions. The efficiency of sphere formation was assessed at day 10 as the number of spheres per 1000 cells. Data is presented as fold change from vehicle control (set to 1; indicated by dashed line) for cells maintained in either normoxic or hypoxic culture conditions. Treatment of cells with rCCN2$_{domain4}$ induced a significant increase in sphere formation compared to vehicle control when cells were maintained in normoxia (N=3-4). **(B)** U-CH1 cells were maintained in normoxic conditions and treated with 100 ng/mL of rCCN2$_{domain4}$ or vehicle control and cell number was quantified every 24 hours over 8 days. No change in cell growth was detected following treatment with rCCN2$_{domain4}$ compared to vehicle control (n=3, N=3). (Unpaired Student's t test (A); 2-way ANOVA with Tukey's test (B); *= $P \leq 0.05$; scale bar= 250 μm)

side scatter profiles) act as progenitor cells that give rise to the larger vacuolated cells (with high side scatter profiles) [50]. We first assessed cell populations maintained in either normoxia or hypoxia and found a significant decrease (*P= 0.03*) in the percentage of vacuolated cells in hypoxia compared to cells maintained in normoxia (3.8 ± 0.6% *vs*. 6.0 ± 0.3%, respectively). Interestingly, the addition of $rCCN2_{domain4}$ did not significantly alter the percentage of U-CH1 cells demonstrating a vacuolated morphology when cells were treated in either normoxia (5.7 ± 0.9 % control *vs*. 5.8 ± 1.1% rCCN2) or hypoxia (3.7 ± 0.6% control vs. 3.9 ± 0.4% rCCN2) (**Figure 2.10A**).

2.3.9. Expression of mesenchymal stromal cell differentiation markers CD90 and CD105 in U-CH1 cells

We next investigated expression of cell surface markers CD90 and CD105, as they have been found highly expressed in U-CH1 cells [57] and act as differentiation markers in mesenchymal stromal cells [58-59]. No significant changes in the percentage of CD90+ or CD105+ U-CH1 cells were detected in normoxic or hypoxic culture conditions or with the addition of $rCCN2_{domain4}$. We found there was a trend towards a decrease in CD90+ U-CH1 cells under normoxia compared to hypoxia (20.1 ± 5.7% in normoxia *vs*. 37 ± 2.5% in hypoxia). In contrast, there was a trend towards an increase in CD105+ UCH-1 cells under normoxia compared to hypoxia (18.7 ± 10.5% in normoxia *vs*. 6.7 ± 1.8% in hypoxia). (**Figure 2.10A and B**).

To investigate if a cancer stem cell population could be detected in U-CH1 cells, the expression of CD133 and the activity of aldehyde dehydrogenase (ALDH) were

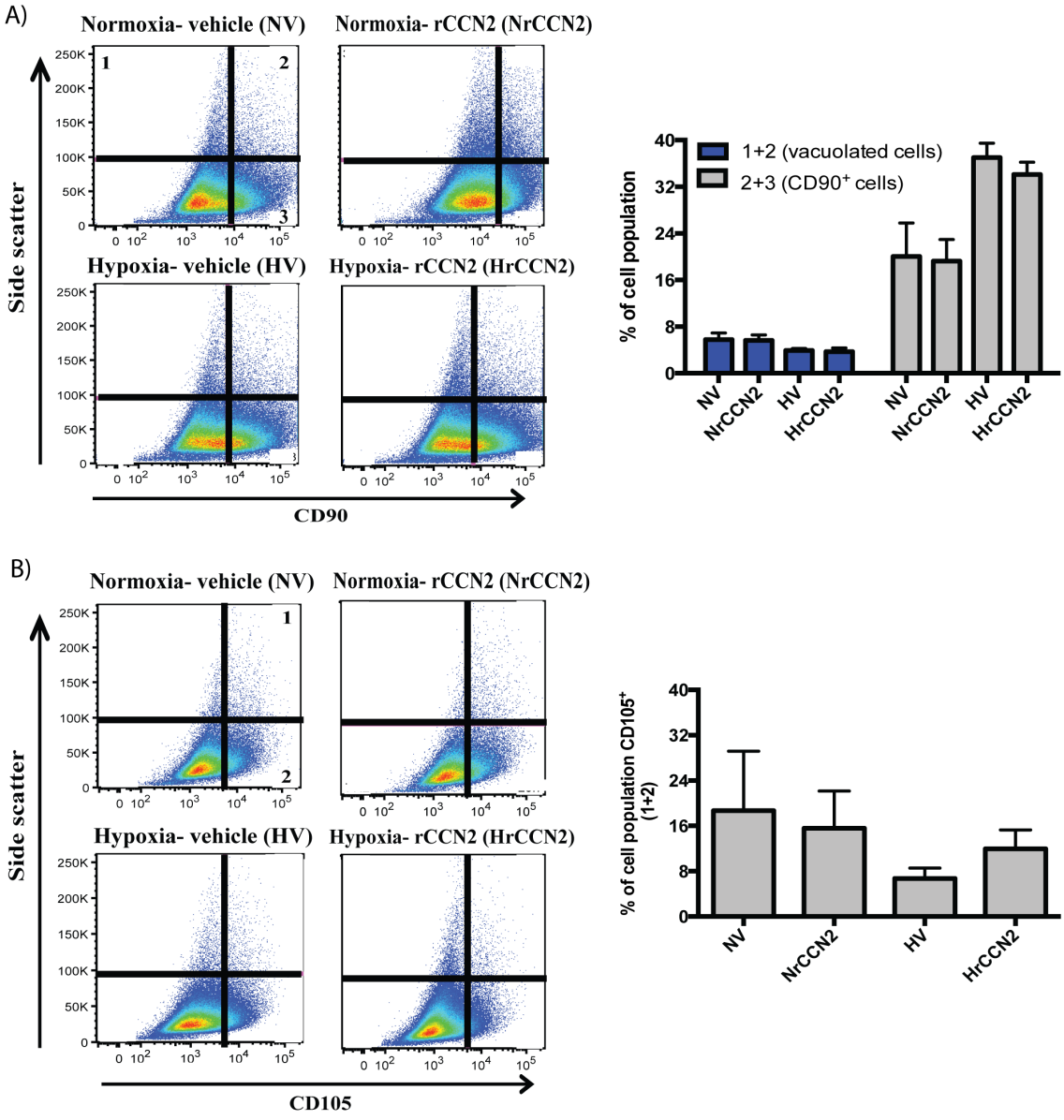

Figure 2.10. Side scatter distributions and expression of cell surface markers CD90 and CD105 in U-CH1 cells maintained in normoxic or hypoxic conditions with or without rCCN2$_{domain4}$ in normoxic (20% O_2) or hypoxic (2% O_2) conditions. (A) Cluster gating was used to determine the intracellular complexity of U-CH1 cells. There was a significant increase in the number of vacuolated cells (side scatter high) under normoxia compared to hypoxia with minimal changes with the addition of rCCN2$_{domain4}$. When placed under normoxia, U-CH1 cells showed a trend towards decreased expression of **(A)** CD90 and increased expression of **(B)** CD105 (N=3).

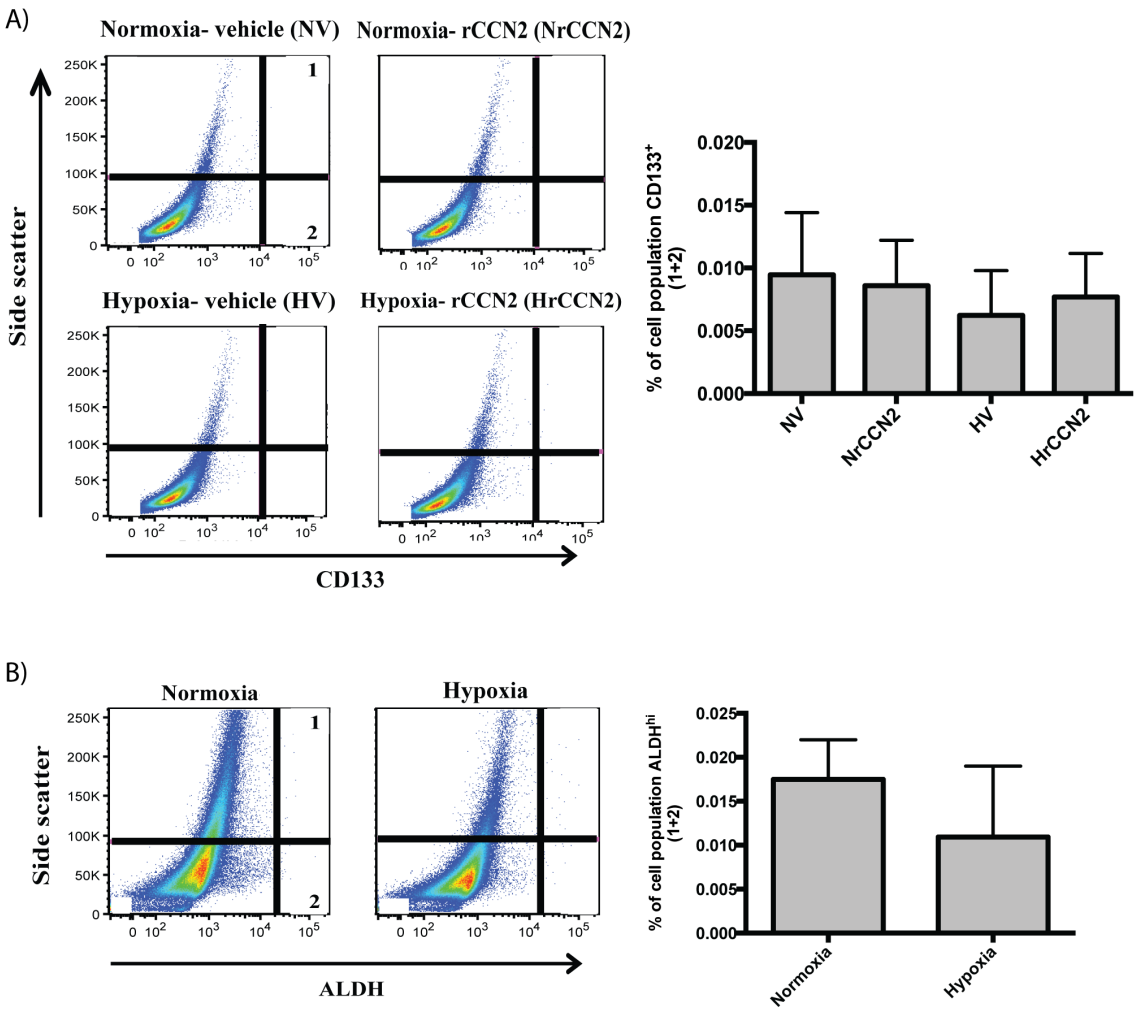

Figure 2.11. Expression of cell surface marker CD133 and ALDH^{hi} activity using rCCN2$_{domain4}$ in normoxic (20% O_2) or hypoxic (2% O_2) conditions. Expression of **(A)** CD133 **and (B)** ALDH^{hi} activity. There was minimal expression of **(A)** CD133 (N=3) and **(B)** ALDH^{hi} activity under all treatment conditions (N=2).

determined as they are common markers of cancer stem cells 51–56. We detected minimal expression of CD133 (>0.01% positive cells) in U-CH1 cells in all culture conditions (Figure 2.11A). Similarly, we detected minimal ALDH activity (>0.02% ALDHhi cells) in U-CH1 cells in all culture conditions (Figure 2.11B).

2.4 Discussion

The tumor microenvironment is a complex environment composed of a variety of different cell types such as cancer cells, stromal fibroblasts, endothelial cells, as well as secreted proteins, oxygen levels and components of the extracellular matrix, including matricellular CCN proteins [60]. The current study investigated the effects of hypoxia and the specific matricellular protein CCN2 on U-CH1 cells, as there is strong indication that these factors could be involved in the regulation of chordoma cell biology [4-5]. In our study, we found that hypoxia had the greatest ability to promote progenitor-like properties in U-CH1 cells compared to the addition of $rCCN2_{domain4}$. We also found the expression of CCN family members in U-CH1 cells and demonstrated their expression to be regulated by the chordoma microenvironment. In addition, we demonstrated that the effects of $rCCN2_{domain4}$ and hypoxia were additive for the expression of a specific subset of notochord progenitor markers.

In this study, we demonstrate the expression of CCN matricellular proteins in U-CH1 cells through immunolocalization and gene expression analysis. To our knowledge, this is the first investigation of *CCN1*, *CCN3* and *CCN5* expression in chordoma and suggests they could have a potential role in chordoma cell biology. Through gene

expression analysis, we found increased expression of *CCN3* and *CCN5* under hypoxia. These findings are in keeping with previous studies that found increased expression of matricellular proteins under hypoxia compared to normoxia. Specifically, *CCN1* and *CCN3* were increased human choriocarcinoma cells [61], *CCN1* was also increased in retinal vascular endothelial cells [62], and *CCN2* was increased in primary tubular epithelial cells [63] under hypoxia compared to normoxia. In addition, we also found localization of CCN1 in the perinuclear and cytoplasmic region of cells, as well as localization of CCN2 in the nucleus and cytoplasmic region under normoxia and hypoxia. Previous studies have shown the localization of CCN1 in nuclei of prostate carcinoma [64], stretched bladder smooth muscle cells [65] and breast cancer cells [66] and CCN2 in melanoma cells [67]. The exact role of CCN proteins within the nucleus remains unknown, and is a future area of study.

When U-CH1 cells were maintained in hypoxia, we found an increase in the expression of early notochord markers (*T, CD24, FOXA1, ACAN* and *CA12*), sphere formation and cell growth. There are currently opposing reports as to the effects of hypoxia on human chordoma cell growth [37, 68]; our finding are consistent with those of Ostroumov *et al*., which reported an increase in cell growth in a primary human chordoma cell line over 5 days under hypoxia compared to normoxia. Further validating a change in U-CH1 cell phenotype in hypoxia, we demonstrated a decrease in the number of vacuolated U-CH1 cells under hypoxia compared to normoxia, which is in keeping with a recent study suggesting that vacuolated cells represent a more differentiated cell type within the heterogeneous U-CH1 cell population [50]. Our findings are well aligned

with studies in other cancers such as in glioma and glioblastoma [22] and ovarian cancer [23], which reported the promotion of stem and progenitor cell properties following culture of cells in hypoxia. Interrogating the expression of CD90 and CD105 demonstrated that these cell surface markers are expressed in U-CH1 cells, and further studies are warranted to determine if they could be used as markers of chordoma cell differentiation.

In hypoxic conditions, cells often demonstrate increased activity of HIF1-α, a transcription factor that binds to hypoxia-response elements to activate the expression of genes involved in a variety of cellular processes including proliferation, angiogenesis, metabolism, apoptosis and the maintenance of an undifferentiated state in cancer cells [69–73]. For example, vascular endothelial growth factor (VEGF) and glucose transporter 1 (GLUT1) are direct downstream targets of HIF1-α involved in angiogenesis and glycolysis, respectively [74]. Under normoxic conditions, the α subunit of the HIF1-α protein is rapidly degraded through hydroxylation of two key proline residues in the oxygen-dependent degradation domain [75]. However, under hypoxic conditions, HIF1-α becomes stabilized and binds to the aryl hydrocarbon receptor nuclear translocator in the nucleus. In our study, we did not detect the induction of *HIF1α* gene expression in U-CH1 cells maintained in hypoxia, however; we detected a significant up-regulation of *VEGF-A* and *GLUT1* gene expression, suggesting increased HIF1-α activity. Studies using ovarian [23] and glioma [73] cancer cells have shown increased HIF1-α expression under hypoxia and future studies should quantify nuclear and cytoplasmic fractions of HIF1-α to directly asssess HIF1-α activity in U-CH1 cells.

Compared to the effects of hypoxia on U-CH1 cells, we found that treatment of cells with exogenous CCN2 induced the expression of fewer notochord markers (*T, CD24, FOXA1* and *ACAN*) and SOX family members (*SOX5* and *SOX6*). To accompany these changes in gene expression, we found an increase in sphere formation but no changes in cell growth. Interestingly, we found that addition of $rCCN2_{domain4}$ to cells grown in hypoxia induced even fewer changes in the expression of notochord progenitor markers, no change in the expression of SOX family members, and did not promote sphere formation. These differences in the effect of exogenous CCN2 treatment in normoxic or hypoxic conditions may be related to the cell-type specific effects of CCN proteins. We demonstrated that U-CH1 cells are more progenitor-like under hypoxia than in normoxia, suggesting that in these conditions, cells may be expressing different integrins, cell surface receptors or CCN binding proteins that mediate CCN2-dependent signalling. Furthermore, recent studies have established an intriguing direct feedback between HIF1-α and CCN2 in related cell types. In chondrocytes, HIF1-α has been shown to directly interact with the *CCN2* promoter and the addition of rCCN2 was shown to increase HIF1-α mRNA and protein levels [75]. In nucleus pulposus cells, the loss of HIF1-α was reported to increase *CCN2* expression [76]. Based on these findings, we speculate there could be interaction between HIF1-α and CCN2 in chordoma cells, such that $rCCN2_{domain4}$ is decreasing HIF1-α activity under hypoxia but promoting HIF1-α activity under normoxia. In addition, there could also be separate pathways downstream of CCN2 interactions with U-CH1 cells that are HIF1-α independent, such as AP1 or Smad signalling [77] that could be involved in regulating progenitor-like properties. Future studies could interrogate the mechanisms responsible for the differential effects of

rCCN2 observed in normoxia and hypoxia, using specific pharmacological manipulation of candidate signalling pathways.

Despite the interesting outcomes of these studies, we acknowledge some inherent limitations. The first is the use of *in vitro* assays, which are not entirely reflective of the tumor microenvironment in its entirety or the heterogeneous clinical presentation of chordomas. Future experiments should therefore incorporate xenotransplantation experiments to assess the effects of CCN2 *in vivo.* To investigate the effects of exogenous CCN2, we also used a peptide fragment corresponding to the fourth domain of CCN2 as opposed to the full-length peptide. Although this CCN2 peptide fragment has been shown to modulate cell adhesion, migration, angiogenesis and differentiation in other cell types [41,76,79–79] and can be found in the tissue microenvironment following endogenous CCN2 cleavage [80–83] it may not effectively recapitulate all functions of the full-length CCN2 protein. Lastly, we did not perform gain or loss of functions experiments using CCN2 in U-CH1 cells, and this is a future area of study.

Taken together, findings from this study highlight the importance of the tumor microenvironment in the regulation of human chordoma cell phenotype. We demonstrate that components of the microenvironment (i.e. hypoxia and CCN2) influence the chordoma cell phenotype and that cells respond to hypoxia and CCN2 by up-regulating progenitor-like properties. Since there is mutual interaction between the microenvironment and tumor cells, we suggest that future studies focus on examining

more components of the microenvironment, as this would provide further insight into chordoma pathogenesis.

2.5 References

1. McMaster ML, Goldstein M, Bromley CM, Ishibe N & Parry DM. Chordoma: incidence and survival patterns in the United States, 1973-1995. *Cancer Causes Control* **12,** 1–11 (2001).

2. Bjornsson J, Wold LE, Ebersold MJ & Laws ER. Chordoma of the mobile spine. A clinicopathologic analysis of 40 patients. *Cancer.* **71,** 735–40 (1993).

3. McCann MR, Tamplin OJ, Rossant J, S. C. Tracing notochord-derived cells using a Noto-cre mouse: implications for intervertebral disc development. *Dis. Model. Mech.* **5,** 73–82 (2012).

4. Choi KS, Cohn MJ & Harfe BD. Identification of nucleus pulposus precursor cells and notochordal remnants in the mouse: implications for disk degeneration and chordoma formation. *Dev. Dyn.* **237,** 3953–3958 (2009).

5. Lehtonen E, Stefanovic V & Saraga-Babic M. Changes in the expression of intermediate filaments and desmoplakins during development of human notochord. *Differentiation.* **59,** 43–9 (1995).

6. Salisbury JR. Demonstration of cytokeratins and an epithelial membrane antigen in chondroid chordoma. *J. Pathol.* **153,** 37–40 (1987).

7. Nakamura Y, Becker LE & Marks A. S100 protein in human chordoma and human and rabbit notochord. *Arch. Pathol. Lab. Med.* **107,** 118–120 (1983).

8. Herrmann BG. Expression pattern of the Brachyury gene in whole-mount embryos mutant. *Development.* **917,** 913–917 (1991).

9. Wilkinson DG, Bhatt S & Herrmann BG. Expression pattern of the mouse T gene and its role in mesoderm formation. *Nature.* **343**, 657-9 (1990).

10. Presneau N, Shalaby A, Ye H, Pillay N, Halai D, Idowu B, Tirabosco R, Whitwell D, Jacques TS, Kindblom LG, Brüderlein S, Möller P, Leithner A, Liegl B, Amary

FM, Athanasou NN, Hogendoorn PC, Mertens F, Szuhai K & Flanagan AM. Role of the transcription factor T (brachyury) in the pathogenesis of sporadic chordoma: a genetic and functional-based study. *J. Pathol.* **223,** 327–35 (2011).

11. Yang XR, Ng D, Alcorta DA, Liebsch NJ, Sheridan E, Li S, Goldstein AM, Parry DM & Kelley MJ. T (Brachyury) gene duplication confers major susceptibility to familial chordoma. *Nat. Genet.* **41,** 1176–1178 (2010).

12. Barrionuevo, F., Taketo, M. M., Scherer, G. & Kispert, A. Sox9 is required for notochord maintenance in mice. *Dev. Biol.* **295,** 128–40 (2006).

13. Smits P. Sox5 and Sox6 are required for notochord extracellular matrix sheath formation, notochord cell survival and development of the nucleus pulposus of intervertebral discs. *Development.* **130,** 1135–1148 (2003).

14. Maier JA, Lo Y & Harfe BD. Foxa1 and Foxa2 are required for formation of the intervertebral discs. *PLoS One.* **8,** e55528 (2013).

15. Bundya J, Rogersa R, Hoffman S & Conwaya SJ. Segmental expression of aggrecan in the non-segmented perinothochordal sheath underlines normal segmentation of the vertebral column. *Mech Dev.* **79,** 213–217 (1998).

16. Sive JI, Baird P, Jeziorsk M, Watkins A, Hoyland JA & Freemont AJ. Expression of chondrocyte markers by cells of normal and degenerate intervertebral discs. *Mol Pathol*. **55**, 91–98 (2002).

17. McKeown SR. Defining normoxia, physoxia and hypoxia in tumours-implications for treatment response. *Br. J. Radiol.* **87,** 20130676 (2014).

18. Höckel M & Vaupel P. Tumor hypoxia: definitions and current clinical, biologic, and molecular aspects. *J. Natl. Cancer Inst.* **93,** 266–76 (2001).

19. Mamede AC, Abrantes AM, Pedrosa L, Casalta-Lopes JE, Pires AS, Teixo RJ, Gonçalves AC, Sarmento-Ribeiro AB, Maia CJ & Botelho MF. Beyond the limits

of oxygen: effects of hypoxia in a hormone-independent prostate cancer cell line. *ISRN Oncol.* **2013,** 918207 (2013).

20. Nagelkerke A, Bussink J, Mujcic H, Wouters BG, Lehmann S, Sweep FC & Span PN. Hypoxia stimulates migration of breast cancer cells via the PERK/ATF4/ LAMP3-arm of the unfolded protein response. *Breast Cancer Res.* **15,** R2 (2013).

21. Hongo K1, Tsuno NH, Kawai K, Sasaki K, Kaneko M, Hiyoshi M, Murono K, Tada N, Nirei T, Sunami E, Takahashi K, Nagawa H, Kitayama J & Watanabe T. Hypoxia enhances colon cancer migration and invasion through promotion of epithelial-mesenchymal transition. *J. Surg. Res.* **182,** 75–84 (2013).

22. Li P, Zhou C, Xu L & Xiao H. Hypoxia enhances stemness of cancer stem cells in glioblastoma: an in vitro study. *Int. J. Med. Sci.* **10,** 399–407 (2013).

23. Liang D, Ma Y, Liu J, Trope CG, Holm R, Nesland JM & Suo Z. The hypoxic microenvironment upgrades stem-like properties of ovarian cancer cells. *BMC Cancer.* **12,** 201 (2012).

24. Tamplin OJ, Cox BJ & Rossant J. Integrated microarray and ChIP analysis identifies multiple Foxa2 dependent target genes in the notochord. *Dev. Biol.* **360,** 415–25 (2011).

25. Bedore J, Sha W, McCann MR, Liu S, Leask A & Séguin CA. Impaired Intervertebral Disc Development and Premature Disc Degeneration in Mice With Notochord-Specific Deletion of CCN2. *Arthritis Rheum.* **65,** 2634–2644 (2013).

26. Chiou M, Chao T, Wu J, Kuo C & Chen J. The physiological role of CTGF/CCN2 in zebrafish notochond development and biological analysis of the proximal promoter region. *Biochem Biophys Res Commun.* **349,** 750–758 (2006).

27. Garcia P, Leal P, Ili C, Brebi P, Alvarez H & Roa JC. Inhibition of connective tissue growth factor (CTGF/CCN2) in gallbladder cancer cells leads to decreased growth in vitro. *Int. J. Exp. Pathol.* **94,** 195–202 (2013).

28. Sounni NE & Noel A. Targeting the tumor microenvironment for cancer therapy. *Clin. Chem.* **59,** 85–93 (2013).

29. Lee CH, Shah B, Moioli EK & Mao JJ. CTGF directs fibroblast differentiation from human mesenchymal stem/stromal cells and defines connective tissue healing in a rodent injury model. *J. Clin. Invest*. **120,** 3340-9 (2010).

30. Yang AT, Wang P, Tong XF, Cong M, Liu TH, Cong R, Wu P, Jia JD, Wang BE & You H. Connective tissue growth factor induces hepatic progenitor cells to differentiate into hepatocytes. *Int. J. Mol. Med.* **32,** 35–42 (2013).

31. Park SA & Kim HS. F-18 FDG PET/CT evaluation of sacrococcygeal chordoma. *Clin. Nucl. Med.* **33,** 906–8 (2008).

32. Nelson AC, Pillay N, Henderson S, Presneau N, Tirabosco R, Halai D, Berisha F, Flicek P, Stemple DL, Stern CD, Wardle FC & Flanagan AM. An integrated functional genomics approach identifies the regulatory network directed by brachyury (T) in chordoma. *J. Pathol.* **3**, 274–285 (2012).

33. Scheil S, Brüderlein S, Liehr T, Starke H, Herms J, Schulte M & Möller P. Genome-wide analysis of sixteen chordomas by comparative genomic hybridization and cytogenetics of the first human chordoma cell line, U-CH1. *Genes. Chromosomes Cancer.* **32,** 203–11 (2001).

34. Yue PY, Leung EP, Mak NK & Wong RN. A simplified method for quantifying cell migration/wound healing in 96-well plates. *J. Biomol. Screen.* **15,** 427–33 (2010).

35. Wang Y, Bailey J, Rovira M & Leach S. Sphere-forming assays for assessment of benign and malignant pancreatic stem cells. *Methods Mol Biol.* **980,** 281–290 (2013).

36. Putman DM, Liu KY, Broughton HC, Bell GI & Hess DA. Umbilical cord blood-derived aldehyde dehydrogenase-expressing progenitor cells promote recovery from acute ischemic injury. *Stem Cells.* **30,** 2248–60 (2012).

37. Yang C, Hornicek FJ, Wood KB, Schwab JH, Choy E, Iafrate J, Rosenberg A, Nielsen GP, Xavier RJ, Mankin H & Duan Z. Characterization and analysis of human chordoma cell lines. *Spine.* **35,** 1257–1264 (2013).

38. Brüderlein S, Sommer JB, Meltzer PS, Li S, Osada T, Ng D, Möller P, Alcorta DA & Kelley MJ. Molecular Characterization of Putative Chordoma Cell Lines. *Sarcoma*. **2010,** 630129 (2010).

39. Espinoza I, Menendez JA, Kvp CM & Lupu R. CCN1 promotes vascular endothelial growth factor secretion through αvβ 3 integrin receptors in breast cancer. *J. Cell Commun. Signal.* **1**, 23-7 (2013).

40. Haque I, Mehta S, Majumder M, Dhar K, De A, McGregor D, Van Veldhuizen PJ, Banerjee SK & Banerjee S. Cyr61/CCN1 signaling is critical for epithelial-mesenchymal transition and stemness and promotes pancreatic carcinogenesis. *Mol. Cancer.* **10,** 8 (2011).

41. Chien W, O'Kelly J, Lu D, Leiter A, Sohn J, Yin D, Karlan B, Vadgama J, Lyons KM & Koeffler HP. Expression of connective tissue growth factor (CTGF/CCN2) in breast cancer cells is associated with increased migration and angiogenesis. *Int. J. Oncol.* **38,** 1741–1747 (2013).

42. Bennewith KL, Huang X, Ham CM, Graves EE, Erler JT, Kambham N, Feazell J, Yang GP, Koong A & Giaccia AJ. The role of tumor cell-derived connective tissue growth factor (CTGF/CCN2) in pancreatic tumor growth. *Cancer Res.* **69,** 775–84 (2009).

43. Gupta N, Wang H, McLeod TL, Naus CC, Kyurkchiev S, Advani S, Yu J, Perbal B & Weichselbaum RR. Inhibition of glioma cell growth and tumorigenic potential by CCN3 (NOV). *Mol. Pathol.* **54,** 293–9 (2001).

44. Chen PC, Cheng HC & Tang CH. CCN3 promotes prostate cancer bone metastasis by modulating the tumor-bone microenvironment through RANKL-dependent pathway. *Carcinogenesis.* **34,** 1669–79 (2013).

45. Dhar G, Mehta S, Banerjee S, Gardner A, McCarty BM, Mathur SC, Campbell DR, Kambhampati S & Banerjee SK. Loss of WISP-2/CCN5 signaling in human pancreatic cancer: a potential mechanism for epithelial-mesenchymal-transition. *Cancer Lett.* **254,** 63–70 (2007).

46. Fritah A, Saucier C, De Wever O, Bracke M, Bièche I, Lidereau R, Gespach C, Drouot S, Redeuilh G & Sabbah M. Role of WISP-2/CCN5 in the maintenance of a differentiated and noninvasive phenotype in human breast cancer cells. *Mol. Cell. Biol.* **28,** 1114–23 (2008).

47. Erwin WM, Ashman K, O'Donnel P & Inman RD. Nucleus pulposus notochord cells secrete connective tissue growth factor and up-regulate proteoglycan expression by intervertebral disc chondrocytes. *Arthritis Rheum.* **54,** 3859–67 (2006).

48. Tran CM, Smith HE, Symes A, Rittié L, Perbal B, Shapiro IM & Risbud MV. Transforming Growth Factor B Controls CCN3 Expression in Nucleus Pulposus Cells of the Intervertebral Disc. *Arthritis Rheum.* **63,** 3022–3031 (2011).

49. Abbott RD, Purmessur D, Monsey RD, Brigstock DR, Laudier DM & Iatridis JC. Degenerative Grade Affects the Responses of Human of Human Nucleus Pulposus Cells to Link-N, CTGF, and TGFB3. *J Spinal Discord Tech.* **26,** 86–94 (2013).

50. El-Heliebi A, Kroneis T, Wagner K, Meditz K, Kolb D, Feichtinger J, Thallinger GG, Quehenberger F, Liegl-Atzwanger B & Rinner B. Resolving tumor heterogeneity: genes involved in chordoma cell development identified by low-template analysis of morphologically distinct cells. *PLoS One.* **9,** e87663 (2014).

51. Ginestier C, Hur MH, Charafe-Jauffret E, Monville F, Dutcher J, Brown M, Jacquemier J, Viens P, Kleer CG, Liu S, Schott A, Hayes D, Birnbaum D, Wicha MS & Dontu G. ALDH1 is a marker of normal and malignant human mammary stem cells and a predictor of poor clinical outcome. *Cell Stem Cell.* **1,** 555–567 (2008).

52. Eramo A, Lotti F, Sette G, Pilozzi E, Biffoni M, Di Virgilio A, Conticello C, Ruco L, Peschle C & De Maria R. Identification and expansion of the tumorigenic lung cancer stem cell population. *Cell Death Differ.* **15,** 504–14 (2008).

53. Hermann PC, Huber SL, Herrler T, Aicher A, Ellwart JW, Guba M, Bruns CJ & Heeschen C. Distinct populations of cancer stem cells determine tumor growth and metastatic activity in human pancreatic cancer. *Cell Stem Cell.* **1,** 313–23 (2007).

54. Ricci-Vitiani L, Lombardi DG, Pilozzi E, Biffoni M, Todaro M, Peschle C, De Maria R. Identification and expansion of human colon-cancer-initiating cells. *Nature.* **445,** 111–5 (2007).

55. O'Brien CA, Pollett A, Gallinger S & Dick JE. A human colon cancer cell capable of initiating tumour growth in immunodeficient mice. *Nature.* **445,** 106–10 (2007).

56. Bao S, Wu Q, McLendon RE, Hao Y, Shi Q, Hjelmeland AB, Dewhirst MW, Bigner DD & Rich JN. Glioma stem cells promote radioresistance by preferential activation of the DNA damage response. *Nature.* **444,** 756–60 (2006).

57. Aydemir E, Bayrak OF, Sahin F, Atalay B, Kose GT, Ozen M, Sevli S, Dalan AB, Yalvac ME, Dogruluk T, T. U. Characterization of cancer stem-like cells in chordoma. *J. Neurosurg.* **116,** 810–820 (2012).

58. Dominici M, Le Blanc K, Mueller I, Slaper-Cortenbach I, Marini F, Krause D, Deans R, Keating A, Prockop Dj & Horwitz E. Minimal criteria for defining multipotent mesenchymal stromal cells. The International Society for Cellular Therapy position statement. *Cytotherapy.* **8,** 315–7 (2006).

59. Notta F, Doulatov S, Laurenti E, Poeppl A, Jurisica I & Dick JE. Isolation of single human hematopoietic stem cells capable of long-term multilineage engraftment. *Science.* **333,** 218–21 (2011).

60. Chong HC, Tan CK, Huang RL & Tan NS. Matricellular proteins: a sticky affair with cancers. *J. Oncol.* **2012,** 351089 (2012).

61. Wolf N, Yang W, Dunk CE, Gashaw I, Lye SJ, Ring T, Schmidt M, Winterhager E & Gellhaus A. Regulation of the matricellular proteins CYR61 (CCN1) and NOV (CCN3) by hypoxia-inducible factor-1{alpha} and transforming-growth factor-{beta}3 in the human trophoblast. *Endocrinology.* **151,** 2835–45 (2010).

62. You JJ, Yang CM, Chen MS & Yang CH. Regulation of Cyr61/CCN1 expression by hypoxia through cooperation of c-Jun/AP-1 and HIF-1α in retinal vascular endothelial cells. *Exp. Eye Res.* **91,** 825–836 (2010).

63. Higgins DF, Biju MP, Akai Y, Wutz A, Johnson RS & Haase VH. Hypoxic induction of Ctgf is directly mediated by Hif-1. *Am J Physiol Renal Physiol.* **6144,** 1223–1232 (2004).

64. Franzen CA, Chen CC, Todorović V, Juric V, Monzon RI & Lau LF. The matrix protein CCN1 is critical for prostate carcinoma cell proliferation and TRAIL-induced apoptosis. *Mol. Cancer. Res.* **7,** 1045–1055 (2010).

65. Tamura I, Rosenbloom J, Macarak E & Chaqour B. Regulation of Cyr61 gene expression by mechanical stretch through multiple signaling pathways. *Am J Physiol Cell Physiol.* **281,** C1524–C1532 (2001).

66. Hirschfeld M, zur Hausen A, Bettendorf H, Jäger M & Stickeler E. Alternative splicing of Cyr61 is regulated by hypoxia and significantly changed in breast cancer. *Cancer Res.* **69,** 2082–90 (2009).

67. Sha W & Leask A. CCN2 expression and localization in melanoma cells. *J. Cell Commun. Signal.* **5,** 219–26 (2011).

68. Ostroumov E & Hunter CJ. The role of extracellular factors in human metastatic chordoma cell growth in vitro. *Spine.* **32,** 2957–64 (2007).

69. Yu JL, Rak JW, Carmeliet P, Nagy A, Kerbel RS & Coomber BL. Heterogeneous Vascular Dependence of Tumor Cell Populations. *Am. J. Pathol.* **158,** 1325–1334 (2001).

70. Chen C, Pore N, Behrooz A, Ismail-Beigi F & Maity A. Regulation of glut1 mRNA by hypoxia-inducible factor-1. Interaction between H-ras and hypoxia. *J. Biol. Chem.* **276 ,** 9519–9525 (2001).

71. Suzuki H, Tomida A & Tsuruo T. Dephosphorylated hypoxia-inducible factor 1alpha as a mediator of p53-dependent apoptosis during hypoxia. *Oncogene.* **20,** 5779–88 (2001).

72. Carmeliet P, Dor Y, Herbert JM, Fukumura D, Brusselmans K, Dewerchin M, Neeman M, Bono F, Abramovitch R, Maxwell P, Koch CJ, Ratcliffe P, Moons L, Jain RK, Collen D & Keshert E. Role of HIF-1[alpha] in hypoxia-mediated apoptosis, cell proliferation and tumour angiogenesis. *Nature.* **394,** 485–90 (1998).

73. Soeda A, Park M, Lee D, Mintz A, Androutsellis-Theotokis A, McKay RD, Engh J, Iwama T, Kunisada T, Kassam AB, Pollack IF & Park DM. Hypoxia promotes expansion of the CD133-positive glioma stem cells through activation of HIF-1alpha. *Oncogene.* **28,** 3949–59 (2009).

74. Tammela T, Enholm B, Alitalo K & Paavonen K. The biology of vascular endothelial growth factors. *Cardiovasc. Res.* **65 ,** 550–563 (2005).

75. Keith B & Simon MC. Hypoxia-inducible factors, stem cells, and cancer. *Cell.* **129,** 465–72 (2007).

76. Ball DK, Rachfal AW, Kemper SA & Brigstock DR. The heparin-binding 10 kDa fragment of connective tissue growth factor (CTGF) containing module 4 alone stimulates cell adhesion. *J. Endocrinol.* **176,** R1–7 (2003).

77. Tran CM, Markova D, Smith HE, Susarla B, Ponnappan RK, Anderson DG, Symes A, Shapiro IM & Risbud MV. Regulation of CCN2/connective tissue growth factor expression in the nucleus pulposus of the intervertebral disc: role of Smad and activator protein 1 signaling. *Arthritis. Rheum.* **62**, 1983-92 (2010).

78. Gao R & Brigstock DR. Connective tissue growth factor (CCN2) induces adhesion of rat activated hepatic stellate cells by binding of its C-terminal domain to

integrin alpha(v)beta(3) and heparan sulfate proteoglycan. *J. Biol. Chem.* **279,** 8848–55 (2004).

79. Liu BC, Zhang JD, Zhang XL, Wu GQ & Li MX. Role of connective tissue growth factor (CTGF) module 4 in regulating epithelial mesenchymal transition (EMT) in HK-2 cells. *Clin. Chim. Acta.* **373,** 144–50 (2006).

80. Williams EJ, Gaça MD, Brigstock DR, Arthur MJ & Benyon RC. Increased expression of connective tissue growth factor in fibrotic human liver and in activated hepatic stellate cells. *J. Hepatol.* **32,** 754–761 (2000).

81. Gao R & Brigstock DR. Low density lipoprotein receptor-related protein (LRP) is a heparin-dependent adhesion receptor for connective tissue growth factor (CTGF) in rat activated hepatic stellate cells. *Hepatol. Res.* **27,** 214–220 (2003).

82. Huang G & Brigstock DR. Regulation of hepatic stellate cells by connective tissue growth factor. *Front Biosci (Landmark Ed).* **17,** 2495–2507 (2012).

83. Ball DK, Surveyor GA, Diehl JR, Steffen CL, Uzumcu M, Mirando MA & Brigstock DR. Characterization of 16- to 20-kilodalton (kDa) connective tissue growth factors (CTGFs) and demonstration of proteolytic activity for 38-kDa CTGF in pig uterine luminal flushings. *Biol. Reprod.* **59,** 828–35 (1998).

CHAPTER 3

General Discussion

3.1 Summary and conclusions

In this study, we sought to investigate microenvironmental regulation of U-CH1 cell properties by specifically investigating the effects of hypoxia and CCN2, as studies have suggested that these may serve as important regulators of chordoma pathogenesis [1-2]. We hypothesized that hypoxic conditions and/or increased levels of CCN2 would alter the phenotype and functional properties of human chordoma cells, promoting progenitor-like characteristics specific to the notochordal tissue of origin.

We explored our hypothesis with two specific objectives:

1) To examine the effect of hypoxia on human U-CH1 chordoma cells.

2) To examine the effect of CCN2 stimulation and the additive effects of CCN2 and hypoxia on human U-CH1 chordoma cells.

These studies enabled us to conclude that hypoxia and CCN2 both promoted progenitor-like properties in U-CH1 cells, including increased progenitor cell self-renewal and the expression of genes associated with the notochord tissue of origin. Interestingly, hypoxia had the greatest ability to induce progenitor-like properties and the effects of CCN2 were more pronounced when cells were treated in normoxia than in hypoxia (**Figure 3.1**).

3.2 Significance of research

Hypoxia and CCN2 have been shown to regulate stem and progenitor cell differentiation and cancer cell biology; however, there are limited studies examining the

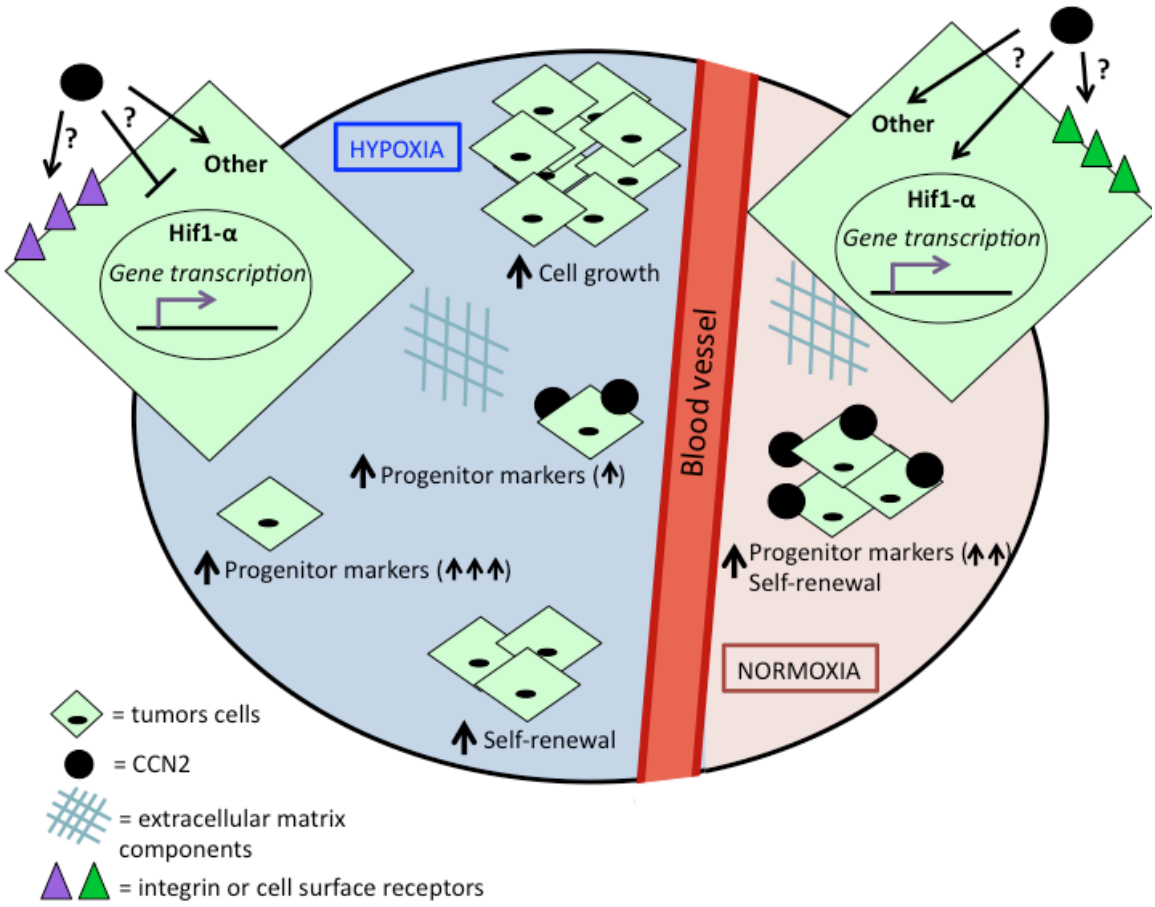

Figure 3.1 Working model illustrating the effects of hypoxia and CCN2 on U-CH1 cells. Results from the current study demonstrate an increase in the expression of notochord progenitor markers, cell growth and self-renewal in chordoma cells in hypoxia compared to normoxia. In normoxia, exogenous CCN2 (indicated as black circles) increased the expression of progenitor markers and sphere formation; however these effects were not as pronounced as hypoxia alone. Lastly, the addition of CCN2 in hypoxia induced the expression of only a subset of progenitor markers. The large green triangles represent chordoma cells in either microenvironment, with potential mechanisms underlying the change in cell phenotype illustrated. In hypoxia, we demonstrated increased HIF1-α activity, which may be decreased by the addition of CCN2. In contrast, in normoxia, where endogenous HIF1-α activity is lower, the addition of CCN2 may alter the U-CH1 phenotype by increasing HIF1-α activity. Modulation of HIF1-α activity may contribute to the differences in progenitor-like properties reported in U-CH1 cells. Given the change detected in the chordoma cell phenotype, it may be that CCN2 is interacting with different integrin or cell surface receptors or downstream pathways independent of HIF1-α (such as AP-1 or SMAD) on U-CH1 cells under hypoxia compared to normoxia, resulting in differential downstream effects.

effects of hypoxia on human chordoma cells and no studies examining the effects of CCN2 on human chordoma cells. There are two studies that examined the effects of hypoxia on cell growth in chordoma cells. The first study used primary human chordoma cells maintained under normoxia (20% O_2) or hypoxia (5% O_2) under low (1 g/L) or high (4.5 g/L) glucose concentrations over 5 days [3]. The authors report an increase in cell proliferation under hypoxia compared to normoxia over 5 days, which was independent of the glucose concentration in the culture media. The second study used U-CH1, CH 8 and GB 60 human chordoma cells maintained under normoxia (20% O_2) or hypoxia (5% O_2) for 7 days with or without glucose (ranging from 2-6 g/L) and measured cell growth after 7 days [4]. The study reported no difference in cell proliferation under hypoxia compared to normoxia for all 3 cell lines, and similarly reported no effects of glucose. The increase we demonstrate in U-CH1 cell growth under hypoxia may be attribute to the lower oxygen level (2% O_2) used in the current study. In addition, we maintained our cells in hypoxia for at least 1-2 passages before performing our cell growth assay, whereas the study using U-CH1 cells did not, which could also explain differences in the findings. Furthermore, the study using primary chordoma cells also found that the optimal pH for chordoma cells was alkaline as this increased cell proliferation and intracellular tyrosine phosphorylation without inducing apoptosis [3].

Our study highlights the importance of the tumor microenvironment, as we demonstrated that hypoxia and CCN2 have important roles in the maintenance of a progenitor-like population in U-CH1 cells. We demonstrated that hypoxia has the greatest ability to promote progenitor-like properties in U-CH1 cells and that the effects of CCN2

were more pronounced under normoxia than under hypoxia. Hypoxia increased the expression of the majority of the notochord markers and increased both cell proliferation and sphere formation compared to rCCN2. We also found additive effects of rCCN2 and hypoxia on the gene expression of a subset of notochord progenitor markers. It is important to note that the increase in progenitor-cell characteristics could be interpreted as either increased expression of these markers in all cells or an increase in the number of progenitor cells in the heterogeneous population. Our data suggests there may be an increase in the number of progenitor cells within the heterogeneous cell population. While we did not directly assess the percentage of U-CH1 cells expressing progenitor markers in the current study, the increases observed in the efficiency of sphere formation in hypoxia suggest an increase in the number of progenitor cells within the heterogeneous population under these conditions.

The differences observed in the effect of exogenous CCN2 treatment of U-CH1 cells in normoxic or hypoxic conditions may be related to the cell-type specific effects of CCN proteins. Since we demonstrated that U-CH1 cells are more progenitor-like in hypoxia than in normoxia, cells may consequently be expressing different integrins, cell surface receptors or CCN2 binding proteins that mediate CCN2-dependent signalling. Furthermore, previous studies have showed that HIF1-α and CCN2 each regulate the expression of the other [5–7]. As such there could be differences in the interaction between HIF1-α and CCN2 in U-CH1 cells, such that $rCCN2_{domain4}$ is decreasing HIF1-α activity under hypoxia but promoting HIF1-α activity under normoxia. In addition, there could also be separate pathways downstream of CCN2 that are HIF1-α independent, such as

AP1 or Smad signalling that could be involved in regulating the response of UCH-1 cells to CCN2 and the induction of progenitor-like properties [8].

Given the change in cell phenotype observed, future experiments could focus on examining differences in the expression of CCN2-binding integrin receptors (such as αvβ1 and αvβ3 [9-10]) in U-CH1 cells maintained in normoxia or hypoxia using immunolocalization and real-time PCR gene expression analysis. Differences in the expression of additional cell surface receptors could likewise be examined in U-CH1 cells maintained under normoxia or hypoxia could be assessed using flow cytometry. To detect differences in expression of extracellular CCN2 binding proteins (ex. fibronectin, vitronectin or decorin [11]) by U-CH1 cells in normoxia versus hypoxia, western blot analysis could be conducted on the media or extracellular matrix fraction of confluent U-CH1 cell cultures. HIF1-α levels could be quantified in U-CH1 cells under normoxia or hypoxia, with or without $rCCN2_{domain4}$ by western blot analysis of both the nuclear and cytoplasmic proteins to quantify changes in expression level, or subcellular localization. Lastly, western blot analysis could be used to determine changes in the activation of Smad or AP-1 signaling pathways under normoxia and hypoxia, and with the addition of $rCCN2_{domain4}$.

Currently, there are very few treatment options available for patients with chordoma. Most patients undergo resection of the tumor, but this is often associated with a high rate of recurrence and decreased survival [3-4]. In addition, the use of radiation therapy has mixed results on patients with chordoma [5-6] complicated by the proximity of

the tumor to the spinal cord, which makes it difficult to administer high doses of radiation. There are no drugs approved by the FDA for the majority of patients of chordomas with a major issue being that chordomas are slow growing tumors and most chemotherapy drugs target rapidly proliferating cells. Since our study demonstrates U-CH1 progenitor properties are significantly increased under hypoxia, with increased cell proliferation and self-renewal, it could be worthwhile to explore hypoxia signaling pathways as potential therapeutic targets. Studies have shown that regions of hypoxia have increased resistance to drug therapy and that HIF1-α can act on a variety of different pathways to increase drug efflux pumps such as MDR1 [16] and inhibit anti-apoptotic genes such as BCL2 [17]. Further studies could explore if patients with chordomas would benefit from HIF-targeting drugs in combination with surgery for a more efficient treatment option. A variety of drugs, including PX-12 and YC-1 have shown to decrease HIF1-α levels in *in vivo* mouse xenograft models using breast cancer and human colon carcinoma [18], and hepatoma, stomach carcinoma, renal carincoma, cervical carcinoma and neuroblastoma cells cancer and breast cancer cells [19]. In these studies, the tumors showed decreased tumor growth [18-19] and angiogenesis [19]. Future studies should use *in vivo* mouse xenograft models with U-CH1 cells with HIF1-α targeting drugs to determine if they reduce cell growth or self-renewal properties in tumors.

3.3 Limitation of the research and suggestions for future studies

In addition to the suggestions for future studies mentioned above, one major limitation of our research is the use of the rCCN2 peptide. This 253-349 amino acid peptide corresponds to the fourth domain of the CCN2 protein, which contains heparin

and integrin binding sites. These sites allow binding of CCN2 with heparin-sulfate-containing-proteoglycans (e.g. perlecan [19]) and cell surface integrin receptors (e.g. αvβ1 and αvβ3 [9-10]) and could potentially induce different biological effects than the full-length CCN2 protein. This domain has been shown to have roles in cell adhesion, migration, angiogenesis and differentiation in other cell types [9,21–23]. Interestingly, studies have shown have shown that CCN2 can be cleaved between domains 3 and 4, producing endogenous CCN2 fragments corresponding to the fourth domain. Studies performed in rat hepatic stellate [9] and pig uterine luminal flushings [24] demonstrated the presence of both full length CCN2 and the fragment corresponding to the fourth domain of CCN2. Therefore, determining the functional effects of module four of CCN2 on chordoma cell regulation is of importance. Future studies should compare the biological response of chordoma cells to the full-length rCCN2 or the fourth domain fragment of the protein. It should be noted that we also attempted to knock-down endogenous CCN2 expression in U-CH1 cells using shRNA to investigate the effects of the loss of CCN2. In all three experimental attempts to generate a stable CCN2 knockdown cell line, we noted increased cell apoptosis and a loss of cell adhesion, preventing cell expansion and experimentation. To complement the gain-of-function experiments presented in the current study, future experiments could attempt to generate CCN2-depleted U-CH1 cells using inducible shRNA constructs to permit the creation of a stable transgenic cell line prior to CCN2 knockdown.

Another limitation of our study is the use of *in vitro* experiments, which makes it difficult to determine the effect of the entire tumor microenvironment. Future studies

should examine the effects of CCN2 using *in vivo* mouse xenograft models overexpressing CCN2 in U-CH1 cells to investigate the effects of the complete tumor microenvironment on the regulation of human chordoma cells. In addition, it may be worthwhile examining the effects of other CCN matricellular proteins, as we detected the expression of *CCN1, CCN2, CCN3* and *CCN5* in U-CH1 cells with an increase in *CCN3* and *CCN5* in response to hypoxia. To our knowledge, there are currently no studies that investigate the role of CCN proteins in chordomas, which have all been shown to regulate cancer properties including cell proliferation [18-19], metastasis [27] and migration [28]. Additionally, studies have shown increased expression of CCN proteins under hypoxia compared to normoxia, such as increases in CCN1 and CCN3 in human choriocarcinoma cells [29] and CCN1 in retinal vascular endothelial cells [30]. This suggests and CCN5 may be involved in the increased progenitor-like properties we see under hypoxia. Furthermore, we also found increased expression of *CCN1*, *CCN3* and *CCN5* following treatment of U-CH1 cells with $rCCN2_{domain4}$ under normoxia and hypoxia. We suggest that future studies focus on investigating the effects of these CCN members on U-CH1 cells and determining the mechanisms through which CCN2 regulates the expression of other CCN family members.

3.4 References

1. Park SA & Kim HS. F-18 FDG PET/CT evaluation of sacrococcygeal chordoma. *Clin. Nucl. Med.* **33,** 906–8 (2008).

2. Nelson AC, Pillay N, Henderson S, Presneau N, Tirabosco R, Halai D, Berisha F, Flicek P, Stemple DL, Stern CD, Wardle FC & Flanagan AM. An integrated functional genomics approach identifies the regulatory network directed by brachyury (T) in chordoma. *J Pathol.* **228**, 274–285 (2012).

3. Ostroumov E & Hunter CJ. The role of extracellular factors in human metastatic chordoma cell growth in vitro. *Spine.* **32,** 2957–64 (2007).

4. Yang C, Hornicek FJ, Wood KB, Schwab JH, Choy E, Iafrate J, Rosenberg A, Nielsen GP, Xavier RJ, Mankin H & Duan Z. Characterization and analysis of human chordoma cell lines. *Spine.* **35,** 1257–1264 (2013).

5. Higgins DF, Biju MP, Akai Y, Wutz A, Johnson RS & Haase VH. Hypoxic induction of Ctgf is directly mediated by Hif-1. *Am J Physiol Renal Physiol.* **6144,** 1223–1232 (2004).

6. Nishida T, Kondo S, Maeda A, Kubota S, Lyons KM & Takigawa M. CCN family 2/connective tissue growth factor (CCN2/CTGF) regulates the expression of Vegf through Hif-1a expression in a chondrocytic cell line, HCS-2/8, under hypoxic condition. *Bone.* **44,** 24–31 (2009).

7. Tran CM, Fujita N, Huang BL, Ong JR, Lyons KM, Shapiro IM & Risbud MV. Hypoxia-inducible Factor (HIF) -1alpha and CCN2 Form a Regulatory Circuit in Hypoxic Nucleus Pulposus Cells. *J Biol Chem*. **288**, 2654-66 (2013).

8. Tran CM, Markova D, Smith HE, Susarla B, Ponnappan RK, Anderson DG, Symes A, Shapiro IM & Risbud MV. Regulation of CCN2/connective tissue growth factor expression in the nucleus pulposus of the intervertebral disc: role of Smad and activator protein 1 signaling. *Arthritis. Rheum.* **62**, 1983-92 (2010).

9. Gao R & Brigstock DR. Connective tissue growth factor (CCN2) induces adhesion of rat activated hepatic stellate cells by binding of its C-terminal domain to integrin alpha(v)beta(3) and heparan sulfate proteoglycan. *J. Biol. Chem.* **279,** 8848–55 (2004).

10. Hoshijima M, Hattori T, Inoue M, Araki D, Hanagata H, Miyauchi A & Takigawa M. CT domain of CCN2/CTGF directly interacts with fibronectin and enhances cell adhesion of chondrocytes through integrin α5β1. *FEBS Lett.* **580,** 1376–1382 (2006).

11. Jun J and Lau LF. Taking aim at the extracellular matrix: CCN proteins as emerging therapeutic targets. *Nat Rev Drug Discov.* **10,** 945–63 (2011).

12. Bergh P, Kindblom LG, Gunterberg B, Remotti F, Ryd W & Meis-Kindblom JM. Prognostic factors in chordoma of the sacrum and mobile spine: a study of 39 patients. *Cancer.* **88,** 2122–34 (2000).

13. Boriani S, Bandiera S, Biagini R, Bacchini P, Boriani L, Cappuccio M, Chevalley F, Gasbarrini A, Picci P & Weinstein JN. Chordoma of the mobile spine: fifty years of experience. *Spine.* **31,** 493–503 (2006).

14. Sciubba DM, Cheng JJ, Petteys RJ, Weber KL, Frassica DA & Gokaslan ZL. Chordoma of the Sacrum and Vertebral Bodies. *J. Am. Acad. Orthop. Surg.* **17 ,** 708–717 (2009).

15. Koutourousiou M, Snyderman CH, Fernandez-Miranda J & Gardner PA. Skull Base Chordomas. *Otolaryngol. Clin. North Am.* **44,** 1155–1171 (2011).

16. Comerford KM, Wallace TJ, Karhausen J, Louis NA, Montalto MC & Colgan SP. Hypoxia-inducible Factor-1-dependent Regulation of the Multidrug Resistance (MDR1) Gene. *Cancer Res.* **62 ,** 3387–3394 (2002).

17. Chen N, Chen X, Huang R, Zeng H, Gong J, Meng W, Lu Y, Zhao F, Wang L & Zhou Q. BCL-xL Is a Target Gene Regulated by Hypoxia-inducible Factor-1α. *J. Biol. Chem.* **284 ,** 10004–10012 (2009).

18. Welsh SJ, Williams RR, Birmingham A, Newman DJ, Kirkpatrick DL & Powis G. The Thioredoxin Redox Inhibitors 1-Methylpropyl 2-Imidazolyl Disulfide and Pleurotin Inhibit Hypoxia-induced Factor 1 α and Vascular Endothelial Growth Factor Formation The Thioredoxin Redox Inhibitors 1-Methylpropyl 2-Imidazolyl Disulfide and Pleurotin I. *Mol Cancer Ther.* **3**, 235-43 (2003).

19. Tsui L, Fong TH & Wang IJ. YC-1: A Potential Anticancer Drug Targeting. *Mol Vis.* **95**, 1594-603 (2003).

20. Takigawa M. CCN2: a master regulator of the genesis of bone and cartilage. *J. Cell Commun. Signal.* **7,** 191–201 (2013).

21. Ball DK, Rachfal AW, Kemper SA & Brigstock DR. The heparin-binding 10 kDa fragment of connective tissue growth factor (CTGF) containing module 4 alone stimulates cell adhesion. *J. Endocrinol.* **176,** R1–7 (2003).

22. Liu BC, Zhang JD, Zhang XL, Wu GQ & Li MX. Role of connective tissue growth factor (CTGF) module 4 in regulating epithelial mesenchymal transition (EMT) in HK-2 cells. *Clin. Chim. Acta.* **373,** 144–50 (2006).

23. Chien W, O'Kelly J, Lu D, Leiter A, Sohn J, Yin D, Karlan B, Vadgama J, Lyons KM & Koeffler HP. Expression of connective tissue growth factor (CTGF/CCN2) in breast cancer cells is associated with increased migration and angiogenesis. *Int. J. Oncol.* **38,** 1741–1747 (2013).

24. Ball DK, Surveyor GA, Diehl JR, Steffen CL, Uzumcu M, Mirando MA & Brigstock DR. Characterization of 16- to 20-kilodalton (kDa) connective tissue growth factors (CTGFs) and demonstration of proteolytic activity for 38-kDa CTGF in pig uterine luminal flushings. *Biol. Reprod.* **59,** 828–35 (1998).

25. Leask, A. A sticky situation: CCN1 promotes both proliferation and apoptosis of cancer cells. *J. Cell Commun. Signal.* **4,** 71–2 (2010).

26. Gupta N, Wang H, McLeod TL, Naus CC, Kyurkchiev S, Advani S, Yu J, Perbal B & Weichselbaum RR. Inhibition of glioma cell growth and tumorigenic potential by CCN3 (NOV). *Mol. Pathol.* **54,** 293–9 (2001).

27. Haque I, Mehta S, Majumder M, Dhar K, De A, McGregor D, Van Veldhuizen PJ, Banerjee SK & Banerjee S. Cyr61/CCN1 signaling is critical for epithelial-mesenchymal transition and stemness and promotes pancreatic carcinogenesis. *Mol. Cancer* **10,** 8 (2011).

28. Ouellet V, Tiedemann K, Mourskaia A, Fong JE, Tran-Thanh D, Amir E, Clemons M, Perbal B, Komarova SV & Siegel PM. CCN3 impairs osteoblast and stimulates osteoclast differentiation to favor breast cancer metastasis to bone. *Am. J. Pathol.* **178,** 2377–88 (2011).

29. Wolf N, Yang W, Dunk CE, Gashaw I, Lye SJ, Ring T, Schmidt M, Winterhager E & Gellhaus A. Regulation of the matricellular proteins CYR61 (CCN1) and NOV (CCN3) by hypoxia-inducible factor-1{alpha} and transforming-growth factor-{beta}3 in the human trophoblast. *Endocrinology.* **151,** 2835–45 (2010).

30. You JJ, Yang CM, Chen MS & Yang CH. Regulation of Cyr61/CCN1 expression by hypoxia through cooperation of c-Jun/AP-1 and HIF-1α in retinal vascular endothelial cells. *Exp. Eye Res.* **91,** 825–836 (2010).

APPENDIX A

Copyright Permission to Use Figure from *Disease Models & Mechanisms*

Close

APPENDIX B

Copyright permission to use figure from *The Journal of Cell Science*

Confirmation Number: 11197388

Special Rightsholder Terms & Conditions

The following terms & conditions apply to the specific publication under which they are listed

Journal of cell science
Permission type: Republish or display content
Type of use: Republish in a thesis/dissertation

TERMS AND CONDITIONS

The following terms are individual to this publisher:

The acknowledgement should state "Reproduced / adapted with permission" and give the source journal name. The acknowledgement should either provide full citation details or refer to the relevant citation in the article reference list. The full citation details should include authors, journal, year, volume, issue and page citation.

Where appearing online or in other electronic media, a link should be provided to the original article (e.g. via DOI):

Development: dev.biologists.org

Disease Models & Mechanisms: dmm.biologists.org

Journal of Cell Science: jcs.biologists.org

The Journal of Experimental Biology: jeb.biologists.org

Other Terms and Conditions:

None

STANDARD TERMS AND CONDITIONS

1. Description of Service; Defined Terms. This Republication License enables the User to obtain licenses for republication of one or more copyrighted works as described in detail on the relevant Order Confirmation (the "Work(s)"). Copyright Clearance Center, Inc. ("CCC") grants licenses through the Service on behalf of the rightsholder identified on the Order Confirmation (the "Rightsholder"). "Republication", as used herein, generally means the inclusion of a Work, in whole or in part, in a new work or works, also as described on the Order Confirmation. "User", as used herein, means the person or entity making such republication.

2. The terms set forth in the relevant Order Confirmation, and any terms set by the Rightsholder with respect to a particular Work, govern the terms of use of Works in connection with the Service. By using the Service, the person transacting for a republication license on behalf of the User represents and warrants that he/she/it (a) has been duly authorized by the User to accept, and hereby does accept, all such terms and conditions on behalf of User, and (b) shall inform User of all such terms and conditions. In the event such person is a "freelancer" or other third party independent of User and CCC, such party shall be deemed jointly a "User" for purposes of these terms and conditions. In any event, User shall be deemed to have accepted and agreed to all such terms and conditions if User republishes the Work in any fashion.

3. Scope of License; Limitations and Obligations.

3.1 All Works and all rights therein, including copyright rights, remain the sole and exclusive property of the Rightsholder. The license created by the exchange of an Order Confirmation (and/or any invoice) and payment by User of the full amount set forth on that document includes only those rights expressly set forth in the Order Confirmation and in these terms and conditions, and conveys no other rights in the Work(s) to User. All rights not expressly granted are hereby reserved.

3.2 General Payment Terms: You may pay by credit card or through an account with us payable at the end of the month. If you and we agree that you may establish a standing account with CCC, then the following terms apply: Remit Payment to: Copyright Clearance Center, Dept 001, P.O. Box 843006, Boston, MA 02284-3006. Payments Due: Invoices are payable upon their delivery to you (or upon our notice to you that they are available to you for downloading). After 30 days, outstanding amounts will be subject to a service charge of 1-1/2% per month or, if less, the maximum rate allowed by applicable law. Unless otherwise specifically set forth in the Order Confirmation or in a separate written agreement signed by CCC, invoices are due and payable on "net 30" terms. While User may exercise the rights licensed immediately upon issuance of the Order Confirmation, the license is automatically revoked and is null and void, as if it had never been issued, if complete payment for the license is not received on a timely basis either from User directly or through a payment agent, such as a credit card company.

Confirmation and these terms and conditions or any rights granted hereunder; provided, however, that User may assign such license in its entirety on written notice to CCC in the event of a transfer of all or substantially all of User's rights in the new material which includes the Work(s) licensed under this Service.

8.4 No amendment or waiver of any terms is binding unless set forth in writing and signed by the parties. The Rightsholder and CCC hereby object to any terms contained in any writing prepared by the User or its principals, employees, agents or affiliates and purporting to govern or otherwise relate to the licensing transaction described in the Order Confirmation, which terms are in any way inconsistent with any terms set forth in the Order Confirmation and/or in these terms and conditions or CCC's standard operating procedures, whether such writing is prepared prior to, simultaneously with or subsequent to the Order Confirmation, and whether such writing appears on a copy of the Order Confirmation or in a separate instrument.

8.5 The licensing transaction described in the Order Confirmation document shall be governed by and construed under the law of the State of New York, USA, without regard to the principles thereof of conflicts of law. Any case, controversy, suit, action, or proceeding arising out of, in connection with, or related to such licensing transaction shall be brought, at CCC's sole discretion, in any federal or state court located in the County of New York, State of New York, USA, or in any federal or state court whose geographical jurisdiction covers the location of the Rightsholder set forth in the Order Confirmation. The parties expressly submit to the personal jurisdiction and venue of each such federal or state court.If you have any comments or questions about the Service or Copyright Clearance Center, please contact us at 978-750-8400 or send an e-mail to info@copyright.com.

v 1.1

Close

APPENDIX C

Copyright permission to use figure from *Arthritis & Rheumatism*

Order Completed

Thank you very much for your order.

This is a License Agreement between University of Western Ontario -- Priya Patel ("You") and John Wiley and Sons ("John Wiley and Sons"). The license consists of your order details, the terms and conditions provided by John Wiley and Sons, and the payment terms and conditions.

Get the printable license.

License Number	3372061361936
License date	Apr 18, 2014
Licensed content publisher	John Wiley and Sons
Licensed content publication	Arthritis & Rheumatism
Licensed content title	Impaired Intervertebral Disc Development and Premature Disc Degeneration in Mice With Notochord-Specific Deletion of CCN2
Licensed copyright line	Copyright © 2013 by the American College of Rheumatology
Licensed content author	Jake Bedore,Wei Sha,Matthew R. McCann,Shangxi Liu,Andrew Leask,Cheryle A. Séguin
Licensed content date	Sep 24, 2013
Start page	2634
End page	2644
Type of use	Dissertation/Thesis
Requestor type	University/Academic
Format	Print and electronic
Portion	Figure/table
Number of figures/tables	1
Original Wiley figure/table number(s)	Figure 1
Will you be translating?	No
Title of your thesis / dissertation	Investigating microenvironmental regulation of human chordoma cell behaviour
Expected completion date	May 2014
Expected size (number of pages)	100
Total	0.00 USD

ORDER MORE... CLOSE WINDOW

Curriculum Vitae

Priya Patel

University educational background:

September 2012- July 2014	Masters in Anatomy and Cell Biology (M.Sc.) Department of Anatomy and Cell Biology University of Western Ontario (Western), London, ON
September 2008- April 2012	Honours Bachelor of Medical Sciences (B.M.Sc.) University of Western Ontario (Western), London, ON

Honours and awards:

1) Ontario Graduate Scholarship (September 2013- August 2014)- $15,000

2) Poster presentation award at Canadian Connective Tissue Conference (June 2013)- $300

3) Canadian Institutes of Health Research (CIHR) Master's Award: Fredrick Banting and Charles Best Canada Graduate Scholarship (September 2012- August 2013)- $17,500

4) Ontario Graduate Scholarship (September 2012- August 2013)- *declined*- $15,000

5) Western Graduate Scholarship (September 2012- August 2014)- $9,000

6) Member of Dean's Honour Roll (2008-2012)

7) Western Scholar Distinction (2009-2012)

8) CIHR Summer Undergraduate Award in Mobility, Musculoskeletal Health and Arthritis (May- August 2012) - $4,950

9) Canadian Red Cross Volunteer Appreciation Award (2011-2012)

10) CIHR Summer Undergraduate Award in Mobility, Musculoskeletal Health and Arthritis (May- August 2011)- $4,950

11) CIHR Joint Motion Program's Summer Undergraduate Studentship Award (May- August 2011)- $1,050

12) Canadian Red Cross Volunteer Appreciation Award (2009-2010)

13) Western Scholarship of Distinction (2008)- $1,000

Related work experience:

Supervisory Experience

1. Gurkeet Lalli, 4th year undergraduate thesis student
   September 2013- April 2014
   Project entitled: The effects of whole body vibration on joint health
   Dr. Cheryle Séguin's Lab, University of Western Ontario, London, ON

2. Michael Barblinardo, 1st year dentistry student
   May-August 2012
   Project entitled: The effects of chronic vibration on the intervertebral discs.
   Dr. Cheryle Séguin's Lab, University of Western Ontario, London, ON

Teaching Assistant **September 2012- February 2013**
Department of Anatomy and Cell Biology, University of Western Ontario

- Facilitated weekly gross anatomy (Anatomy 9501) lab sessions for first-year physiotherapy students by utilizing cadavers for dissections and anatomical prossections
- Proctored and evaluated course examinations

Undergraduate Research Student **May 2011- August 2012**
Dr. Cheryle Séguin, Department of Physiology and Pharmacology, University of Western Ontario

- Investigated the effects of whole-body vibration platforms on intervertebral discs of the spinal column using *ex vivo* and *in vivo* mice models

Undergraduate Research Student **May 2010- January 2011**
Odette Cancer Centre, Sunnybrook Health Sciences Centre, University of Toronto

- Examined the use of total quality culture management in staffing models for both national and international hospitals and radiation therapy departments
- Investigated the effects of whole brain radiation therapy in the treatment of multiple brain metastases for a novel patient case

Publications:

1. McCann MR, **Patel P**, Pest M, Ratneswaran A, Kamphuis M, Esmail Z, Lee J, Barbilinardo M, Beaucage K, Holdsworth DW, Beier F, Dixon SJ, Séguin CA. Repeated exposure to high-frequency low-amplitude vibration induces degeneration of intervertebral disc and knee joints in a murine model. (In-preparation for submission to Arthritis and Rheumatology)
2. Matthew R. McCann, **Priya Patel**, Yizhi Xiao, Walter L. Siqueira, Cheryle A. Séguin. Proteomic Signature of the Murine Intervertebral Disc. (Submitted to PLOS One June 2014)
3. Matthew R. McCann*, **Priya Patel***, Kim L. Beaucage, Yizhi Xiao, Corey Bacher, Walter L. Siqueira, David W. Holdsworth, S. Jeffrey Dixon, Cheryle A. Séguin. Acute vibration induces transient expression of anabolic genes in the

murine intervertebral disc. (Arthritis & Rheumatism 2013 July; 65(7): 1853-1864.) **equal first-author contribution*

4. **Patel P**, Mitera G. A Systematic Scoping Literature Review of Incorporating a Total Quality Culture Within Radiotherapy Staffing Models: A Management Strategy to Improve Patient Safety and Quality of Care in Radiation Therapy Departments. (Journal of Medical Imaging and Radiation Sciences 2011 June;42(2):81-85.)
5. **Patel P**, Mitera G. Management of symptomatic brain metastases. (Radiation Therapist 2011 March;20(1):81-84.)

Oral presentations

**equals presenting author at conference*

1. Matthew R. McCann*, **Priya Patel**, Michael Barbalinardo, Michael A. Pest, Kim L. Beaucage, Meg P. Kamphuis, Frank Beier, David W. Holdsworth, S. Jeffrey Dixon, Cheryle A. Séguin. Repeated daily exposure to high-frequency low-amplitude vibration negatively affects cartilaginous joints. London Health Research Day: March 9, 2013, London, Ontario, Canada.
2. McCann MR*, **Patel P**, Beaucage KL, Bacher C, Nikolov N, Pollmann SI, Holdsworth DW, Dixon SJ, Séguin CA. Acute vibration induces transient expression of anabolic genes in the intervertebral disc in a frequency dependent manner. London Health Research Day: March 20, 2012, London, Ontario, Canada.

Poster presentations

**equals presenting author at conference*

1. **Priya Patel,** Courtney Brooks, Dr. Cheryle A. Séguin. Investigating microenvironmental regulation of human chordoma cell behaviour. London Health Research Day: March 18, 2014, London, Ontario, Canada.
2. **Priya Patel***, Courtney Brooks, Cheryle A. Séguin. Investigating the expression of matricellular proteins in human chordoma. Spine Research Symposium: November 6-8, 2013, Philadelphia, Pennsylvania, U.S.A.
3. **Priya Patel***, Courtney Brooks, Cheryle A. Séguin. Investigating the expression of matricellular proteins in human chordoma. The Annual Anatomy and Cell Biology Research Day: November 24, 2013, University of Western Ontario, London, Ontario, Canada.
4. **Priya Patel***, Matthew R. McCann, Kim L. Beaucage, Yizhi Xiao, Corey Bacher, Walter L. Siqueira, David W. Holdsworth, S. Jeffrey Dixon, Cheryle A. Séguin. Acute exposure to whole body vibration significantly alters intervertebral disc homeostasis. Canadian Connective Tissue Conference: May 29-June 1, 2013, Montreal, Quebec, Canada. *(Awarded 1st place for poster presentation)*
5. **Patel P***, McCann MR, Beaucage KL, Bacher C, Nikolov N, Pollmann SI, Holdsworth DW, Dixon SJ, Séguin CA. Acute vibration induces transient expression of anabolic genes in the intervertebral disc in a frequency dependent manner. Annual Bone and Joint Retreat: May 8 2013, University of Western Ontario, London, Ontario, Canada.

6. Matthew R. McCann*, **Priya Patel**, Michael Barbalinardo, Michael A. Pest, Kim L. Beaucage, Meg P. Kamphuis, Frank Beier, David W. Holdsworth, S. Jeffrey Dixon, Cheryle A. Séguin. Repeated daily exposure to high-frequency low-amplitude vibration negatively affects articular joints. Gordon Research Conference on Cartilage Biology and Pathology: April 7-12, 2013, Les Diablerets, Switzerland.
7. **P. Patel***, M.R. McCann, K.L. Beaucage, H. N. Nikolov, S.I. Pollmann, W.L. Siqueira, D.W. Holdsworth, S.J.Dixon, C.A. Séguin. Acute exposure to whole body vibration significantly alters intervertebral disc homeostasis in a frequency-dependent manner. London Health Research Day: March 19, 2013, London, Ontario, Canada.
8. McCann MR*, **Patel P**, Beaucage KL, Bacher C, Nikolov N, Pollmann SI, Holdsworth DW, Dixon SJ, Séguin CA. Acute vibration induces transient expression of anabolic genes in the intervertebral disc in a frequency dependent manner. The Annual Physiology and Pharmacology Research Day: November 6, 2012, University of Western Ontario, London, Ontario, Canada.
9. **Patel P***, McCann MR, Beaucage KL, Bacher C, Nikolov N, Pollmann SI, Holdsworth DW, Dixon SJ, Séguin CA. Acute vibration induces transient expression of anabolic genes in the intervertebral disc in a frequency dependent manner. The Annual Anatomy and Cell Biology Research Day: October 25, 2012, University of Western Ontario, London, Ontario, Canada.
10. **Patel P***, McCann MR, Beaucage KL, Bacher C, Nikolov N, Pollmann SI, Holdsworth DW, Dixon SJ, Séguin CA. Acute vibration induces transient expression of anabolic genes in the intervertebral disc in a frequency dependent manner. Canadian Connective Tissue Conference: June 8-10, 2012, Toronto, Ontario, Canada.
11. McCann MR*, **Patel P**, Beaucage KL, Bacher C, Nikolov N, Pollmann SI, Holdsworth DW, Dixon SJ, Séguin CA. Effect of vibration on intervertebral disc homeostasis in a mouse model. Spine Research Symposium: November 16-18, 2011, Philadelphia, Pennsylvania, U.S.A.
12. McCann MR*, **Patel P**, Beaucage KL, Bacher C, Nikolov N, Pollmann SI, Holdsworth DW, Dixon SJ, Séguin CA. Effect of vibration on intervertebral disc homeostasis in a mouse model. Canadian Arthritis Network Annual Scientific Conference: October 27-29, 2011, Quebec City, Quebec, Canada.
13. **Patel P***, McCann MR, Beaucage KL, Bacher C, Nikolov N, Pollmann SI, Holdsworth DW, Dixon SJ, Séguin CA. Modulating intervertebral disc homeostasis through vibration. Annual CIHR Joint Motion Program Summer Research Symposium: August 4, 2011, London, Ontario, Canada.